

FINAL REPORT

Development of Controls for
TIME-TEMPERATURE CHARACTERISTICS
IN ALUMINUM WELDMENTS

Contract No. NAS8-11930
Control No. DCN 1-5-30-12723-01

REPRODUCED FROM BEST AVAILABLE COPY

FACILITY FORM 602

N67-40194

(ACCESSION NUMBER)

130
(PAGES)

CR#89621

(NASA CR OR TMX OR AD NUMBER)

(THRU)

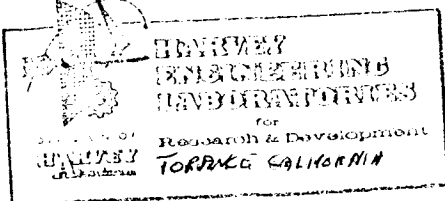
0
(CODE)

15
(CATEGORY)

Reproduced by
NATIONAL TECHNICAL
INFORMATION SERVICE
Springfield, Va. 22151

REPRODUCED FROM BEST AVAILABLE COPY

Ref 47357



HA NO. 2283 PAGE Title

FINAL REPORT

Development of Controls for TIME-TEMPERATURE CHARACTERISTICS IN ALUMINUM WELDMENTS

Contract No. NAS8-11930
Control No. DCN 1-5-30-12723-01

Prepared for
George C. Marshall Space Flight Center
National Aeronautics and Space Administration

October 1966

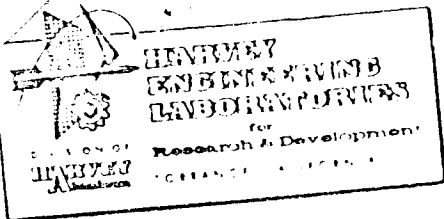
Prepared by: D. Q. Cole

Reviewed by: L. W. Davis

Approved by: P. E. Anderson

ABSTRACT

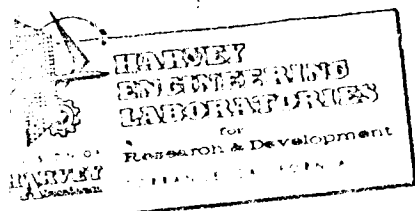
The objective of the NASA sponsored program under which this work was performed is to improve the properties of weldments in aluminum plate by controlling time-temperature relationships during the welding operation. This report contains the results of an experimental study to determine the effects of controlling this relationship by employing a concept for chilling the weldment simultaneously with welding by impingement of liquid CO₂ jets in the vicinity of the weld. Results indicate that this concept is feasible, producing substantial increases in yield strength and reducing distortion markedly. It is also indicated that gross porosity can be reduced. Technical background, experimental procedures, and analysis of results are presented.



ADMINISTRATIVE INFORMATION

This report was prepared by Harvey Engineering Laboratories for Research and Development, a division of HARVEY ALUMINUM (Incorporated), under contract number NAS8-11930 to the George C. Marshall Space Flight Center of the National Aeronautics and Space Administration. The work is administered under the technical direction of the Manufacturing Engineering Laboratory with Mr. Elmer F. Bizarth (R-ME-IT) and Mr. Franklin J. Jackson (R-ME-MW) as technical representatives. Participating technical personnel for Harvey Engineering Laboratories include Mr. L. W. Davis, project manager; Mr. D. Q. Cole, project engineer; Mr. E. V. Sumner, metallurgical engineer; Mr. L. P. Evans, design engineer; Mr. M. R. Ransom, electrical engineer; and Mr. H. Wendling, welding technician.

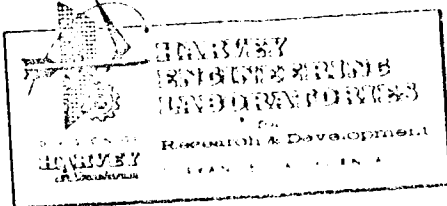
The results of these tests shall not be circulated, referred to, or otherwise used for publicity or advertising purposes or for sales other than those leading to ultimate use by an agency of the Federal Government.



<u>Section</u>	<u>Title</u>	<u>Page</u>
ENDIX V	TENSILE TEST RESULTS	A.V
VI	TABLE OF HEAT INPUT, HEAT EXTRACTION, TENSILE STRENGTH, AND POROSITY DATA	A.VI
VII	TEMPERATURE MEASUREMENT BY INFRARED RADIATION	A.VII
VIII	REFERENCES	A.VIII

TABLE OF CONTENTS

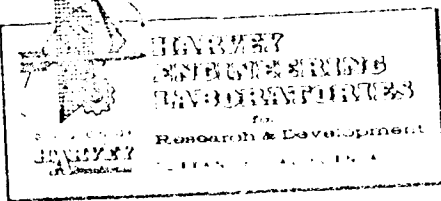
<u>Section</u>	<u>Title</u>	<u>Page</u>
	ADMINISTRATIVE INFORMATION	i
	LIST OF ILLUSTRATIONS	iv
	LIST OF TABLES	x
I	SUMMARY	I.01
II	INTRODUCTION AND TECHNICAL BACKGROUND	II.01-II.03
III	LITERATURE AND INDUSTRY SURVEY	III.01
IV	EXPERIMENTAL WORK	IV.01
	A. GENERAL	IV.01
	B. EQUIPMENT AND INSTRUMENTATION	IV.04
	C. CHILLING FROM THE BACK SIDE OF THE WELDMENT	IV.08
	D. CHILLING FROM THE FRONT SIDE OF THE WELDMENT	V.01
V	DISCUSSION OF RESULTS	VI.01
VI	CONCLUSIONS	VII.01
VII	RECOMMENDATIONS	A.I
APPENDIX I	CALCULATION OF TARGET THERMAL PATTERNS	A.II
II	EXPERIMENTAL THERMAL PATTERNS	A.III
III	CALCULATION OF THERMAL BALANCE	A.IV
IV.	DEVELOPMENT OF CO ₂ SHIELDS FOR FRONT SIDE CHILLING	



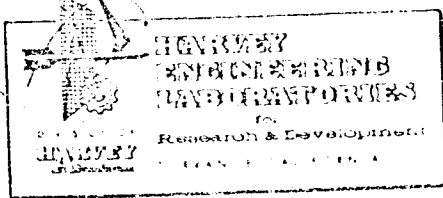
LIST OF ILLUSTRATIONS

Figure

- 1 TIG Welding Equipment and Instrumentation, Metallurgical and Welding Laboratory of the Harvey Engineering Laboratories
- 2 Sketch of Experimental Setup
- 3 Jet System for Chilling from the Back Side
- 4 Efficiency of Glass Tape Backing Materials - Macro-sections of Bead-on-Plate Welds in 5/16-inch 2014-T6 Plate (3X)
- 5 Efficiency of Metal Roll Backing Materials - Macro-sections of Bead-on-Plate Welds in 5/16-inch 2014-T6 Plate (3X)
- 6 Efficiency of Copper Mesh Backing Materials - Macro-sections of Bead-on-Plate Welds in 5/16-inch 2014-T6 Plate (3X)
- 7 Effect of liquid CO₂ chilling on Time-Temperature Curves during Welding of 5/16" 2014-T6 Aluminum Plate Chilled from the Back Side
- 8 Effect of liquid CO₂ Chilling on Time-Temperature Curves during Welding of 1/2" 2014-T6 Aluminum Plate Chilled from the Back Side.
- 9 Effect of liquid CO₂ Chilling on Time-Temperature Curves during Welding of 5/16" 2219-T87 Plate, Weld Centerline, Chilled from the Back Side.
- 10 Effect of liquid CO₂ Chilling on Time-Temperature Curves during Welding of 1/2" 2219-T87 Plate, Weld Centerline, Chilled from the Back Side.

LIST OF ILLUSTRATIONS (cont.)Figure

- 11 Jet System No. 1 for Front Side Chilling of Weldments using a Cryogenic liquid -- Stationary Shield with Metal Foil Seal.
- 12 Jet System No. 14 for Front Side Chilling using a Cryogenic Liquid -- Traveling Shield with Spring Loaded Metallic Wool and Wire Brush Seal, Helium Purged with Metallic Shirt-7 Jet Manifold.
- 13 Effect of Front Side Chilling on Thermal Cycle Curves, Jet System No. 14, Butt Welds in 1/2-inch 2219-T87 Plate.
- 14 Effect of Front Side Chilling on Thermal Cycle Curves, Jet System No. 14, Butt Welds in 5/16-inch 2219-T87 Plate.
- 15 Effect of Front Side Chilling on Thermal Cycle Curves, Jet System No. 14, Butt Welds in 1/2-inch 2014-T6 Plate.
- 16 Effect of Front Side Chilling on Thermal Cycle Curves, Jet System No. 14, Butt Welds in 5/16-inch 2014-T6 Plate.
- 17 Effect of Front Side Chilling on Thermal Cycle Curves, Jet System No. 18, Butt Welds in 5/16" and 1/2" 2014-T6 Plate.
- 18 Effect of Front Side Chilling on Thermal Cycle Curves, Jet System No. 19, Butt Welds in 5/16" 2219-T87 and 2014-T6 Plate.
- 19 Effect of Front Side Chilling on Thermal Cycle Curves for Butt Welds in 5/16" 2014-T6 Plate.
- 20 Effect of Front Side Chilling on Thermal Cycle Curves for Butt Welds in 1/2" 2014-T6 Plate.

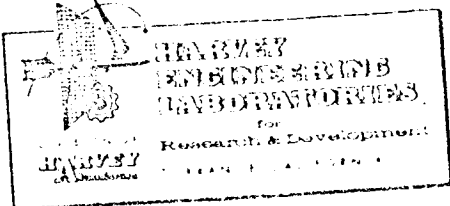
LIST OF ILLUSTRATIONS (cont.)Figure

- 21 Effect of Front Side Chilling on Thermal Cycle Curves for Butt Welds in 5/16" 2219-T87 Plate.
- 22 Effect of Front Side Chilling on Thermal Cycle Curves for Butt Welds in 1/2" 2219-T87 Plate.
- 23 Macrosections Showing the Effects of Liquid CO₂ Chilling from Front Side of Bead on Plate Welds in 5/16-inch 2014-T6 Aluminum Made with Constant Heat Input.
- 24 Macrosections Showing the Effect of Liquid CO₂ Chilling from the Front Side of Bead on Plate Welds in 1/2-inch 2014-T6 Aluminum Made with Constant Heat Input.
- 25 Macrosections Showing Effect of Front Side Chilling of Welds in 5/16-inch 2219-T81 Jet System No. 23.
- 26 Macrosections Showing Effect of Front Side Chilling of Welds in 5/16-inch 2219-T87 Plate - Jet System No. 19.
- 27 Macrosections Showing Effect of Front Side Chilling of Welds in 5/16-inch 2014-T6 Plate - Jet System No. 23.
- 28 Macrosections Showing Effect of Front Side Chilling of Welds in 5/16-inch 2014-T6 Plate - Jet System No. 18.
- 29 Macrosections Showing Effect of Front Side Chilling of Welds in 1/2-inch 2014-T6 Plate - Jet System No. 19.
- 30 Macrosections Showing Effect of Front Side Chilling of Welds in 1/2-inch 2014-T6 Plate - Jet System No. 18.
- 31 Macrosections Showing Effect of Front Side Chilling of Welds in 1/2-inch 2219-T87 Plate - Jet System No. 14.

LIST OF ILLUSTRATIONS (cont.)

Figure

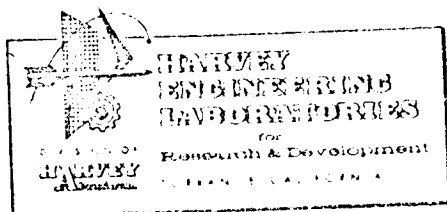
- 32 Macrosections Showing Comparison of the Effect of Three Jet Systems for Front Side of Chilling of Welds in 1/2-inch 2219-T87 Plate.
- 33 Typical X-rays Showing Effect of Front Side Chilling on Porosity in Welds in 1/2-inch 2014-T6 Plate.
- 34 Effect of CO₂ Chilling on Warpage in Aluminum Weldments (Top: Unchilled; Bottom: Chilled from Front Side).
- 35 Calculated Peak Temperatures
- 36 Schematic for Target Thermal Patterns (1)
- 37 Schematic for Target Thermal Patterns (2)
- 38 Thermal Pattern for Weld Panel 1A1 No Chilling, 5/16" 2014-T6, Penetration Pass.
- 39 Thermal Pattern for Weld Panel 1EC1 CO₂ Chilled, 5/16" 2014-T6 Penetration Pass.
- 40 Thermal Pattern for Weld Panel 1F2 No Chilling, 1/2" 2014-T6, Penetration Pass.
- 41 Thermal Pattern for Weld Panel 1D33 CO₂ Chilled, 1/2" 2014-T6, Penetration Pass.
- 42 Thermal Pattern for Weld Panel 2B2-20, No Chilling, 1/2" 2219-T87.
- 43 Thermal Pattern for Weld Panel 2B03-1 CO₂ Chilled, 1/2" 2219-T87.
- 44 Thermal Pattern for Weld Panel 2 ACI-X No Chilling, 5/16", 2219-T87.
- 45 Thermal Pattern for Weld Panel 2AC-1 CO₂ Chilled, 5/16" 2219-T87.



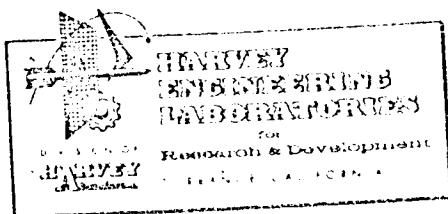
LIST OF ILLUSTRATIONS (Cont.)

Figure

- 46 Sketch of Jet System Arrangement for Chilling Weldments from Front Side using a Stationary Shield.
- 47 Jet System No. 2 for Front Side Chilling of Weldments using a Cryogenic Liquid -- Traveling Shield with Metal Foil Shoe.
- 48 Jet System No. 3 for Front Side Chilling of Weldments using a Cryogenic Liquid -- Traveling Shield with Flexible Skirt Seal.
- 49 Jet System No. 4 for Front Side Chilling of Weldments using a Cryogenic Liquid -- Traveling Shield with Helium Purge Manifold.
- 50 Jet System No. 5 for Front Side Chilling of Weldments using a Cryogenic Liquid -- Traveling Shield with Helium Purge Ring.
- 51 Jet System No. 6 for Front Side Chilling of Weldments using a Cryogenic Liquid -- Traveling Shield with Helium Purge Collar.
- 52 Jet System No. 7 for Front Side Chilling of Weldments using a Cryogenic Liquid -- Traveling Shield with Metallic Wool Seal - 3 Jet Manifold.
- 53 Jet System No. 8 for Front Side Chilling of Weldments using a Cryogenic Liquid -- Traveling Shield with Metallic Wool Seal - 5 Jet Manifold.
- 54 Jet System No. 9 for Front Side Chilling of Weldments using a Cryogenic Liquid -- Traveling Shield with Metallic Wool Seal - 7 Jet Manifold.
- 55 Jet System No. 10 for Front Side Chilling of Weldments using a Cryogenic Liquid -- Traveling Shield with Metallic Wool and Wire Brush Seal - 7 Jet Manifold.

LIST OF ILLUSTRATIONS (cont.)Figure

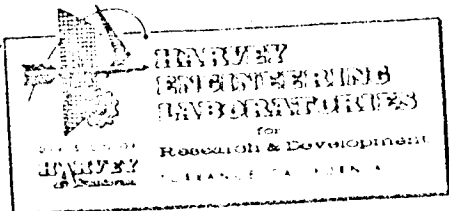
- 56 Jet System No. 11 for Front Side Chilling of Weldments using a Cryogenic Liquid -- Traveling Shield with Spring Loaded Metallic Wool 7 Jet Manifold.
- 57 Jet System No. 12 for Front Side Chilling using a Cryogenic Liquid -- Traveling Shield with Spring Loaded Metallic Wool and Wire Brush Seal - 7 Jet Manifold.
- 58 Jet System No. 13 for Front Side Chilling using a Cryogenic Liquid -- Traveling Shield with Spring Loaded Metallic Wool and Wire Brush Seal, Helium Purged - 7 Jet Manifold.
- 59 Effect of Front Side Chilling on Thermal Cycle Curves Jet System No. 1.
- 60 Effect of Front Side Chilling on Thermal Cycle Curves - Jet System No. 2.
- 61 Effect of Front Side Chilling on Thermal Cycle Curves - Jet System No. 7.
- 62 Effect of Front Side Chilling on Thermal Cycle Curves - Jet System No. 8 (1/2" Plate).
- 63 Effect of Front Side Chilling on Thermal Cycle Curves - Jet System No. 9.
- 64 Trace of Carnes Scanning Radiometer During Welding, Showing Six Consecutive Scans.



LIST OF TABLES

Table

- I Comparison of Tensile Properties of Unchilled Welds and Welds Chilled from the Back Side by Liquid CO₂ 2219-T87 Plate.
- II Comparison of Tensile Properties of Unchilled Welds and Welds Chilled from the Back Side by Liquid CO₂ 2014-T6 Plate.
- III Effect of Back Side Chilling on Weld Porosity.
- IV Typical Welding Parameters - Unchilled Panels.
- V Welding Parameters - Panels Chilled from the Front Side.
- VI Effect of Front Side Chilling on Tensile Properties of Weldments (Artificial Aging).
- VII Effect of Front Side Chilling on Tensile Properties of Weldments (Natural Aging).
- VIII Maximum Increases in Tensile Strength Effected by Front Side Chilling.
- IX Optimum Jet Systems for Improving Tensile Strength Front Side Chilling.
- X Effect of Front Side Chilling on Weld Porosity.
- XI Cooling Available for Altering the Thermal Pattern of Weld Panels Chilled by Liquid CO₂.
- XII Heat Input for the Penetration Pass in Unchilled and Liquid CO₂ Chilled Weld Panels, 5/16" and 1/2" 2014-T6 Plates.
- XIII Heat Extraction Expected by Liquid CO₂ Chilling during Penetration Pass of Weld Panels in 5/16" and 1/2" 2014-T6 Plate.



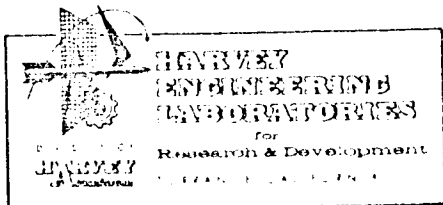
HA NO 2283 PAGE xi

LIST OF TABLES (cont.)

Table

XIV

Summary of Data for Welds Chilled from the Front Side.



1. SUMMARY

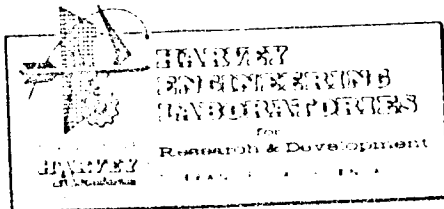
For current aerospace applications it is essential that properties of aluminum alloy weldments be increased to the maximum possible. Properties of heat-treatable alloys, particularly those involving cast structure, are time-temperature dependent.

The work covered in this report was initiated to investigate the feasibility of applying a concept for controlling the time-temperature relationship by impingement of liquid CO₂ jets in the vicinity of the weld concurrent with the welding operation to produce beneficial thermal patterns. Target thermal patterns were those which would increase the thermal gradient in the weld area and shorten the time above critical temperatures to a minimum. Such patterns should produce weldments with finer grained cast structure and narrower heat affected zones, while inhibiting agglomeration of gases and strengthening elements as well as decreasing formation of undesirable compounds.

Materials selected for the experimental work were aluminum alloys 2219-T87 and 2014-T6 in plate thickness of 5/16 and 1/2-inch. The welding process selected was DC-SF tungsten arc, with welding to be accomplished from one side in the "free state" in the horizontal position using 2319 filler wire for both alloys. One pass was prescribed for the 5/16-inch material and two passes for the 1/2-inch material.

Experimental equipment and procedures were developed for welding 12 inch x 48 inch panels with sufficient instrumentation to monitor pertinent heat input and extraction variables. Weldment temperatures were measured by thermocouples embedded in the plate. Limited investigations were conducted for measuring weld temperatures by means of infrared radioneters.

Two series of welded panels were fabricated. Half of each series was welded without chilling and half with liquid CO₂ chilling, attempting to maintain comparable weld bead dimensions. In the first series, chilling was effected from the back side of the weldment using a double layer of glass tape

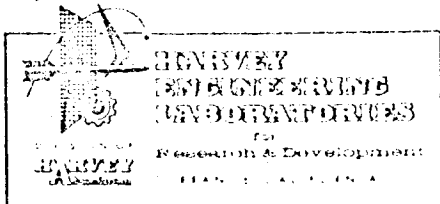


to prevent deformation and contamination of the underbead by the liquid CO_2 . In the second series, weldments were chilled from the front (torch) side using a shield to prevent leakage of CO_2 into the arc area. Several systems of jet orifice sizes and arrangements were used for each series.

Comparable unchilled and chilled weldments for both series were examined by X-ray, fracturing and macrosectioning. Tensile tests were performed after natural aging, artificial aging and after reheat-treating to the T-6 condition.

Macrosections show that chilling markedly reduces the grain size of the cast structure and significantly narrows the heat affected zone. Results of tensile tests indicate substantial improvements in the yield strength (up to 20%) for chilled welds. The effect on ultimate strength was less clearly defined. In some cases increases up to 18% were obtained, and in other cases slight decreases were noted. Changes in porosity were similarly not clearly defined; however, the indications were that chilling does not degrade the weldment in these respects. In some cases particularly in welds chilled from the back side, marked improvements occurred indicating that nucleation and growth of porosity might be inhibited. Chilling from the front side greatly reduced warpage both in longitudinal bow and peaking.

It is concluded that application of chilling by cryogenic liquids is feasible for improving weldment properties, and further development is warranted based on the improvements in yield strength and control of warpage. It is expected greater strength improvements can be realized, and that the concept can be applied to control of warpage and residual stresses. It is therefore recommended that this work be continued to verify and extend results already obtained, and to refine equipment and techniques preparatory to applying the concept to production welding.

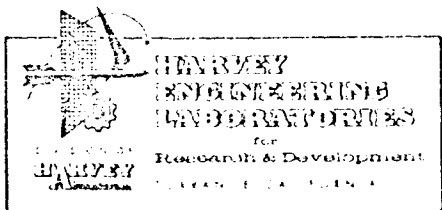


II. INTRODUCTION AND TECHNICAL BACKGROUND

The objective of the program under which this work was performed is to develop methods, tooling concepts, and processes to control the time-temperature characteristics in the weld and heat-affected zone, in order to improve tensile properties and reduce porosity in aluminum weldments. A secondary objective is to advance the state-of-the-art by developing control methods which will aid the welder in consistently producing better welds in all materials.

The need for this work has been brought about by the increasing requirement for higher strength-weight ratio and for greater reliability of weldments in aerospace vehicles, in particular the aluminum components for the Saturn V boosters. Stringent design demands have made it necessary to obtain the maximum properties from the best available materials, as new materials development has not been able to keep pace with these demands. Therefore, the increased design requirements must be realized by improvements and innovations in those areas of materials processing which will raise design allowables of existing materials by decreasing degradation and increasing reliability. The fusion welding process characteristically degrades properties of most high strength materials and also decreases reliability by introducing defects.

The copper bearing heat treatable aluminum alloys are severely affected by fusion welding, as their strength is dependent upon a sensitive time-temperature relationship and welding produces an adverse relationship. A cast structure, which contains large and improperly oriented grains, may be produced. The parent metal adjacent to the weld will be affected by the heat of welding. This zone will contain a portion in which eutectic melting has occurred, a solution annealed area, a partially annealed area, and an overaged area. Depending upon the time-temperature relationship, the heat-affected zones may be wide or narrow and the zone of eutectic melting may contain small or large amounts of coalesced strengthening and grain refining elements as well as undesirable compounds. All of these metallurgical structures affect the strength of



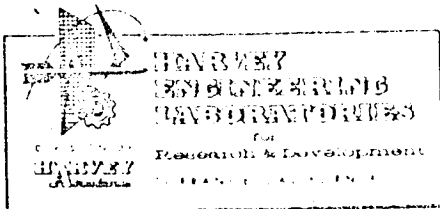
the welded joint. An optimum time-temperature relationship during the welding process will alleviate these degrading effects. An increased cooling rate can reduce grain size and retard agglomeration of strengthening elements; a steeper thermal gradient can reduce the size of the heat-affected zone and alleviate adverse grain orientation in the cast structure.

Fusion welding can also introduce "mechanical" defects, such as gas and shrinkage porosity, into the weld. While these defects are not ordinarily thought of as being time-temperature dependent from the standpoint of welding, it has long been recognized in the making of castings that they are in fact greatly influenced by cooling rate and direction of solidification. Since fusion welds are, in effect, small castings, similar principles should apply. A steep thermal gradient produces smaller dendrites and allows residual liquid metal to more effectively feed the interstices, reducing shrinkage porosity. Unidirectional solidification also promotes escape of gases and alleviates formation of shrinkage porosity. Fast cooling inhibits gas pore growth and results in a reduction of gross porosity.

From the above, it is apparent that an optimum thermal pattern, which would increase the thermal gradient and reduce the time at temperature in critical ranges, will improve weldment properties.

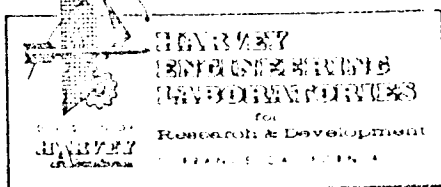
The use of chill bars has long been used to achieve quenching during welding. While this method is perhaps adequate for welds in non-critical structure, it has three distinct disadvantages: (1) Non-uniform contact between the chill bars and the work piece can cause erratic chilling with resultant hot and cold spots along the length of the weld; (2) The degree of chilling is not easily adjustable to the variety of materials, thicknesses, configurations, etc.; and (3) "Hard" tooling cannot always be used.

Efforts to control weld chilling by selection of special chill bar materials, such as titanium and insulator-type materials, have indicated some promise in overcoming erratic chilling but are subject to the other limitations and produce only a limited degree of heat extraction.



The concept chosen for accomplishing the program objective was alteration of the thermal pattern in the weldment during the welding process by impingement of cryogenic liquid jets in the vicinity of the weld. By proper balancing of heat input and heat extraction, the time-temperature relationship for the weld cast structure and heat-affected zone can be controlled to minimize porosity formation, grain growth, overaging and coalescence of grain refining and strengthening.

The program was divided into two phases: a four-month phase for literature and industry survey, and a fourteen-month experimental phase. The purpose of the first phase was to determine the state-of-the-art to avoid duplication of effort and to obtain any information that might be useful in the program. The second phase included all of the experimental work, and was planned to consist of two principal steps. The first was to establish realistic thermal patterns designed to improve the weld properties. The second step was to devise and test various means of providing the time-temperature controls required to attain maximum increase in tensile strength and decrease in porosity. Welding studies were to include two plate thicknesses, 5/16" and 1/2", in each of two aluminum alloys - 2014-T6 and 2219-T87. Welding was to be performed in the horizontal position by the semi-automatic TIG process, using direct current straight polarity, on square-butt joint preparation with 2319 filler wire, if required.



III. LITERATURE AND INDUSTRY SURVEY

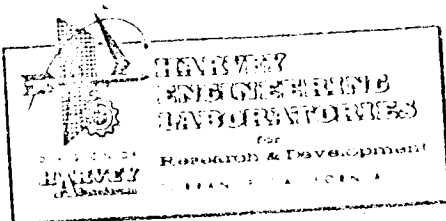
The purpose of the survey was to obtain information which might be helpful in the performance of this program, by avoiding duplication of effort and/or by supplementing the original program concept.

Current abstract bulletins published by the National Aeronautics and Space Administration (STAR) and by the Defense Documentation Center (TAB) were checked for reports of work pertinent to fusion welding of aluminum, and significant reports were acquired for review.

A similar survey was made of applicable technical books and periodicals, including those of the American Welding Society, the American Society for Metals and the American Institute of Mining and Metallurgical Engineers. Particular emphasis was devoted to issues of the Welding Journal published during the past ten years.

Those organizations and individuals who were considered to be involved in work related to this program were contacted for personal interview or for interview by telephone. The cooperation was excellent, and in some cases special data were furnished and tours of plant facilities arranged.

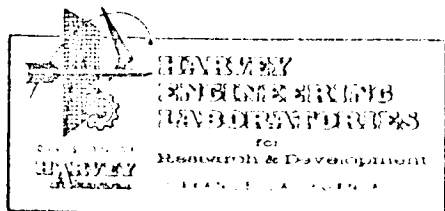
No reported or unreported work was found which would indicate that any part of this program is a duplication of effort. A considerable amount of information was obtained which facilitated the experimental portion of the program, particularly that work pertaining to heat transfer analysis and specific welding techniques currently in use for fabricating aerospace structures by welding the particular materials involved. A large amount of work has been done and is currently in progress to improve the quality of weldments in aerospace components fabricated from aluminum. Although only a few specific studies have apparently been conducted on a laboratory basis for determining the effects of time-temperature on properties of weldments, a good many of the process controls adopted for shop welding are aimed in the direction of controlling thermal patterns.



In some work completed in 1965 by Frankford Arsenal, it was determined that three significant trends were noted in the microstructure which indicate the merit of the use of super-chilling during welding of aluminum: (1) the amount of micro-porosity was substantially lessened, (2) the width of the zone of grain boundary melting at the interface was reduced appreciably, and (3) a finer-grained cast structure was obtained. All of this work was performed on 0.090-inch thick 2014 and 2024 aluminum alloys. In one set of experiments the chill bars (both top and bottom) were cooled with brine at -45°F . In a second set, for which data has been published recently, the chill bars were cooled with liquid nitrogen. In each case, welding was performed after the parts to be welded reached a selected temperature, -30°F and -250°F , respectively. Difficulty with condensation of moisture on the parts was overcome by enclosing the part in a flexible bag containing dry argon or helium.

The cryogenic liquid jet concept of chilling has two advantages over pre-chilling the entire part prior to welding. Condensation of moisture in the area to be welded can be avoided by adjusting the jet arrangement so that this area is not cooled below room temperature until it is shielded by the welding torch atmosphere. Thus, there is no need to perform the welding operation in an environmental chamber. Secondly, the degree of chilling and the chilling pattern can be easily adjusted.

From data obtained from the survey, approximate calculations were made to determine whether or not it would be feasible to achieve the chilling required for changing thermal patterns during the welding process by utilizing liquid CO_2 as a chilling agent. As shown in Appendix I, it appeared entirely possible to accomplish the required cooling, using liquid Carbon Dioxide.



IV. EXPERIMENTAL WORK

A. General

The experimental phase of the program was divided into three major steps. The first step consisted of development of equipment and instrumentation. In the second, experimental studies were performed to determine the effect of chilling the weld from the back side. Studies for chilling the weld from the front side were performed in the third step.

B. Equipment and Instrumentation

Existing equipment was modified as shown in Figure 1 for welding test panels from one side in the horizontal position. The basic equipment consisted of a Miller Model 600/1200 power supply, a Miller high-frequency unit, a Berkeley-Davis side beam and carriage system, an Airco TIG welding torch and wire feed system with mounting brackets, a fixture for 12 in. x 48 in. weld panels, a cryogenic jet spray system and suitable brackets and attachments for mounting radiometers.

Welding Power Supply

A duplex Miller DC rectifier-type welder, Model No. 600/1200, with superimposed high frequency, was used to supply the welding current.

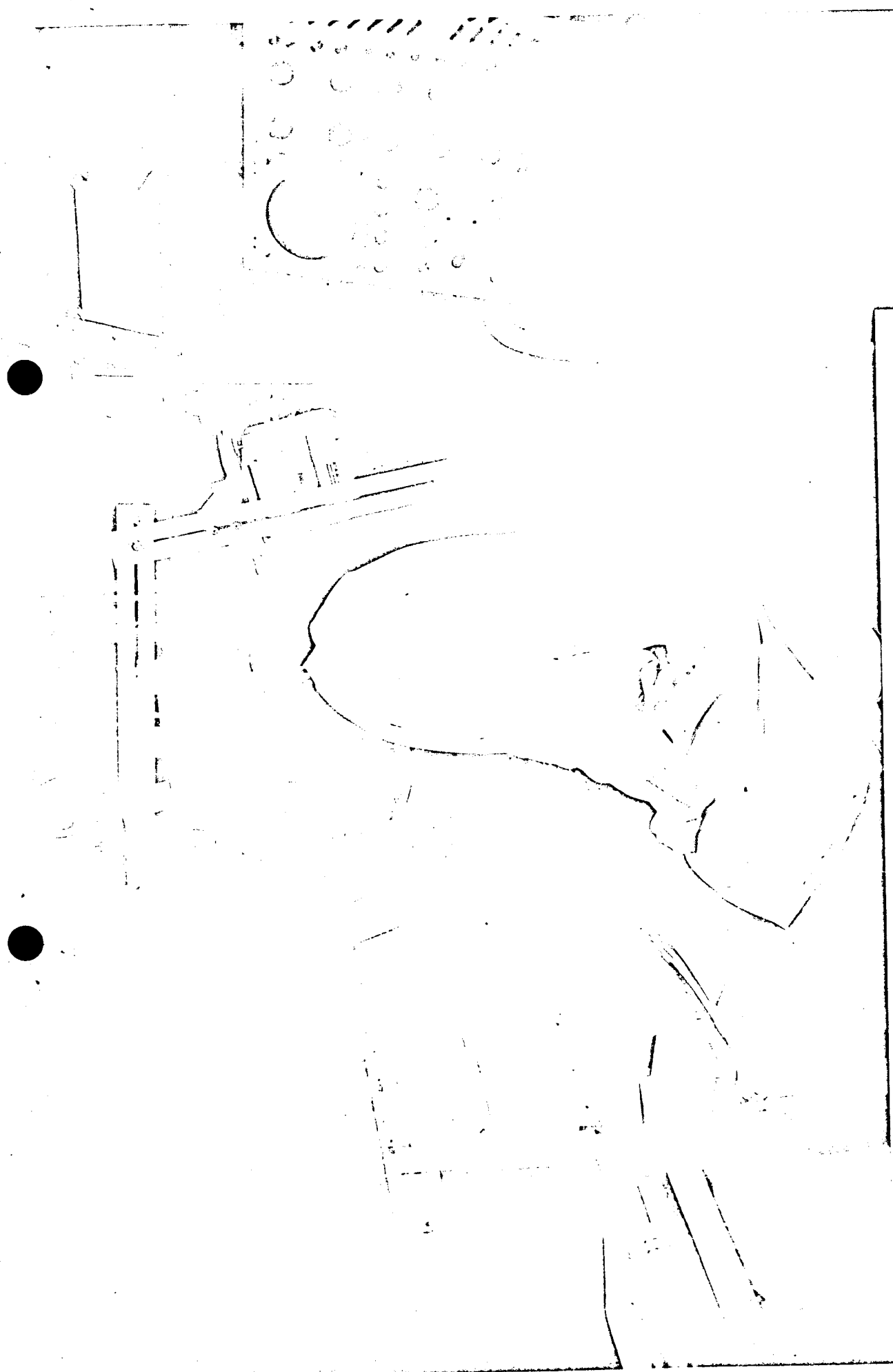
Side Beam and Carriage System

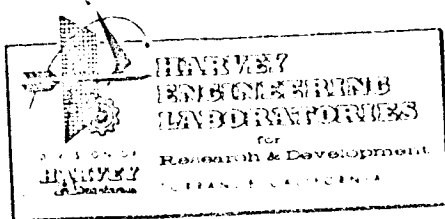
A 12 ft. Berkeley-Davis System Model No. TC4 was mounted on a rectangular support frame fabricated from 2 1/2 in. diameter tubular steel pipe which was anchored to the floor and to the building structural members. The side beam carriage speed was controlled by an electronic governor (Model EG-3) for travel speeds ranging from 4.4 to 72.01 inches per minute.

Welding Torch

An Airco Proximity Control Model EMH-F heliweld unit with metallic nozzles of 5/8-in. and 1/2-in. orifices was adapted for semi-automatic welding using 5/32-in. and 3/16-in., 2% thoriated tungsten electrodes.

Figure 1. TIG Welding Equipment and Instrumentation, Metallurgical and Welding Laboratory
of the Harvey Engineering Laboratories





Wire Feed

An Airco filler wire feed with wire positioner was installed on the carriage system and fitted for 3/64-in. and 1/16-in. wire.

Panel Fixture

The fixture for positioning the weld panels in the horizontal position consisted of a frame fabricated from 1/4-in. x 3 in. x 3 in. stainless steel angle iron, with a "free" area of 4 inches on each side of the weld centerline. The panels were clamped to the fixture by means of angle clamps which were machined for each thickness.

Chilling System

Jets of various orifice size, flexible hose, and liquid CO₂ in 250 lb. tanks were obtained. An attachment bracket for positioning the jets was mounted on the back side of the weld carriage system. The location and number of jets were adjustable.

Instrumentation

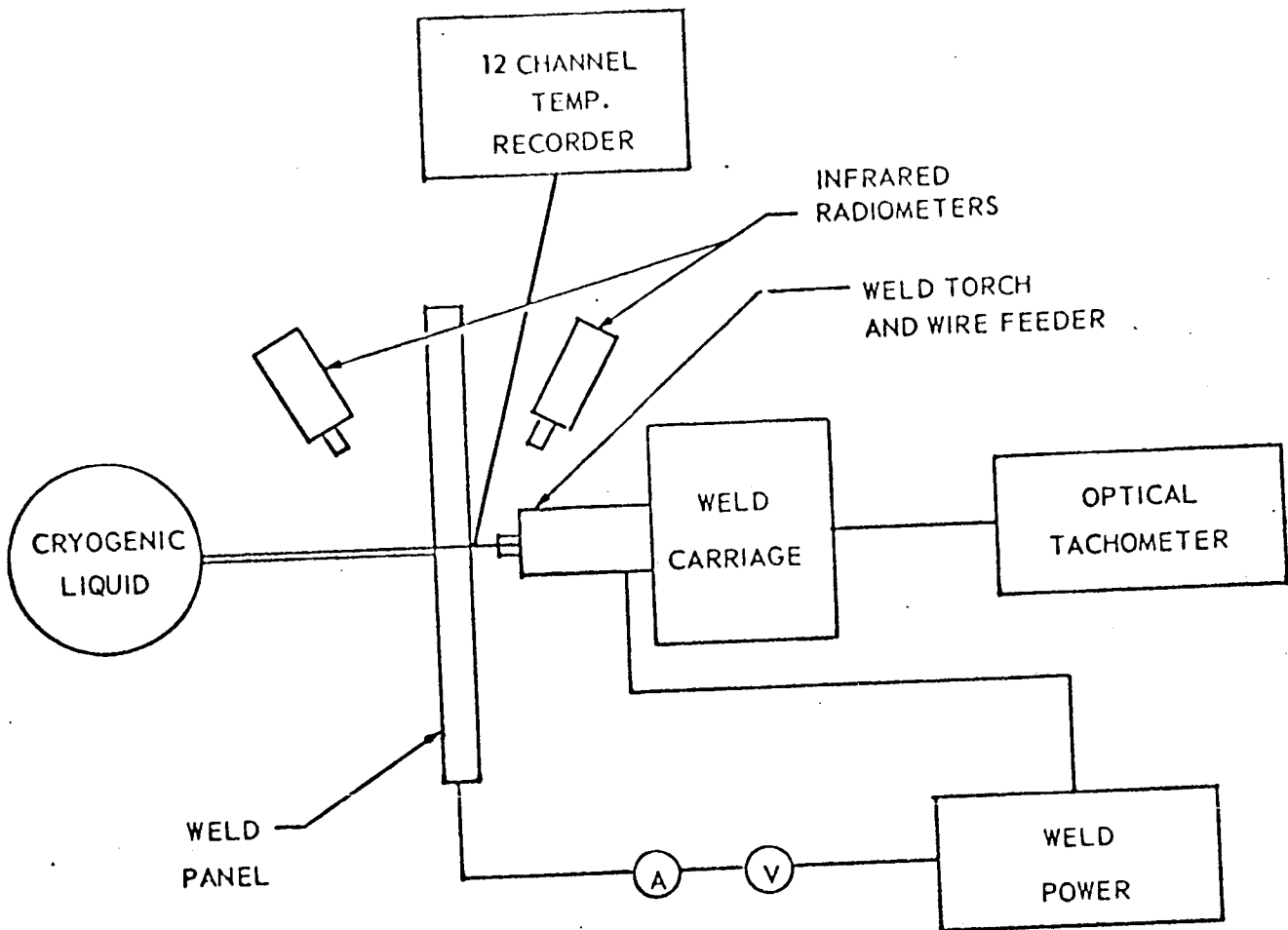
As shown in Figure 2 the instrumentation for monitoring welding process variables and thermal patterns in the weld panels consists of Weston ammeter and voltmeter, an optical tachometer, a Leeds & Northrup 12-channel temperature recorder with thermocouples, an Airco helium flow-meter, an Airco filler wire speed regulator, a Tektronic oscilloscope, and infrared radiation thermometers.

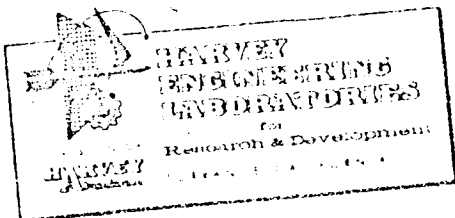
Welding Speed

An optical tachometer, utilizing light reflections from the carriage drive motor shaft, was used to monitor welding speed. The reflected light is directed into a photocell, the signal from which is converted into revolutions per minute by a Hewlett-Packard Frequency Meter, Model 500C. This motor speed is then calibrated in terms of travel speed in inches per minute.

Figure 2

SKETCH OF EXPERIMENTAL SETUP





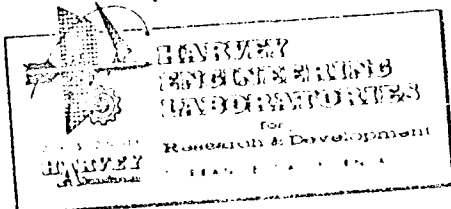
Welding Current

A Weston D.C. Ammeter, Model 1, with a 750 amp. shunt, was installed in the workpiece ground lead, which, in conjunction with a Weston D.C. Voltmeter Model 1, monitors the welding current.

Time-Temperature

A Leeds & Northrup Speedomax 12-channel recorder was modified to accommodate the required temperature range (-300 to 2100°F), using chromel-constantan thermocouples.

A Huggins Mark 1 Infrascopes (infrared radiometer) and a Barnes scanning radiometer (also infrared) were obtained for evaluation.



C. CHILLING FROM THE BACK SIDE OF THE WELDMENT

SUMMARY

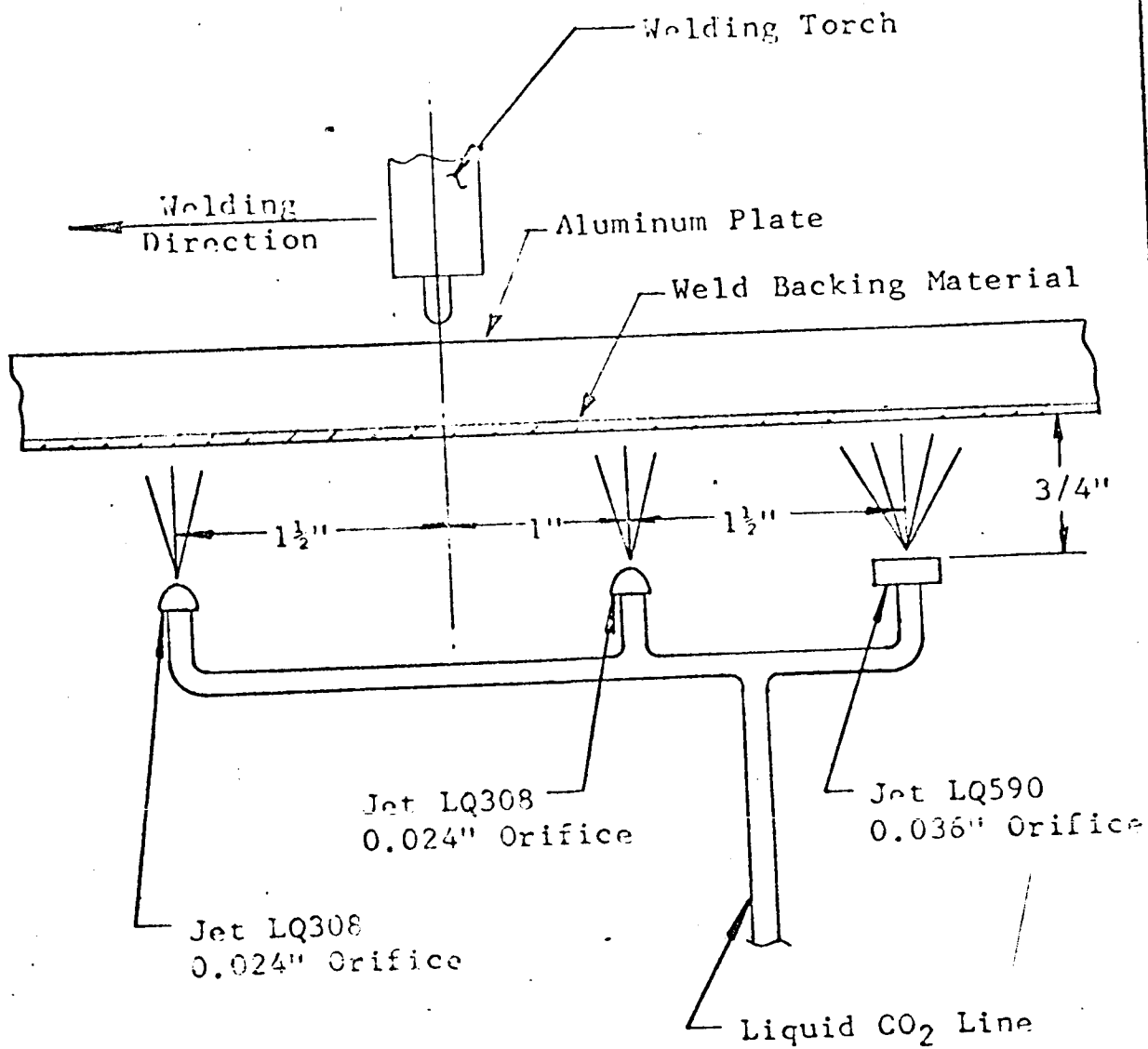
Welding studies were performed to develop welding and chilling parameters, and to determine the effect of chilling on weldment properties. It was demonstrated that chilling from the back side can be successfully accomplished to produce marked improvements in properties. Increases up to 14.5% in the ultimate tensile strength were effected by the chilling systems used. In some cases porosity reductions to one-half were noted. Work on chilling from the back side was discontinued after a decision that only chilling from the front side would be practical for the majority of production weldments.

PROCEDURE AND RESULTS

Systems were fabricated to effect impingement of the liquid CO_2 on the back side of the weld. Figure 3 shows a sketch of a typical system. These systems were designed so that a series of jets could be positioned along the weld seam on the underhead side of the panel. The number and relative position of each jet, as well as orifice size, could be varied making it possible to adjust the amount of CO_2 delivered and the locations of impingement. The jet holder system was attached to the welding carriage so that it moved along with the welding torch keeping the relative position of each jet constant with respect to the torch along the full length of the weld seam. A special flexible tubing delivered the liquid CO_2 from the tank to the jet system.

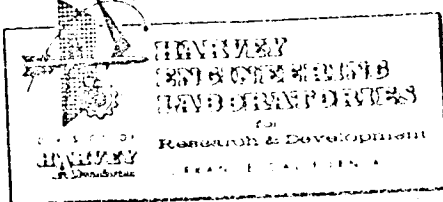
Impingement of CO_2 on the molten metal caused deformation and contamination of the weld underhead. Tests were performed to select weld backing materials that would protect the underhead as well as permit adequate heat transfer for effective chilling.

Backing materials investigated included adhesive and non-adhesive glass tape, fine copper mesh, coarse copper mesh, copper foil and aluminum foil. All materials were cut into strips approximately two inches wide and twelve inches long. These strips were fastened in series over the underhead side



Jet System for Chilling
from the Back Side.

Figure 3



of the plate to be welded using adhesive glass tape. Double glass tape (adhesive glass tape over non-adhesive glass tape) was placed at intervals between the materials being investigated, and additional intervals were left uncovered for comparison.

all welding and chilling variables were kept constant for each plate thickness, and macro-sections were prepared to compare the efficiency of each material for heat extraction.

By comparing the size of the cast weld nuggets as shown in the photographs of macrosections presented in Figures 4 through 6, it appears that copper foil transfers heat most efficiently. However, the size of the heat-affected zone remains essentially the same for the two copper meshes, the copper foil, the aluminum foil, and the single glass tape. Final selection of double glass tape for the backing material was based on a trade-off of poorer heat transfer efficiency with reliability and ease of handling.

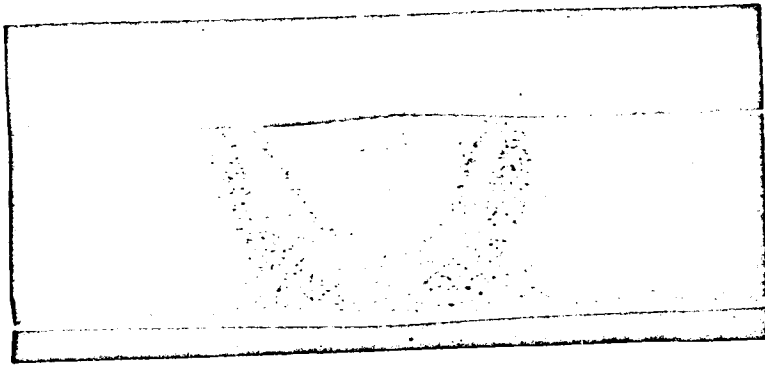
Development of Welding and Chilling Parameters

Welding heat input and CO₂ chilling parameters were varied to obtain welds in each thickness of each plate alloy which were acceptable from the standpoint of physical appearance, while accomplishing a significant change in the cooling rate. Efforts were made to prepare unchilled welds and chilled welds in the same manner so that the number of variables which might influence the characteristics of the weld would be reduced.

Typical thermal cycle curves showing the changes in the cooling rate and time at temperatures above 500°F are shown in Figures 7 through 10.

Thermal patterns for selected weld panels were plotted and are shown in appendix II. By comparison of these patterns for chilled and unchilled welds, it is apparent that substantial chilling has been effected.

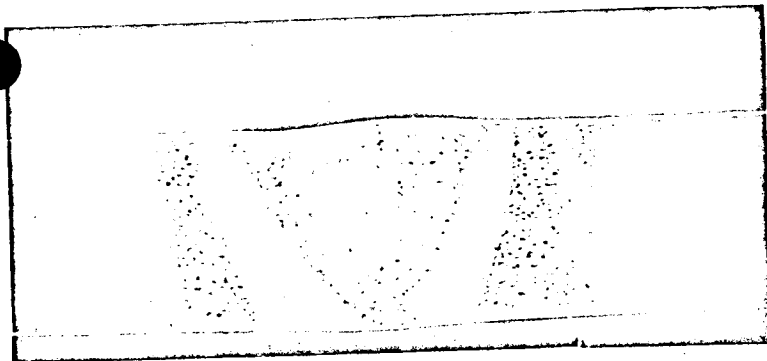
Appendix III shows calculations for heat input and heat extraction for a series of welds in 2014-T6 plate. The calculations show that at 50% efficiency, CO₂ can provide sufficient cooling to produce quench rates required to effect beneficial changes in metallurgical structure.



1ACB-1

Chilling: Liquid CO₂
Jet System No. 1

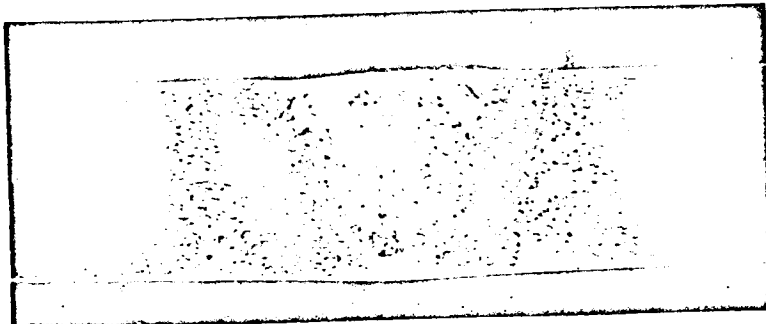
Backing Material:
None



1ACB-2

Chilling: Liquid CO₂
Jet System No. 1

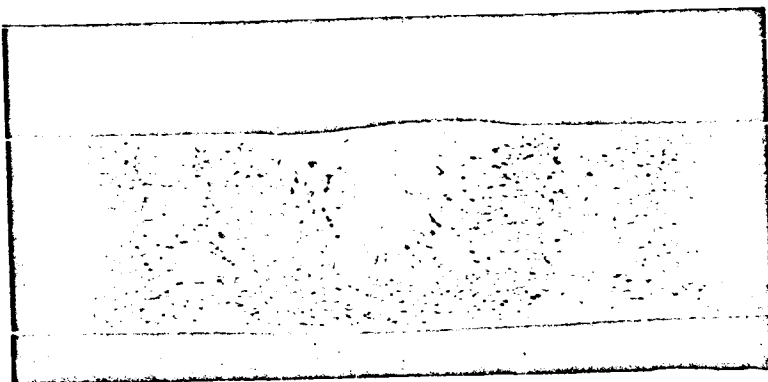
Backing Material:
Single Glass Tape



1ACB-3

Chilling: Liquid CO₂
Jet System No. 1

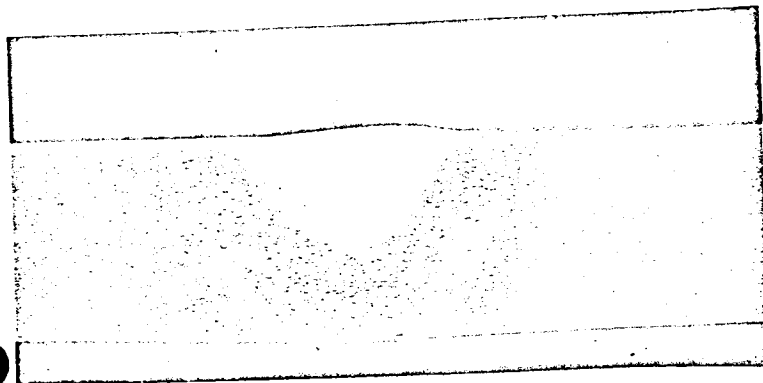
Backing Material:
Double Glass Tape



1ACB-16

Chilling: None
Backing Material:
None

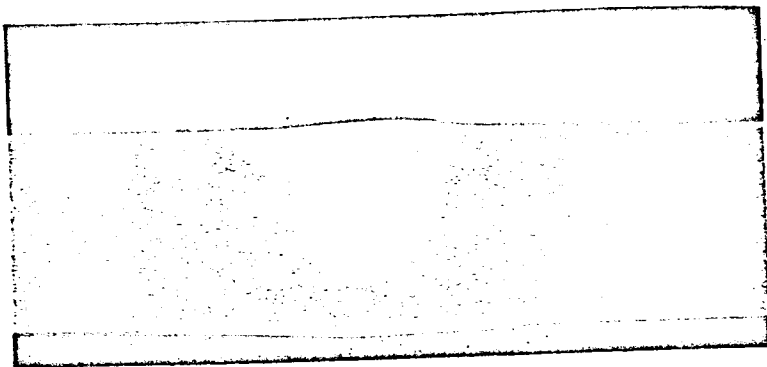
Figure 4. Efficiency of Glass Tape Backing Materials – Macrosections of Bead-on-Plate Welds in 5/16 INCH 2014-T6 Plate (3X)



1ACB-1

Chilling: Liquid CO₂
Jet System No. 1

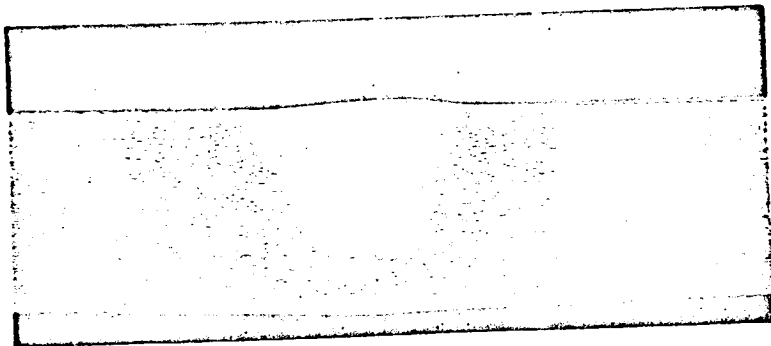
Backing Material:
None



1ACB-12

Chilling: Liquid CO₂
Jet System No. 1

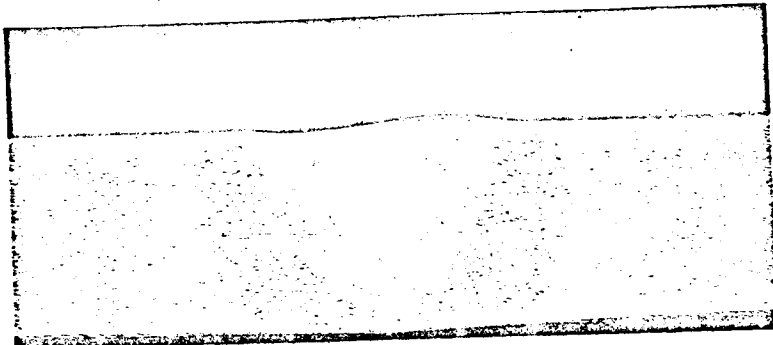
Backing Material:
Coarse Copper Mesh



1ACB-13

Chilling: Liquid CO₂
Jet System No. 1

Backing Material:
Fine Copper Screen



1ACB-16

Chilling: None
Backing Material:
None

Figure 6. Efficiency of Copper Mesh Backing Materials – Macrosections of Bead-on-Plate Welds in 5/16 INCH 2014-T6 Plate (3X)

THERMAL CYCLE CURVES FOR A TYPICAL
 SINGLE POINT ON THE WELD CENTERLINE
 DURING THE WELDING OPERATION

Time at Temperatures above 500F:

Unchilled: 42 sec.

CO₂ Chilled: 27 sec.

Quench Rate 750F to 500F:

Unchilled: 10F/sec.

CO₂ Chilled: 25F/sec.

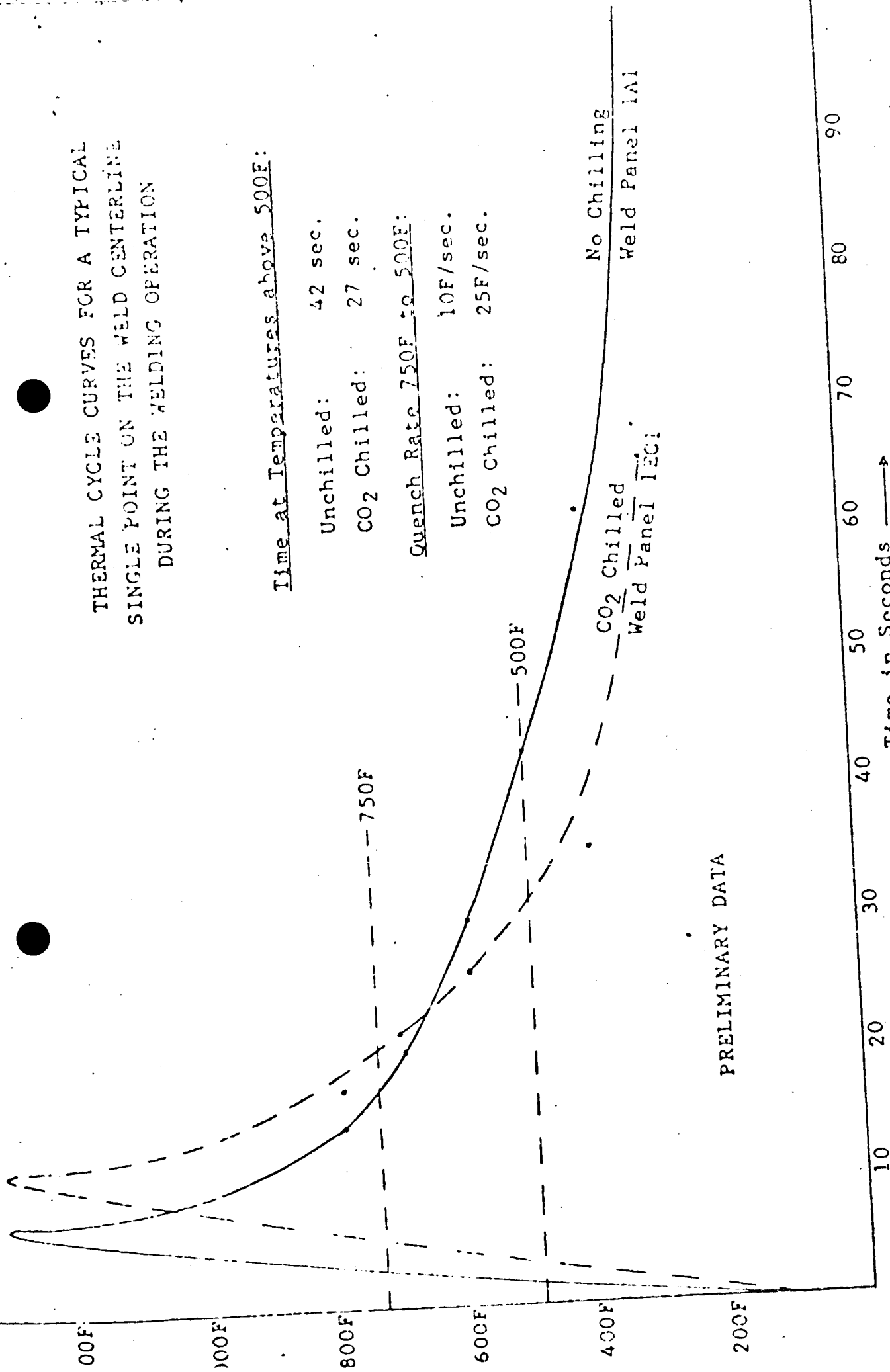


FIGURE 7 - EFFECT OF LIQUID CO₂ CHILLING ON TIME-TEMPERATURE CURVES DURING
 WELDING OF 5/16" 2014-T6 ALUMINUM PLATE CHILLED FROM THE BACK SIDE

WELDING OF 5/16" 2014-T6 ALUMINUM PLATE CHILLED FROM THE BACK SIDE

THERMAL CYCLE CURVES
 SINGLE POINT ON THE WELD CENTERLINE
 DURING THE WELDING OPERATION

Time at Temperatures above 500F:

Unchilled:	30 sec.
CO ₂ Chilled:	21 sec.

Quench Rate 750F to 500F:

Unchilled:	13.9F/sec.
CO ₂ Chilled:	26.4F/sec.

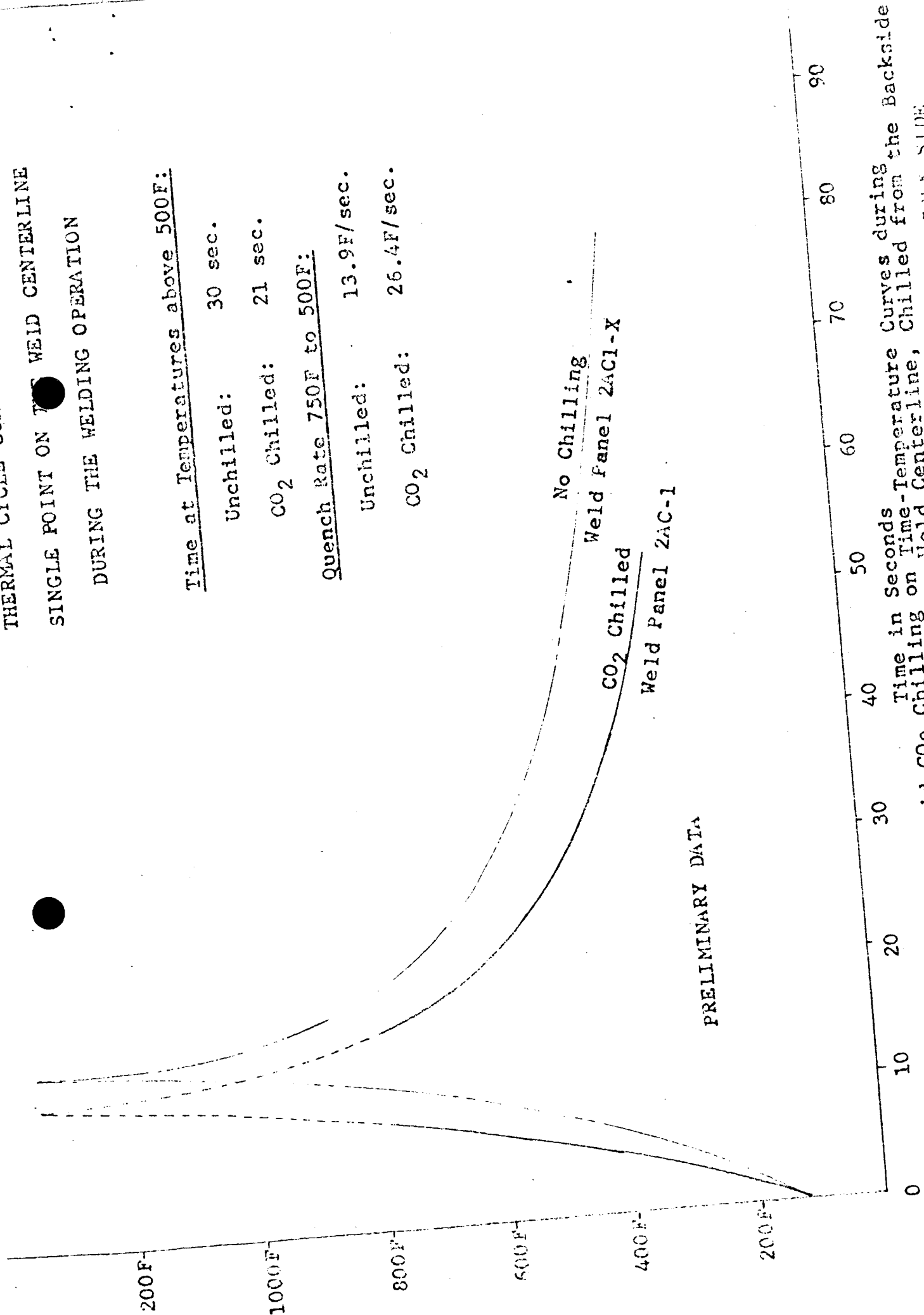


Figure 9. Effect of Liquid CO₂ Chilling on Time-Temperature Curves during the Backside Welding of 5/16" 2219-T87 Plate, Chilled from the Back Side

THERMAL CYCLE CURVES FOR A TYPICAL
SINGLE POINT ON THE WELD CENTERLINE
DURING THE WELDING OPERATION

Time at Temperatures above 500F:

Unchilled: 31 sec.

CO₂ Chilled: 21 sec.

Quench Rate 750F to 500F:

Unchilled: 14.0F/sec.

CO₂ Chilled: 20.8F/sec.

No Chilling

Weld Panel 2B2-20

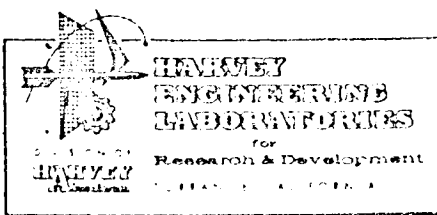
CO₂ Chilled

Weld Panel 2BC3-1

PRELIMINARY DATA

Time in Seconds →

FIGURE 10- EFFECT OF LIQUID CO₂ CHILLING ON TIME-TEMPERATURE CURVES DURING
WELDING OF 1/2" 2219-T87 PLATE, WELD CENTERLINE, CHILLED FROM THE BACK SIDE



Tensile Properties

Tensile specimens were prepared from comparable chilled and unchilled weld panels. A straight-sided tensile bar configuration was adequate as all failures occurred in the vicinity of the weld at values substantially below the strength of the unaffected parent metal. Welded specimens were naturally aged for a minimum of one week prior to testing. Principally "bead on" specimens were considered as this condition was selected as most applicable to current hardware. However, a few tests were also performed to evaluate the effect of chilling on the properties of the cast weld metal. "Bead on" specimens failed at the edge of the weld, while "bead off" specimens failed through the cast structure. Tables I and II show the results of these tests.

Porosity

Welded panels were examined for porosity by radiography and by fracture studies. Table III shows a summary of estimated average porosity for unchilled and chilled welds.

All welds contained some degree of porosity. Those made by one penetration pass without the addition of filler wire contained relatively small amounts of fine scattered porosity. Welds made with filler wire contained substantial amounts of gross porosity. Porosity in 2014-T6 weldments was essentially spherical while porosity in 2219-T87 weldments was principally of the cross type.

For these weldments chilling from the back side reduced the incidence and severity of porosity by a factor of more than two. Although porosity was above acceptable levels, the reduction effected by chilling is significant in that a trend is indicated.

Subsequent studies, performed to determine the effect of front side chilling of welds, indicated that the high level of porosity resulted from incomplete removal of surface oxides from the wire and weld area prior to welding. This was remedied by chemically re-cleaning both materials and scraping

Table I. Comparison of Tensile Properties of Unchilled Welds and Welds Chilled from the Back Side by Liquid CO₂ - 2219-T87 Plate.

Specimen	Test	Tensile Properties		
		Unchilled	Chilled	Improvement
5/16" - Bead-on	Yield (psi)	18,500	19,300	4.3%
	Ultimate (psi)	36,000	37,300	3.6%
	% Elong. in 2"	4.0	4.0	0
5/16" - Bead-off	Yield (psi)	17,000	19,000	11.8%
	Ultimate (psi)	37,100	38,300	3.2%
	% Elong. in 2"	6.0	4.0	---
1/2" - Bead-on	Yield (psi)	18,000	20,400	13.3%
	Ultimate (psi)	38,500	42,000	9.6%
	% Elong. in 2"	4.0	6.0	50 %
1/2" - Bead-off	Yield (psi)	17,600	18,800	6.8%
	Ultimate (psi)	36,300	38,000	4.7%
	% Elong. in 2"	4.0	5.0	25 %

Table II. Comparison of Tensile Properties of Unchilled Welds and Welds Chilled from the Back Side by Liquid CO₂ - 2014-T6 Plate.

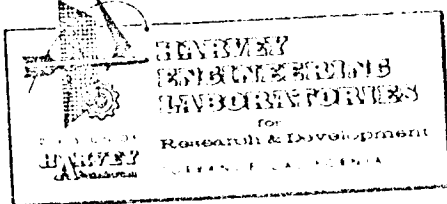
● Specimen	Test	Tensile Properties		
		Unchilled	Chilled	Improvement
5/16" - Bead on	Yield (psi)	27,900	30,300	8.6%
	Ultimate (psi)	42,100	45,500	8.1%
	Elong. in 2"	5.0	7.0	40.0%
5/16" - Bead off	Yield (psi)	26,600	29,800	12.0%
	Ultimate (psi)	36,700	45,000	18.5%
	Elong. in 2"	3.0	6.0	100 %
1/2" - Bead on	Yield (psi)	27,500	31,500	14.5%
	Ultimate (psi)	45,300	47,600	5.8%
	Elong. in 2"	5.5	6.0	9.1%
* 1/2" - Bead off	Yield (psi)	26,800	30,600	14.2%
	Ultimate (psi)	43,200	43,000	---
	Elong. in 2"	4.0	4.0	0%

* Test specimens could not be machined flush due to excessive peaking, therefore, hand grinding was used.

Table III. Effect of Back Side Chilling
on Weld Porosity.

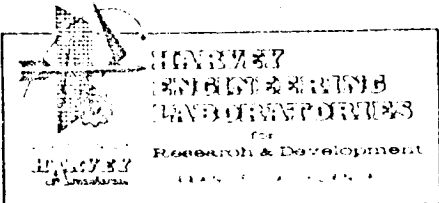
Weldment Material	Test	Unchilled	Back Side Chilled
5/16" 2219-T87	X-ray ⁽¹⁾ % x section ⁽²⁾	D#3 LC 5	D#1 LC 2 1/2
1/2" 2219-T87	X-ray ⁽¹⁾ % x section ⁽²⁾	D#2 LC 2	D#1 LC 1
5/16" 2014-T6	X-ray ⁽¹⁾ % x section ⁽²⁾	G#3 SI 2	G#1 SI 1
1/2" 2014T6	X-ray ⁽¹⁾ % x section ⁽²⁾	G#3 LC 1	G#1 SI 1/2

- (1) NAVORD OD 7574 - X-ray standards for shielded arc welds in aluminum.
- (2) Estimated percent of cross sectional area of fractured specimens.
- (3) D = dross, G = gas, S = scattered, I = intermittent
L = lineal, C = continuous.



HA NO 2283 PAGE IV.07

the surfaces of the plate in the weld area instead of wire brushing. However, work on chilling from the back side has been discontinued, so that it was not evaluated using the new pre-weld cleaning procedures.



D. CHILLING FROM THE FRONT SIDE OF THE WELDMENT

SUMMARY

Devices were fabricated for impingement of liquid CO₂ on the front side of the weld, and for protecting the arc and weld puddle from CO₂ leakage. A number of jet systems and shields with a variety of seals were used to weld a series of panels to determine the effect of front side chilling on tensile properties and porosity. Improvements in tensile yield strength up to 20.3% were obtained, and a significant reduction in the incidence and severity of porosity was noted. Chilling from the front side decreased warpage markedly, and it is indicated that the concept can be applied to reduce warpage and alleviate residual stresses in production parts.

PROCEDURE AND RESULTS:

Jet Systems and Shields

Two concepts for applying chilling to the front side were investigated. The first concept employed fixed shields to prevent CO₂ from leaking into the arc and the second employed traveling shields for this purpose. For both concepts the jet systems moved with the welding torch along the weld seam.

The fixed shield system is depicted in the sketch shown in Figure 11. The aluminum foil seal used in this system did not provide a sufficient degree of uniformity of heat transfer for adequate chilling. Arc disturbances resulting from drafts created by the "chimney effect" also presented a problem; therefore, this concept was abandoned in favor of the traveling shield concept.

The traveling shield concept appeared to offer promise for effecting the required chilling, but leakage of CO₂ into the arc area presented a serious problem. A number of variations of the basic concept were fabricated using several means of effecting a seal between the shield structure and the aluminum plate. These variations are shown in Appendix IV, and a sketch of the shield utilized for the major portion of the fabrication of welded test panels is shown in Figure 12. This shield was

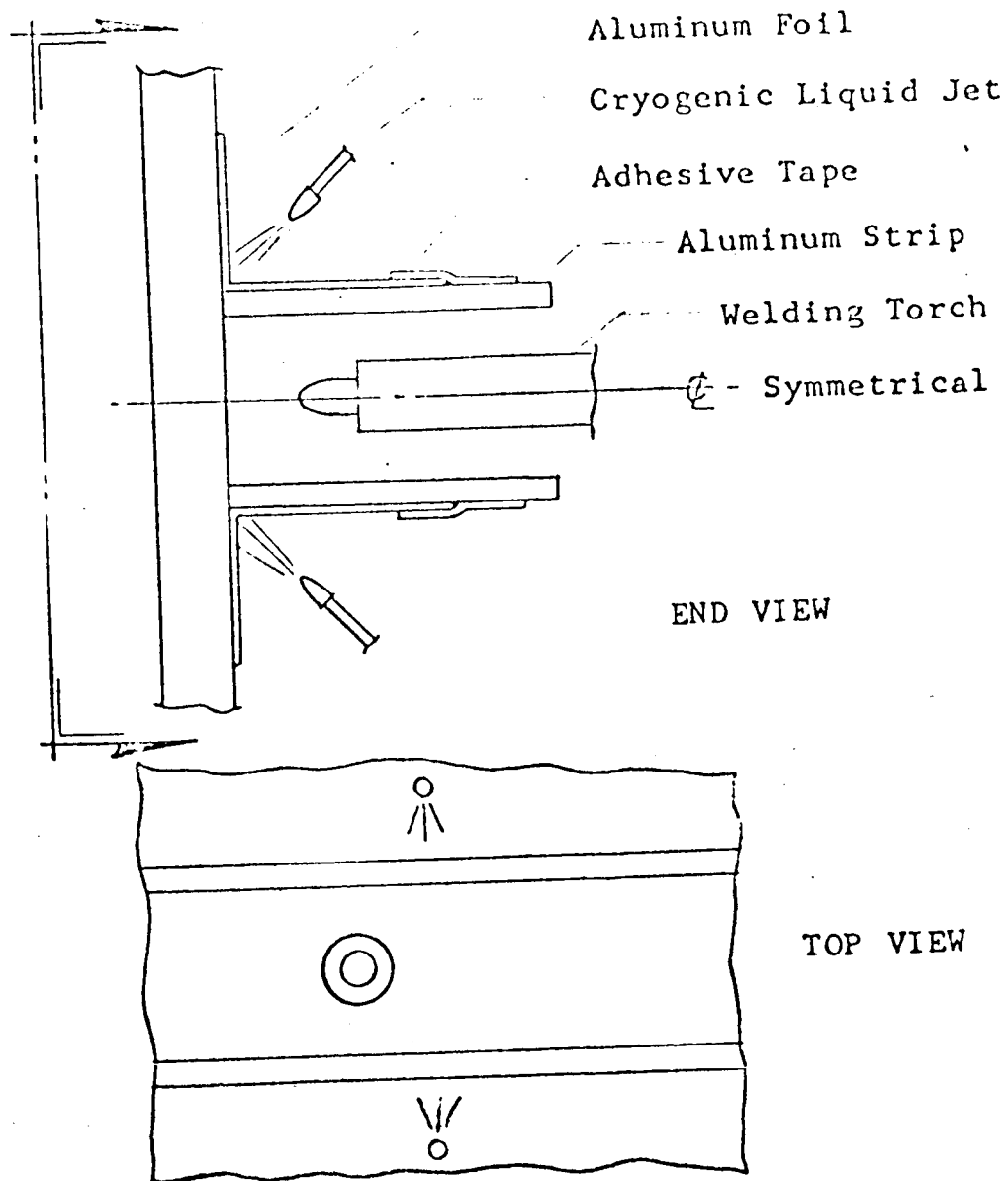


Figure 11. Jet System No. 1 for Front Side Chilling of Weldments using a Cryogenic Liquid — Stationary Shield with Metal Foil Seal

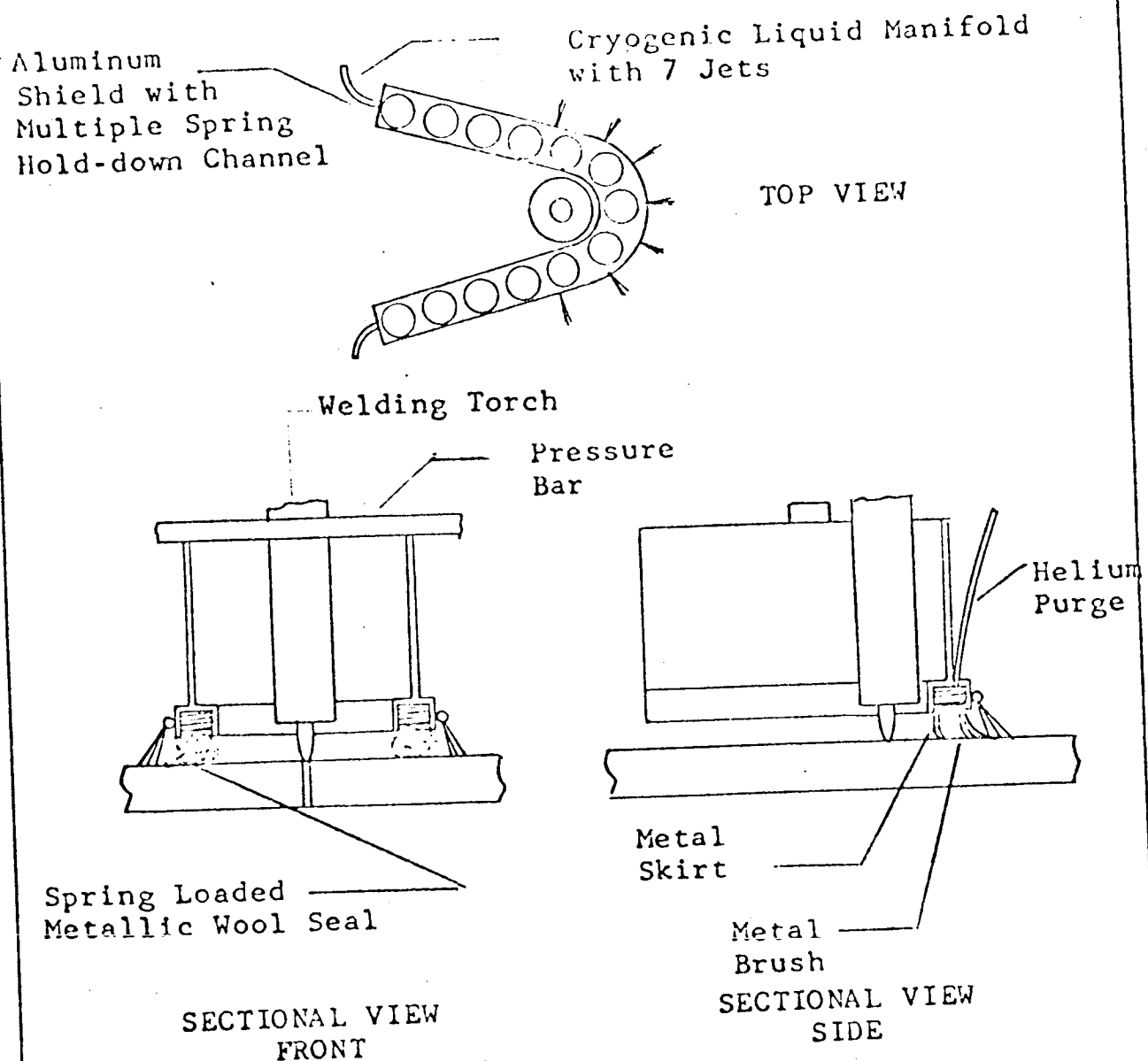
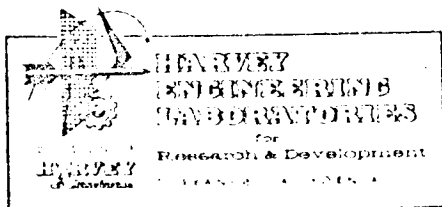


Figure 12. Jet System No. 14 for Front Side Chilling using a Cryogenic Liquid--Traveling Shield with Spring Loaded Metallic Wool and Wire Brush Seal, Helium Purged with Metallic Skirt-7 Jet Manifold



further modified by altering the liquid CO₂ manifold to increase the number and sizes of orifices as well as their position relative to the torch to effect various chilling patterns. In the jet systems used for fabricating panels for mechanical testing, liquid CO₂ was delivered to the weld area at rates varying from 1 to 2 1/2 pounds per inch of weld by arrangements of 12 to 14 jet orifices of varying sizes in the manifold.

These jet systems produced drastic cooling of the weldment, and the shield was reliable enough to permit welding of the required panels. However, combinations of severe irregularities on the weld seam (undercut or highcrown) with variations in fit-up of the shield to the plate made the shield subject to leaks. Such leaks caused arc disturbances and weld contamination, resulting in considerable scrap loss. Sufficient time was not available to rectify these shield deficiencies by redesigning the shield to incorporate a special fine wire brush to compliment or replace the stainless steel wool. Such a shield would not only increase reliability, but could be adapted for warpage control jet systems.

Fabrication of Welded Panels

Unchilled and chilled weld panels were fabricated to determine the effect of chilling on porosity and tensile properties. Identical pre-weld procedures were used for preparing panels to be compared. During the first part of these tests all panels were chemically cleaned followed by draw filing of the faying surface of the butting edges and wire brushing the top and bottom surfaces in the area to be welded. Typical welding parameters are shown in Tables 4 and 5. Welds made in this manner contained a considerable amount of dross. Therefore, wire brushing was replaced by scraping of the top and bottom surfaces. In order to further insure uniform processing of chilled and unchilled weldments, both weldments were made on the same panel; i.e., the first half of the panel was welded with chilling and the remainder was welded without chilling. Thermal cycle temperature measurements were taken for a point 3/8-in. from the weld centerline for all weldments. In some cases temperature measurements were made for additional locations.

TABLE IV.

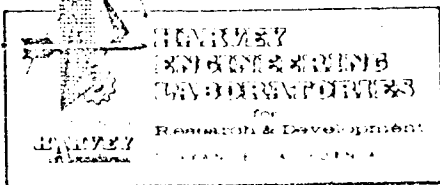
TYPICAL WELDING PARAMETERS - UNCHILLED PANELS

WELD PANEL DESCRIPTION						PENETRATION PASS			FILLER PASS			
Alloy	Thick- ness	Panel No.	No. of Passes	Chill- ing	Amps.	Volts	Carriage Speed	Wire Speed	Amps.	Volts	Carriage Speed	Wire Speed
2014-T6	5/16"	1AUN6161A	Two	None	215	10.5	7.0	None	215	10.5	16.5	80
2014-T6	5/16"	1AUN6161B	One	None	215	10.5	6.4	80	-	-	-	-
2014-T6	5/16"	1AUN6173	One	None	220	11.0	7.7	80	-	-	-	-
2219-T87	5/16"	2AUN6172A	One	None	215	11.5	9.3	80	-	-	-	-
2219-T87	5/16"	2AUN6172B	One	None	215	11.5	10.1	80	-	-	-	-
2219-T87	5/16"	2AUN6201	One	None	215	11.5	10.1	80	-	-	-	-
2014-T6	1/2"	1BUN6131	Two	None	325	11.0	7.1	None	300	11.3	18.5	120
2014-T6	1/2"	1BUN6151	Two	None	325	11.0	7.1	None	310	10.5	17.5	120
2219-T87	1/2"	2BUN6151	Two	None	320	11.5	7.6	None	295	12.0	17.5	120

TABLE V.
WELDING PARAMETERS - PANELS CHILLED FROM THE FRONT SIDE

FILLER PASS

WELDING PASSES												
WELD PANEL DESCRIPTION					PENETRATION PASS							
Alloy	Thick- ness	Panel No.	No. of Passes	Chill- ing	Amps.	Carriage		Wire Speed	Amps.	Volts	Carriage Speed	Wire Speed
						Volts	Speed					
2014-T6	5/16"	1ACFW6212	One	#10	220	11.0	7.0	80	-	-	-	-
2014-T6	5/16"	1ACFW6221	One	#10	200	11.0	7.0	80	-	-	-	-
2014-T6	5/16"	1ACFW6294	One	#10	220	11.0	7.0	80	-	-	-	-
2014-T6	5/16"	1ACFW713	One	#14	225	11.0	7.0	80	-	-	-	-
									-	-	-	-
									-	-	-	-
									-	-	-	-
									-	-	-	-
2219-T87	5/16"	2ACFW6211	One	#10	210	12.0	9.6	98	-	-	-	-
2219-T87	5/16"	2ACFW6291	One	#14	215	12.0	9.8	98	-	-	-	-
2219-T87	5/16"	2ACFW6292	One	#14	215	11.5	9.6	98	-	-	-	-
2219-T87	5/16"	2ACFW711	One	#14	220	12.5	9.6	98	-	-	-	-
2219-T87	5/16"	2ACFW712	One	#14	215	12.5	9.6	98	-	-	-	-
									-	-	-	-
2014-T6	1/2"	1BCFW6101	Two	#9	335	11.0	7.4	-	300	11.5	16.2	120
2014-T6	1/2"	1BCFW6213	Two	#10	335	11.0	7.4	-	300	11.5	16.2	120
2014-T6	1/2"	1BCFW752	Two	#14	340	10.5	7.0	-	310	12.0	16.2	120
2014-T6	1/2"	1BCFW761	Two	#14	325	11.5	7.0	-	300	12.0	16.2	120
									-	-	-	-
2219-T87	1/2"	2BCFW751	Two	#14	325	11.5	7.4	-	300	12.5	16.2	120



Thermal Cycle Curves

Typical thermal cycle curves for weldments made during the development of the shielding device are shown in Appendix IV. Figures 13 through 16 are examples of these thermal cycle curves for points at 3/8-inch and 3/4-inch from the weld centerline on weldments in each material and thickness, comparing unchilled welds with welds chilled by use of Jet System No. 14. Figures 17 through 22 show typical curves for similar series of welds made to determine the effect of other jet systems. Each jet system produced varying degrees of change in the curve with respect to the curve for a comparable unchilled weld. Peak temperatures as well as time at temperature varied with the jet system used and the plate material being welded. A complex relationship exists between the variables which affect heat input and heat extraction as related to the resultant thermal cycle curve. It will be noted from the results of tensile tests, the optimum jet system is not the same for all properties in all materials and thicknesses. Considerably more work would be required to select a specific system to accomplish a given improvement in a given weldment. However, the following curves illustrate that such an accomplishment is possible.

Macrosections

Macrosections were prepared to show changes effected by chilling.

Figures 23 and 24 show the reduction in the extent of the heat-affected zone of bead on plate welds chilled from the front side by one of the earlier traveling shield jet systems.

Figures 25 through 32 show comparisons of macrosections of unchilled welds and welds in each material and thickness chilled from the front side by various jet systems.

In most cases the macrosections show that chilling reduces the extent of the heat-affected zone, and reduces the grain size of the cast structure. The macrosections also show that the degree of chilling effect is different for each jet system, with Jet System No. 23 providing the greatest amount of chilling in most cases.

TYPICAL THERMAL CYCLE CURVES FOR TWO LOCATIONS ON
12 x 48 INCH WELDMENTS - PENETRATION PASS

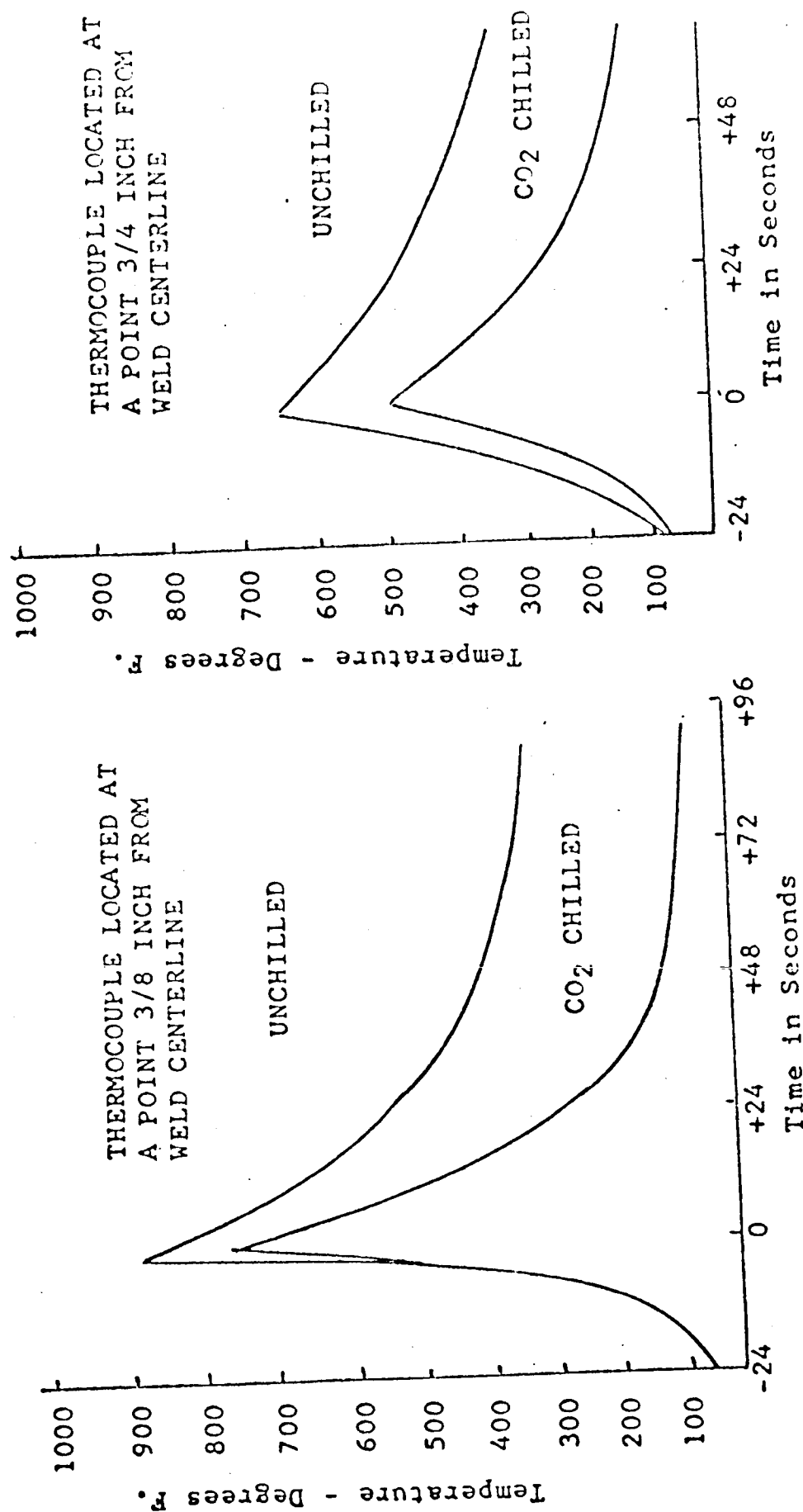


Figure 13. Effect of Front Side Chilling on Thermal Cycle Curves, Jet System No. 14, Butt Welds in 1/2-inch 2219-T87 Plate.

TYPICAL THERMAL CYCLE CURVES FOR TWO LOCATIONS ON 12 x 48 INCH WELDMENTS

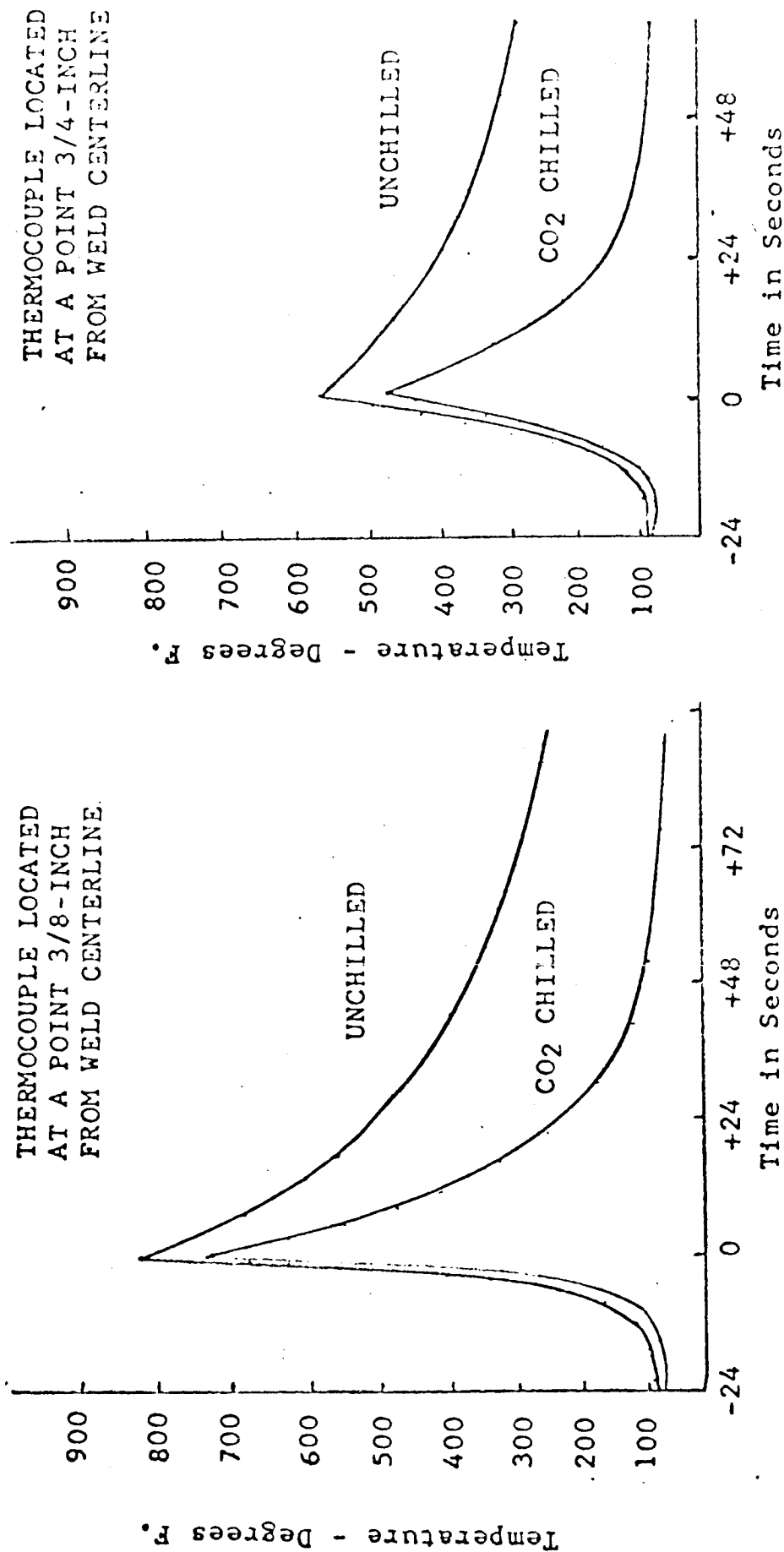


Figure 4. Effect of Front Side Chilling on Thermal Cycle Curves, Jet System No. 14, Butt Welds in 5/16-inch 2219-T87 Plate

TYPICAL THERMAL CYCLE CURVES FOR TWO LOCATIONS ON
12 x 48-INCH WELDMENTS - PENETRATION PASS

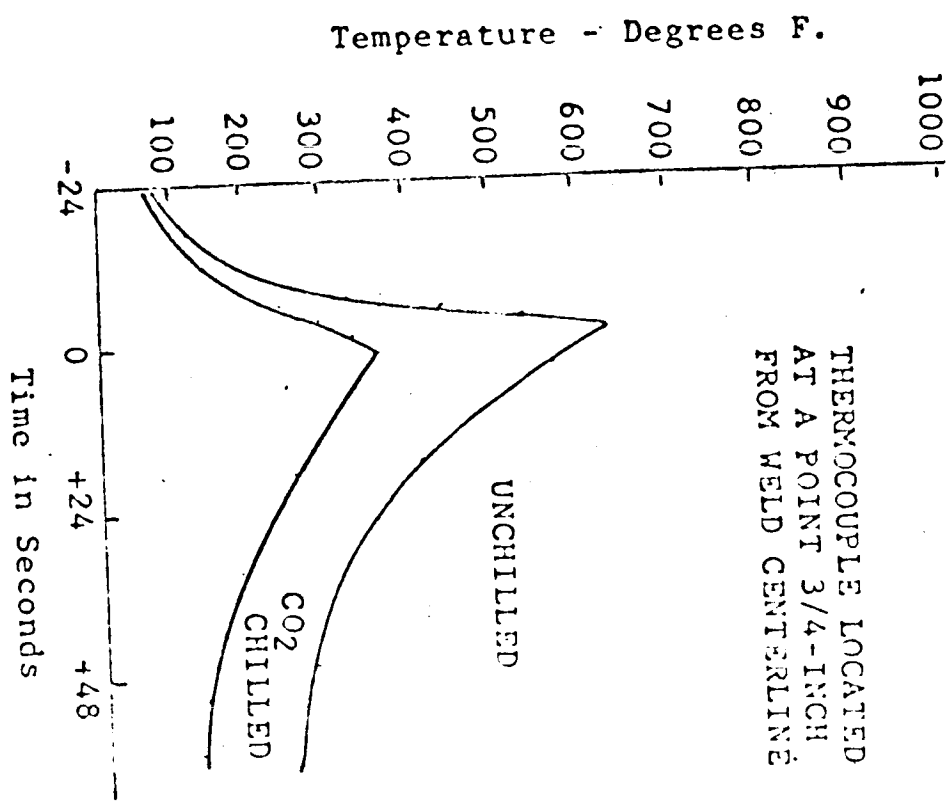
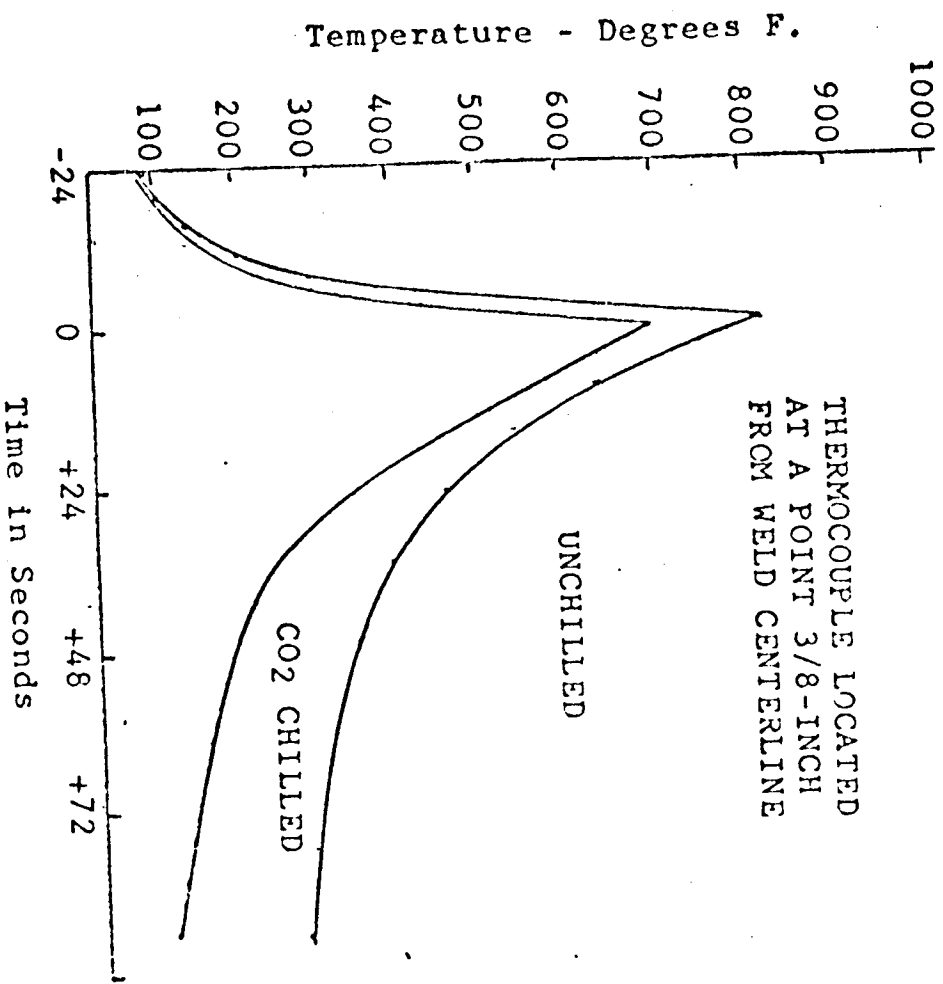


Figure 15. Effect of Front Side Chilling on Thermal Cycle Curves, Jet System No. 14, Butt Welds in 1/2-Inch 2014-T6 Plate.

TYPICAL THERMAL CYCLE CURVES FOR TWO LOCATIONS ON 12 x 48-INCH WELDMENTS

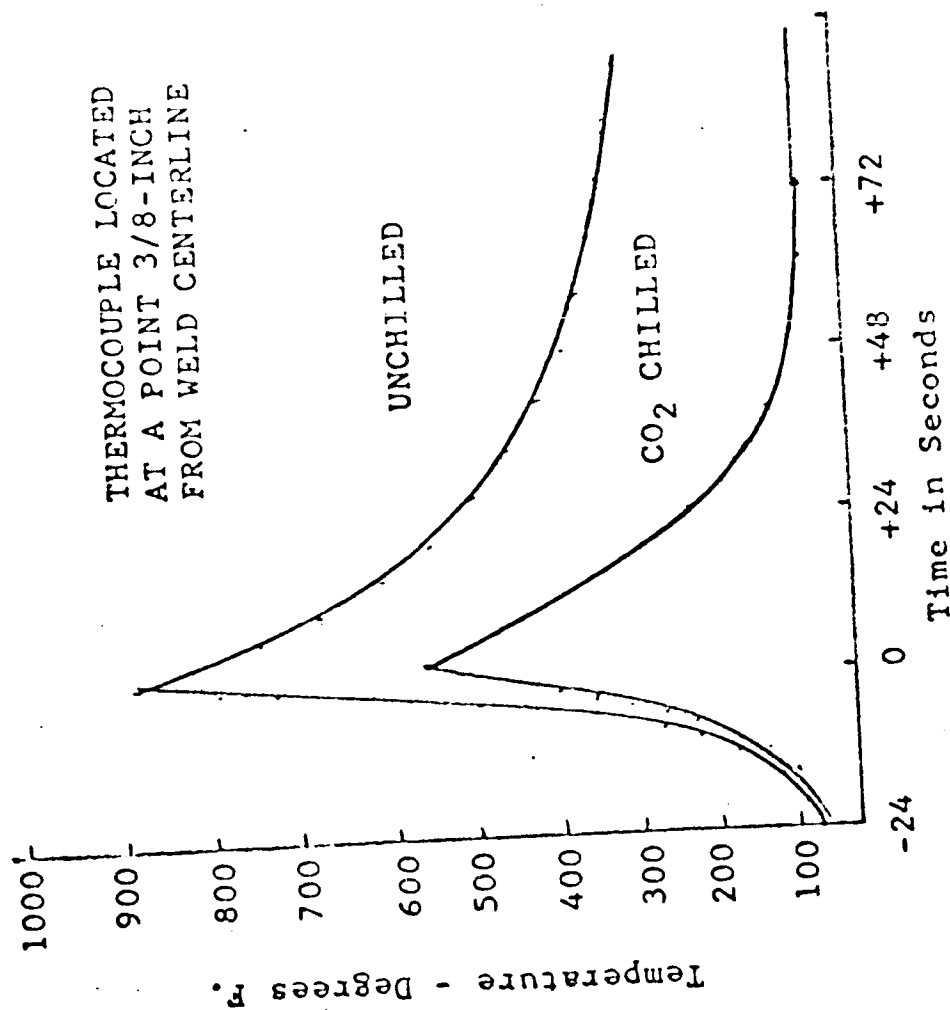
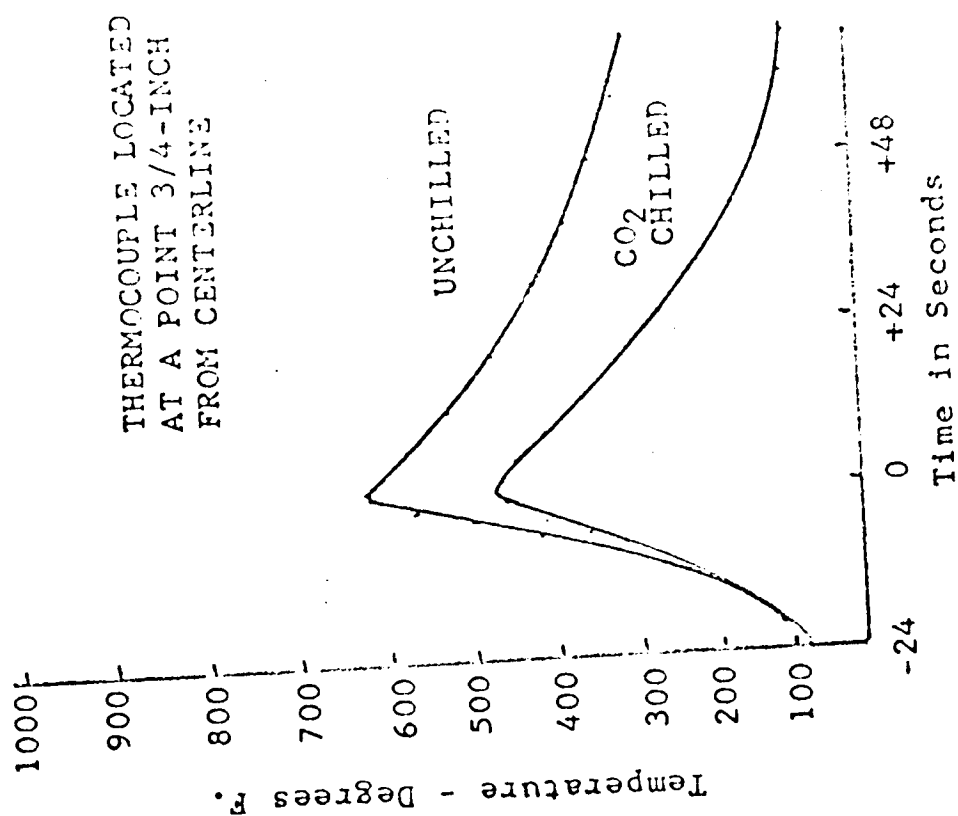


Figure 16. Effect of Front Side Chilling on Thermal Cycle Curves, Jet System No. 14,
 Butt Welds in 5/16-inch 2014-T6 Plate

TYPICAL THERMAL CYCLE CURVES FOR POINTS 3/8" FROM WELD CENTERLINE

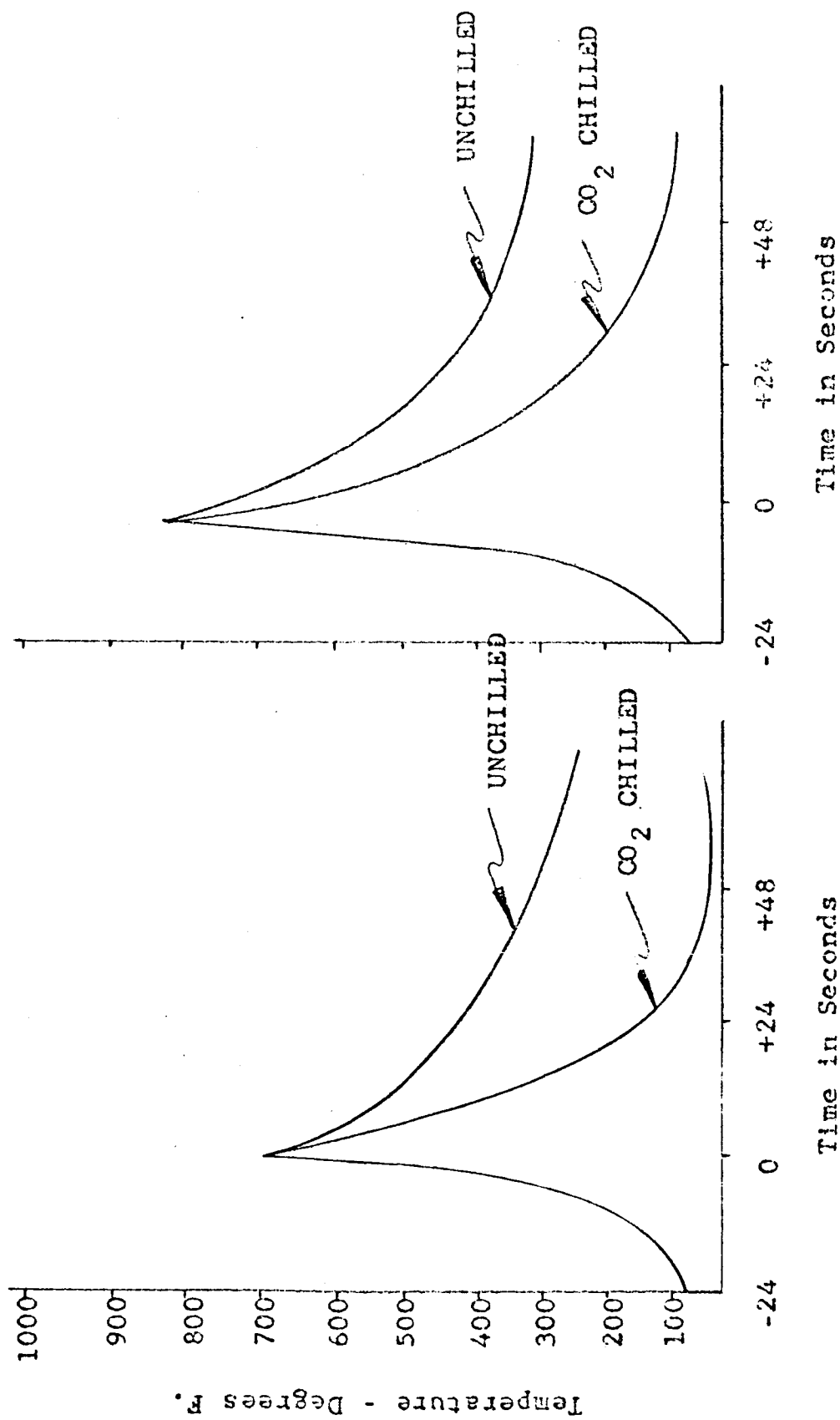


Figure 17. Effect of Front Side Chilling on Thermal Cycle Curves, Jet System No. 18, Butt Welds in 5/16" and 1/2" 2014-T6 Plate

TYPICAL THERMAL CYCLE CURVES FOR POINTS 3/8" FROM WELD CENTERLINE

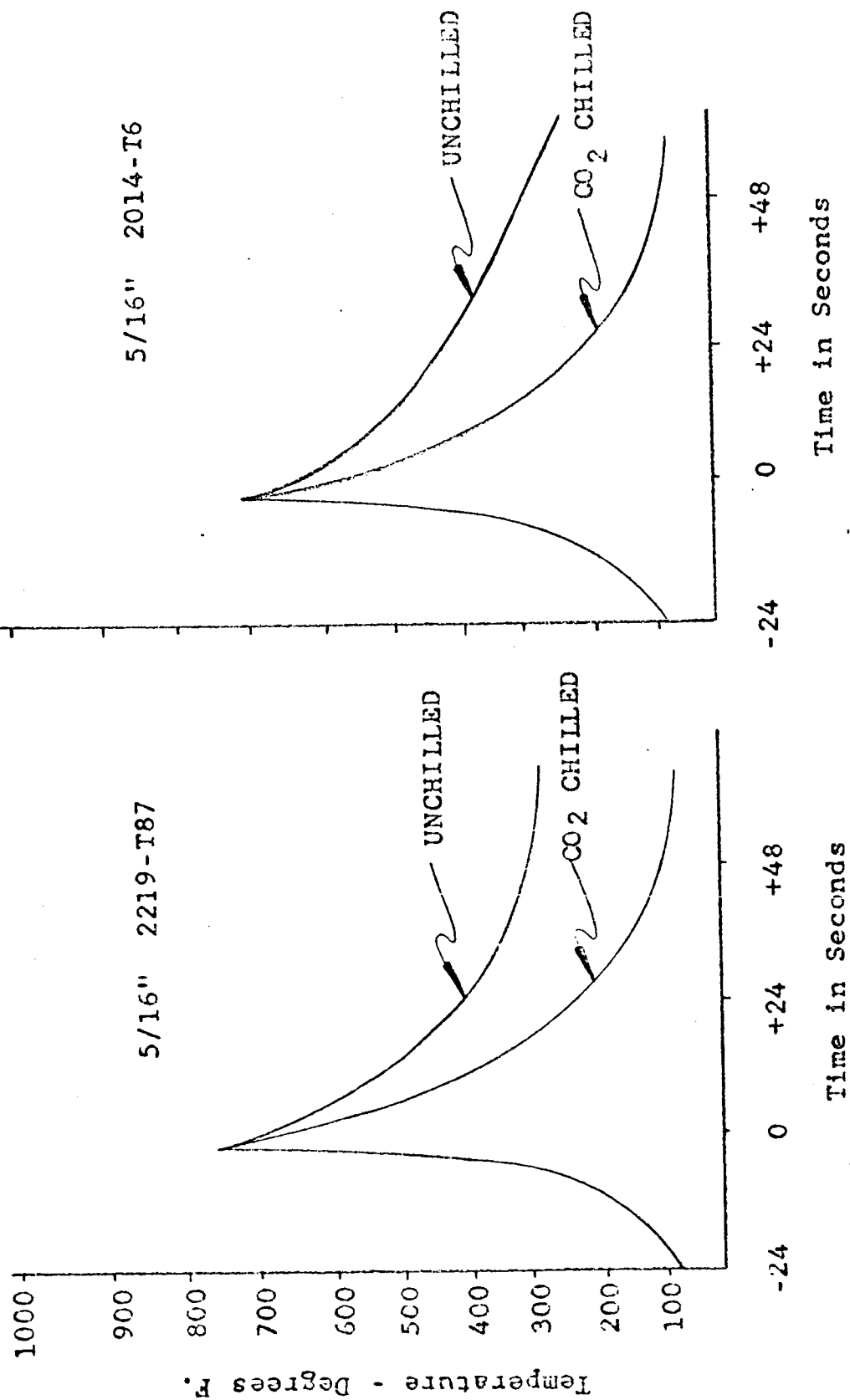


Figure 18. Effect of Front Side Chilling on Thermal Cycle Curves, Jet System No. 19, Butt Welds in 5/16" 2219-T87 and 2014-T6 Plate

TYPICAL THERMAL CYCLE CURVES FOR POINTS 3/8" FROM WELD CENTERLINE

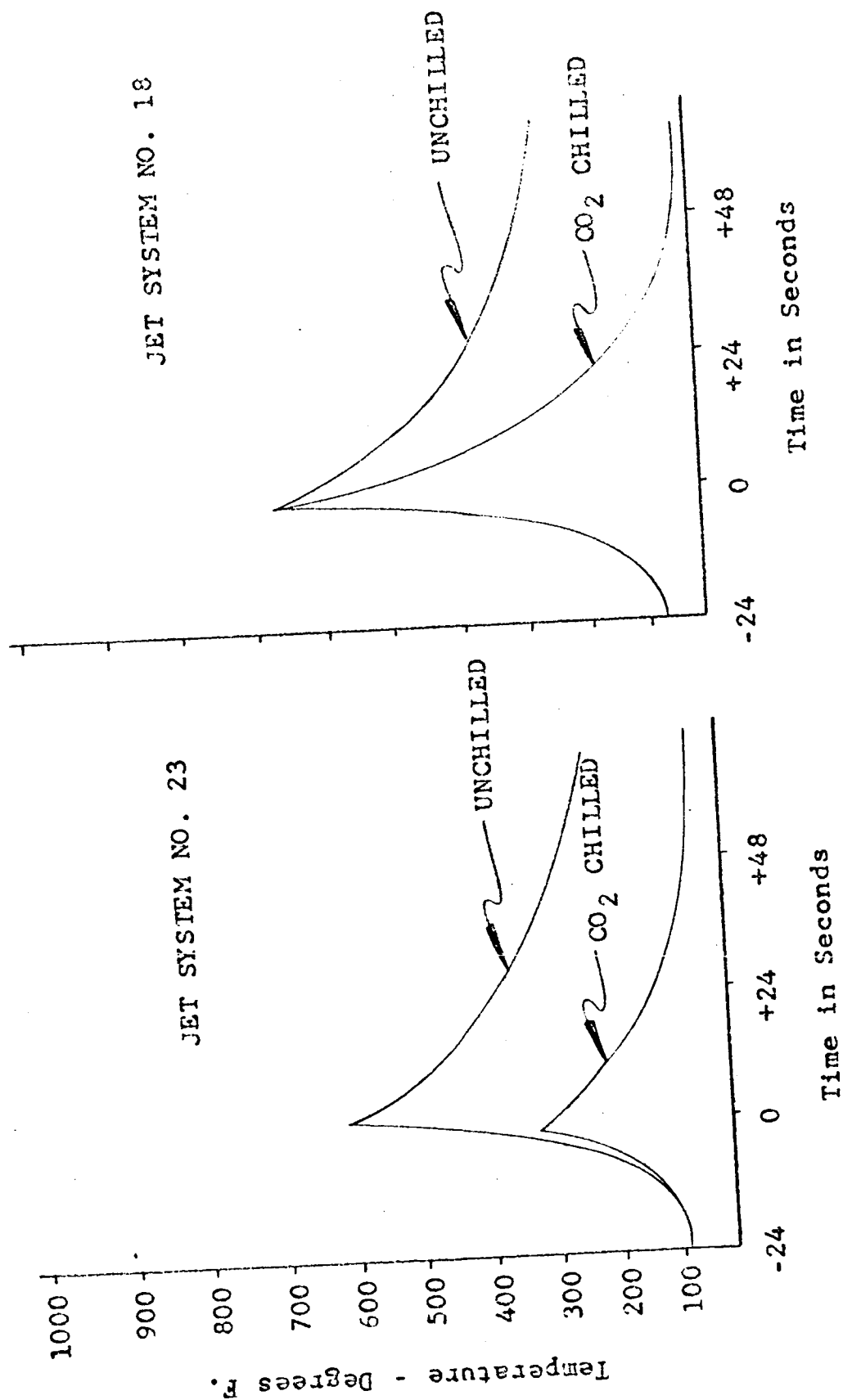


Figure 19. Effect of Front Side Chilling on Thermal Cycle Curves for Butt Welds in 5/16" 2014-T6 Plate

TYPICAL THERMAL CYCLE CURVES FOR POINTS 3/8" FROM WELD CENTERLINE

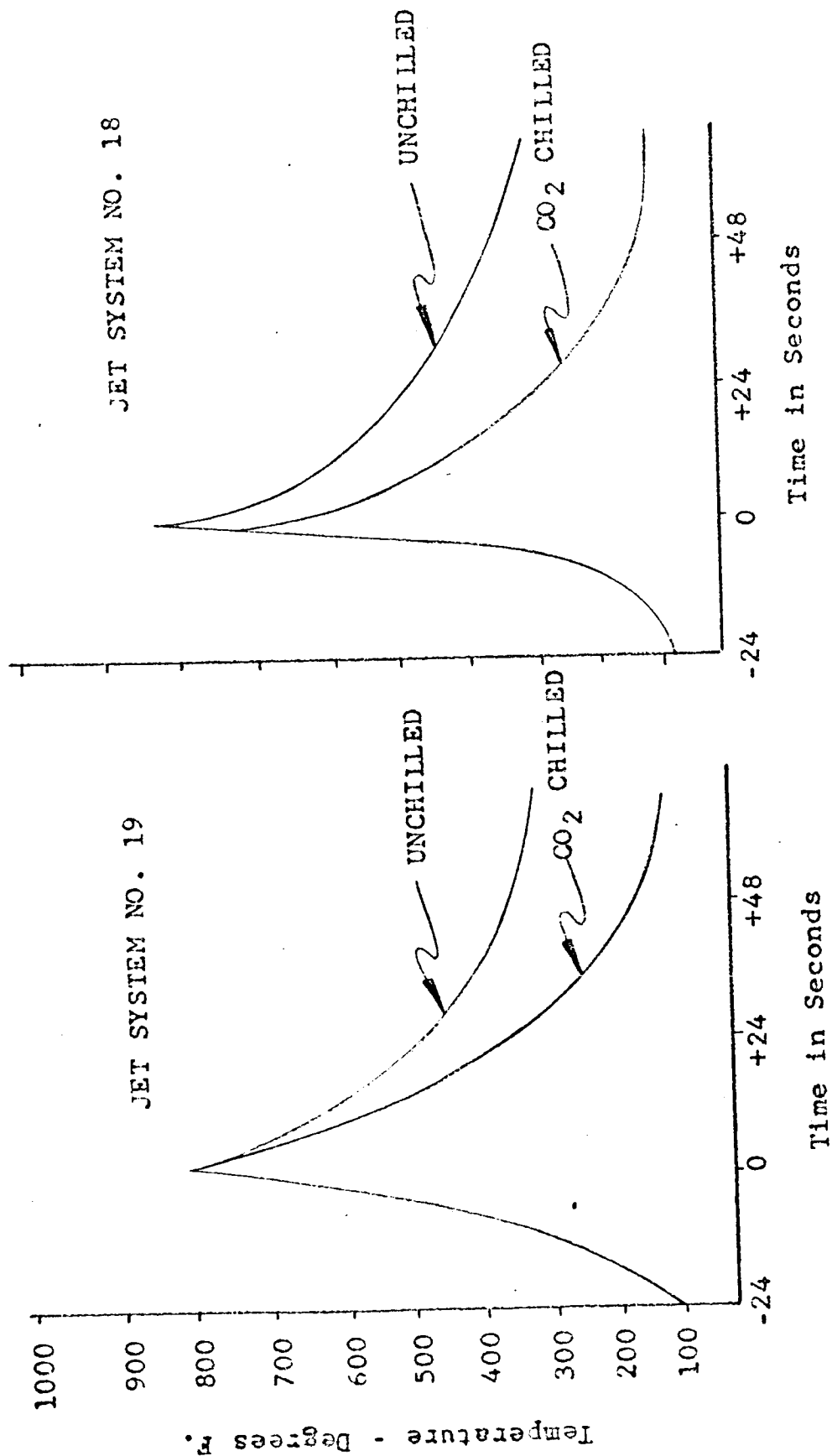


Figure 20. Effect of Front Side Chilling on Thermal Cycle Curves for Butt Welds in 1/2" 2014-T6 Plate

TYPICAL THERMAL CYCLE CURVES FOR POINTS 3/8" FROM WELD CENTERLINE

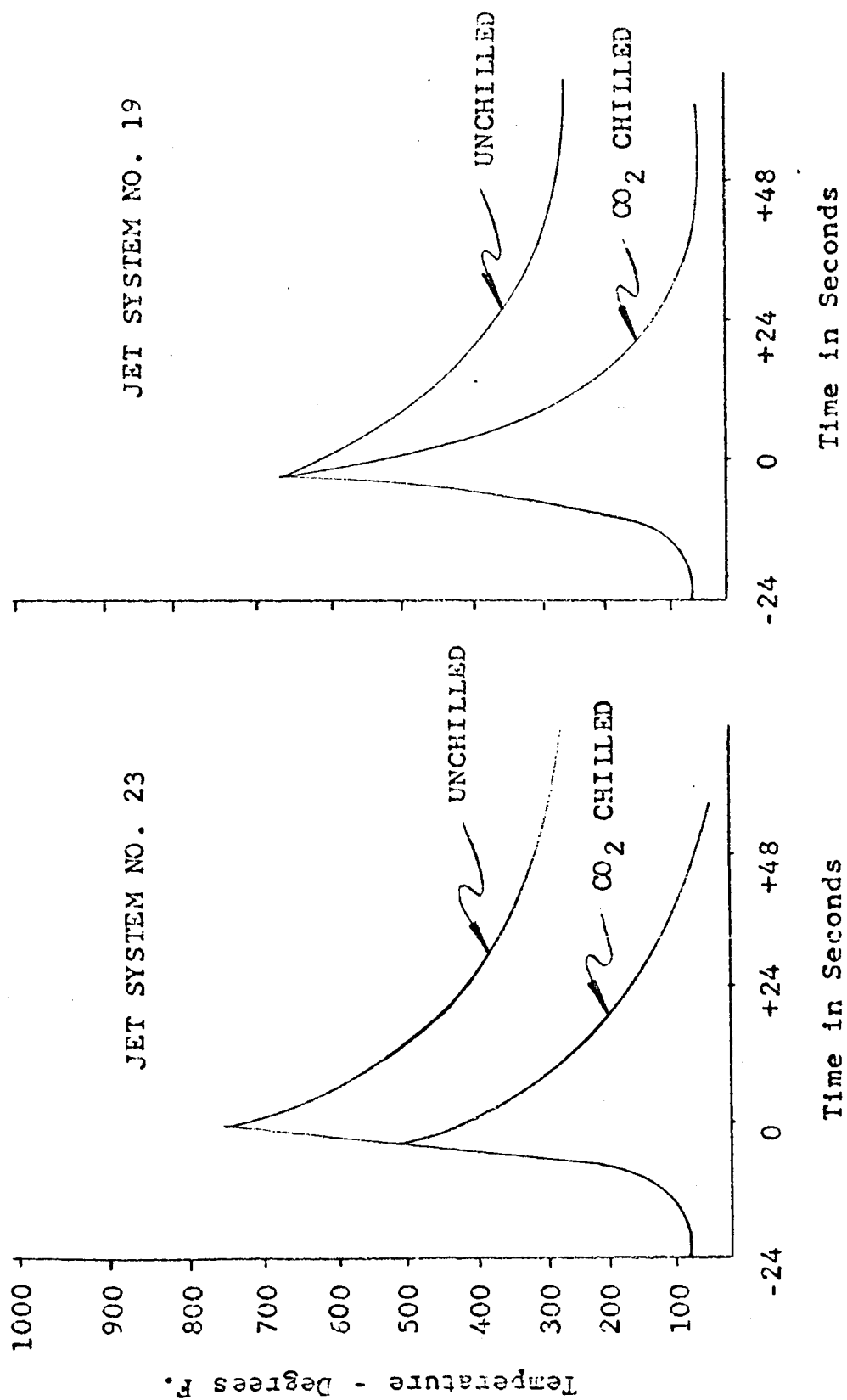


Figure 21. Effect of Front Side Chilling on Thermal Cycle Curves for Butt Welds in 5/16" 2219-T87 Plate

TYPICAL THERMAL CYCLE CURVES FOR POINTS 3/8" FROM WELD CENTERLINE

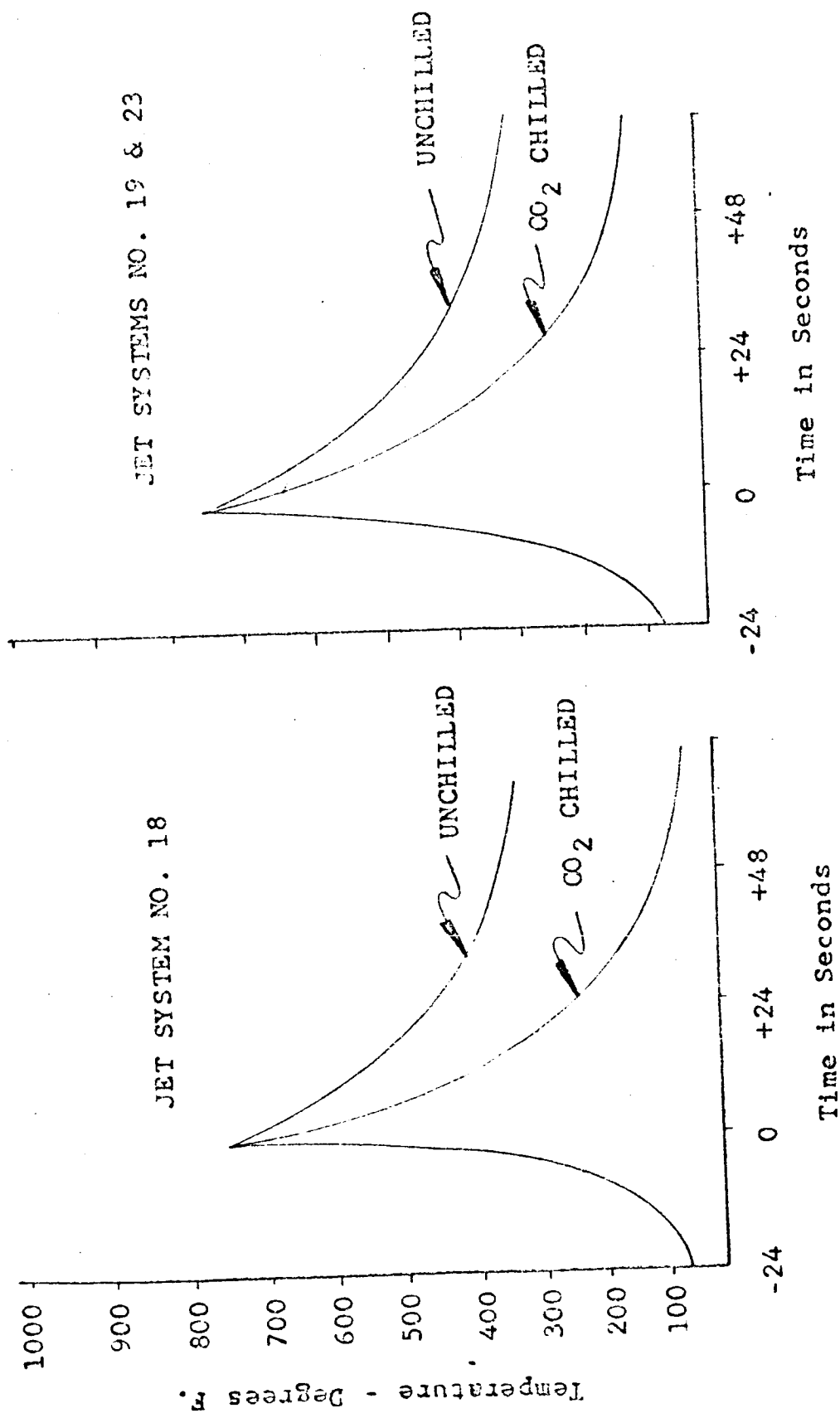
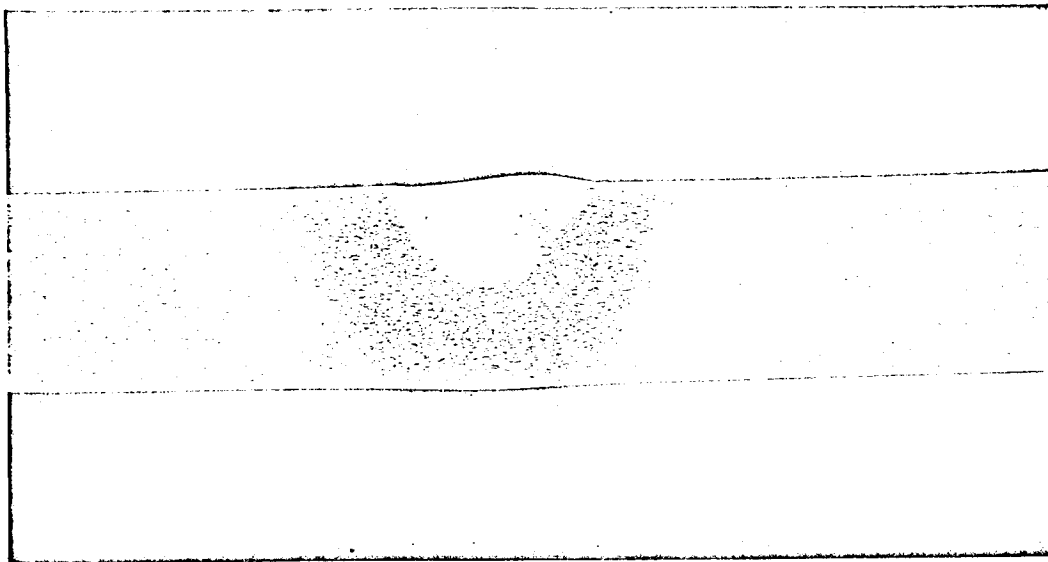
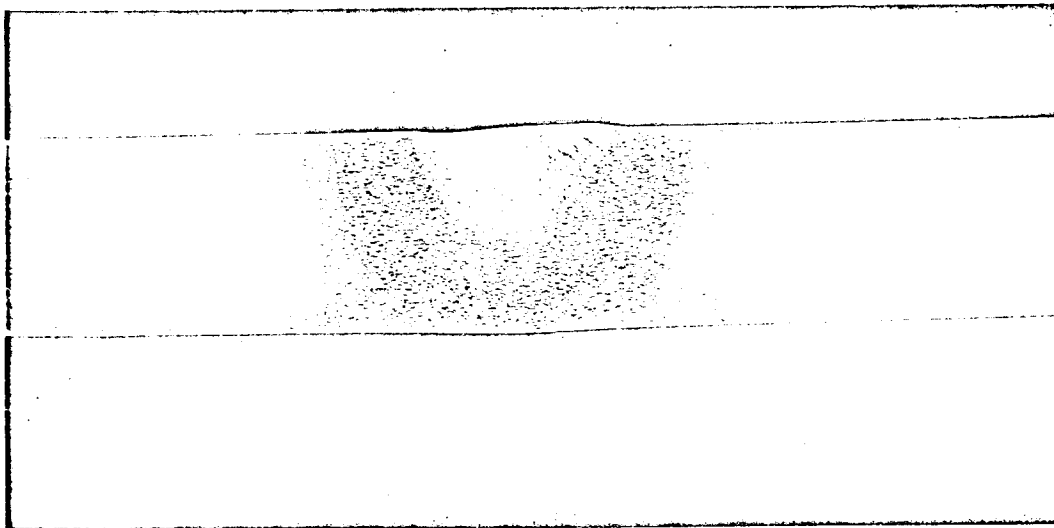


Figure 22. Effect of Front Side Chilling on Thermal Cycle Curves for Butt Welds in 1/2" 2219-T87 Plate

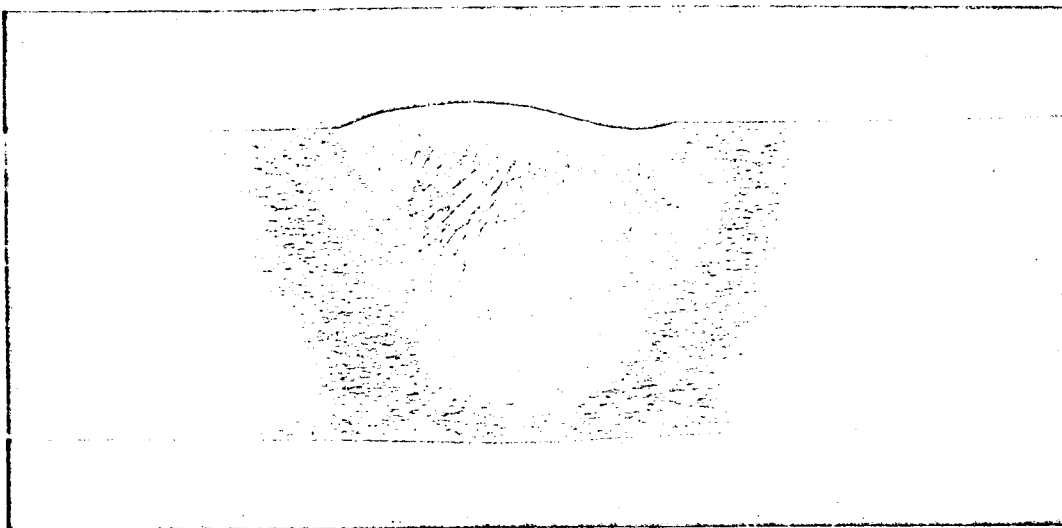


Liquid CO₂ Chilled Weld – Jet Arrangement No. 8

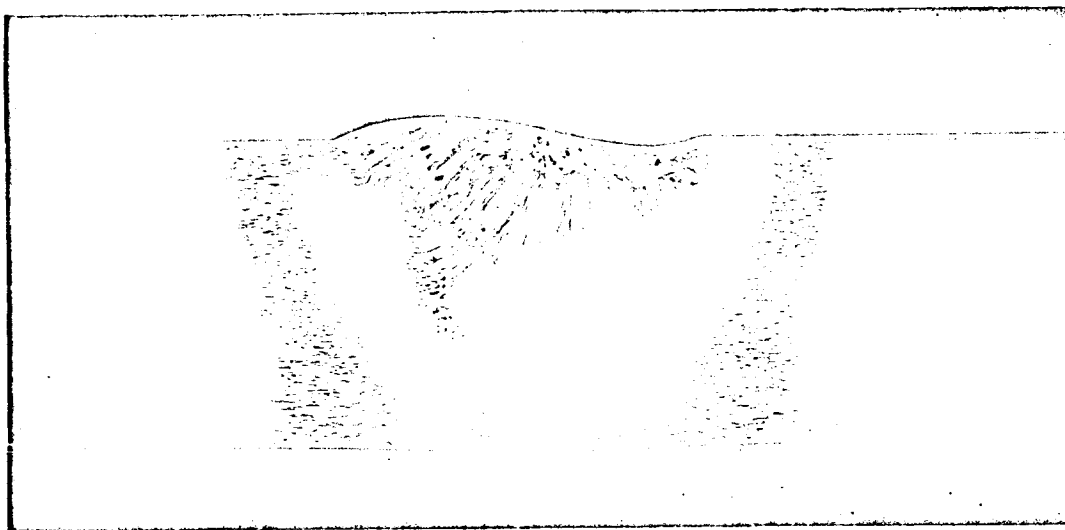


Unchilled Weld

Figure 23.



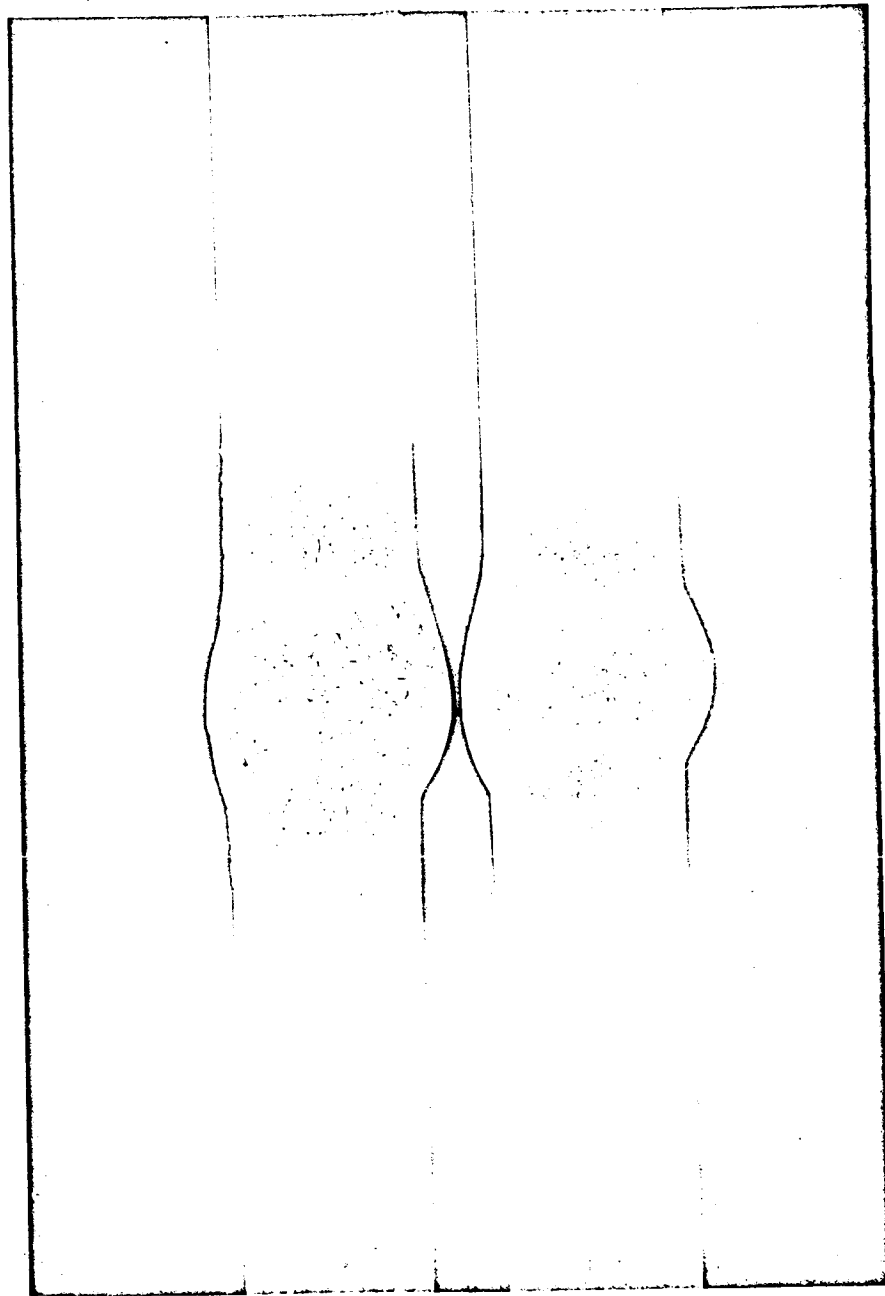
Liquid CO₂ Chilled Weld – Jet Arrangement No. 8



Unchilled Weld

Figure 24.

Macrosection Showing the Effect of Liquid CO₂ Chilling from the Front Side of Bead
on Plate Welds in 1/2-inch 2014-T6 Aluminum Made With Constant Heat Input

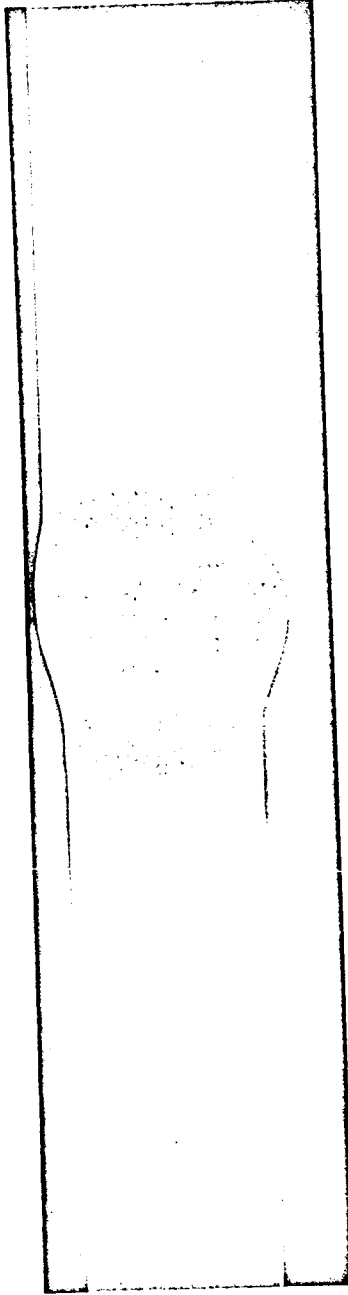


Unchilled
2AUW8182

CO₂ Chilled
2ACFW8181

Figure 25. Macrosections Showing Effect of Front Side Chilling of Welds
in 5/16-in. 2219-T81 - Jet System No. 23

Unchilled,
2AUW8232



CO₂ Chilled
2ACFW8231

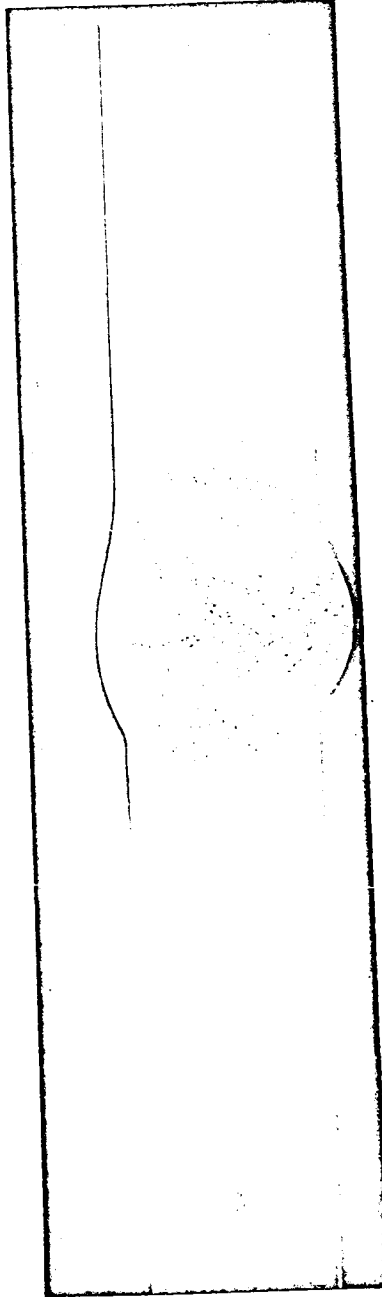
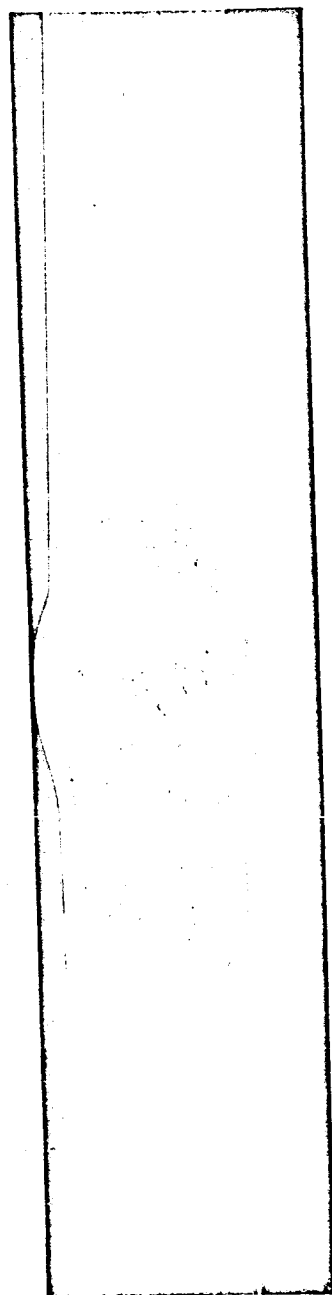
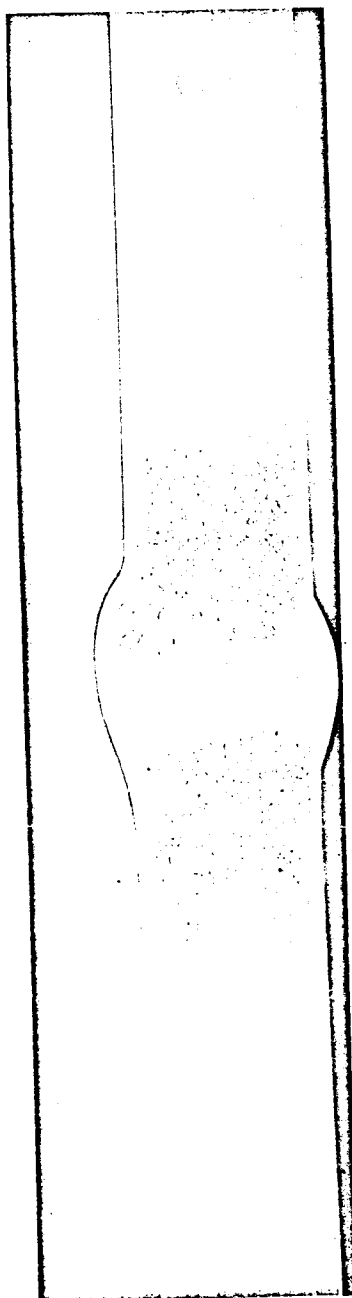


Figure 26. Macrosections Showing Effect of Front Side Chilling of Welds
in 5/16-in 2219-T87 Plate - Jet System No. 19

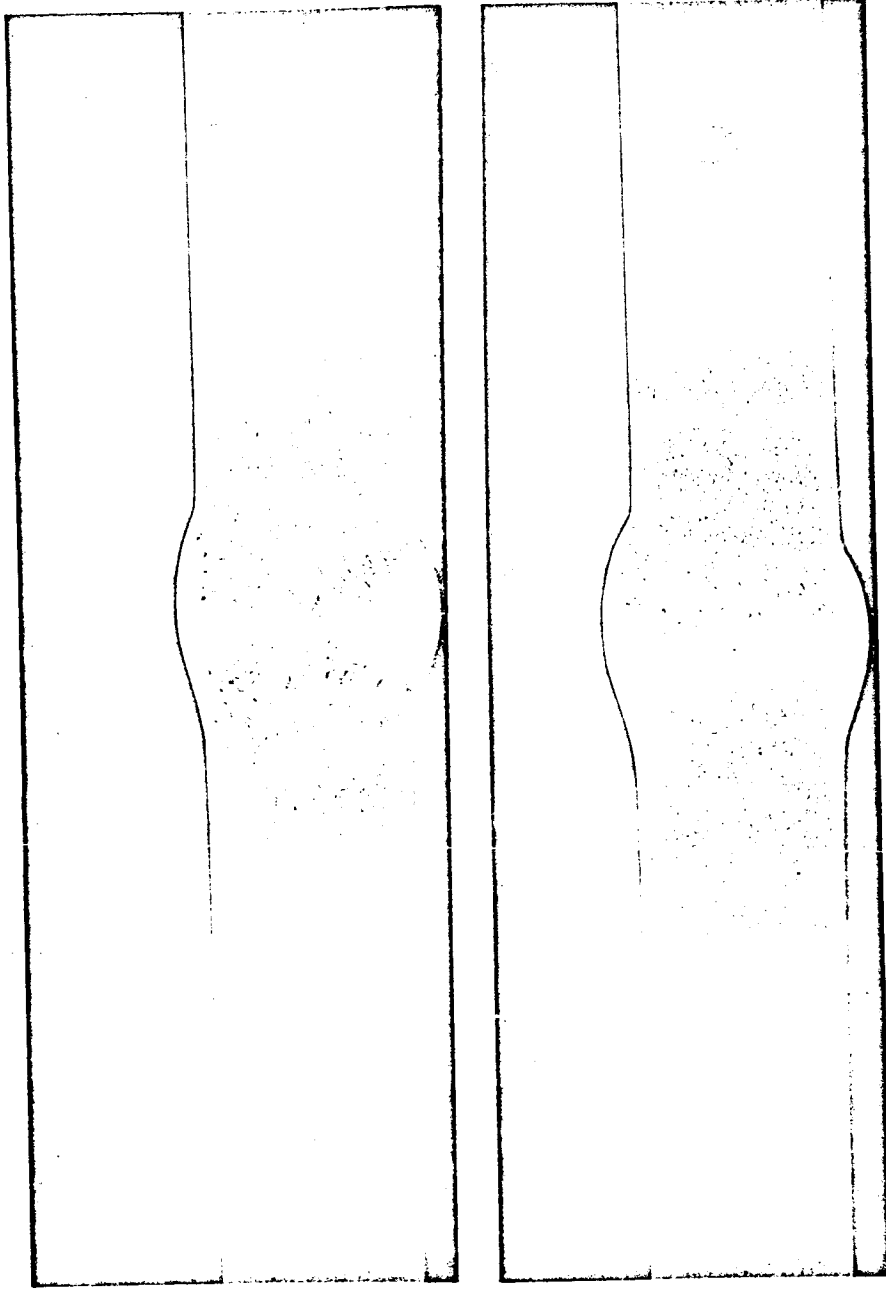


Unchilled
1AUW8186



CO₂ Chilled
1ACFW8185

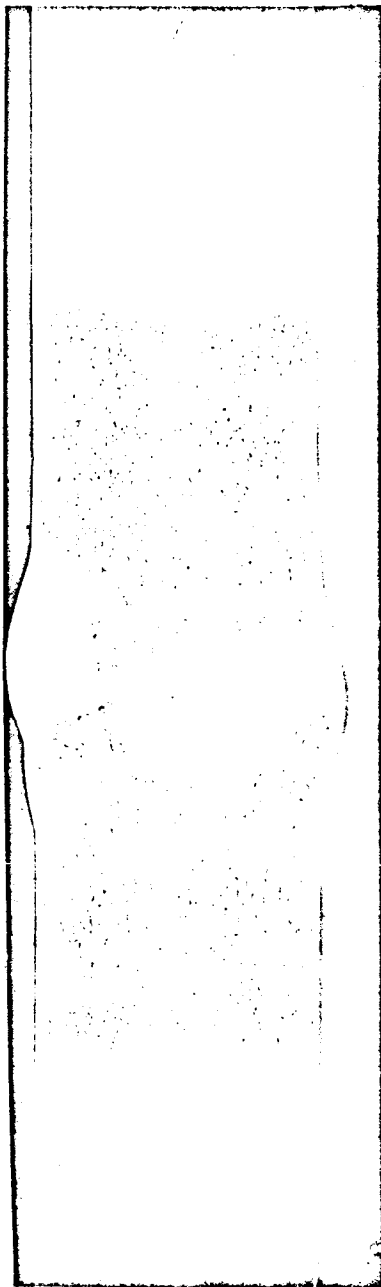
Figure 27. Macrosections Showing Effect of Front Side Chilling of Welds
in 5/16-in. 2014-T6 Plate - Jet System No. 23



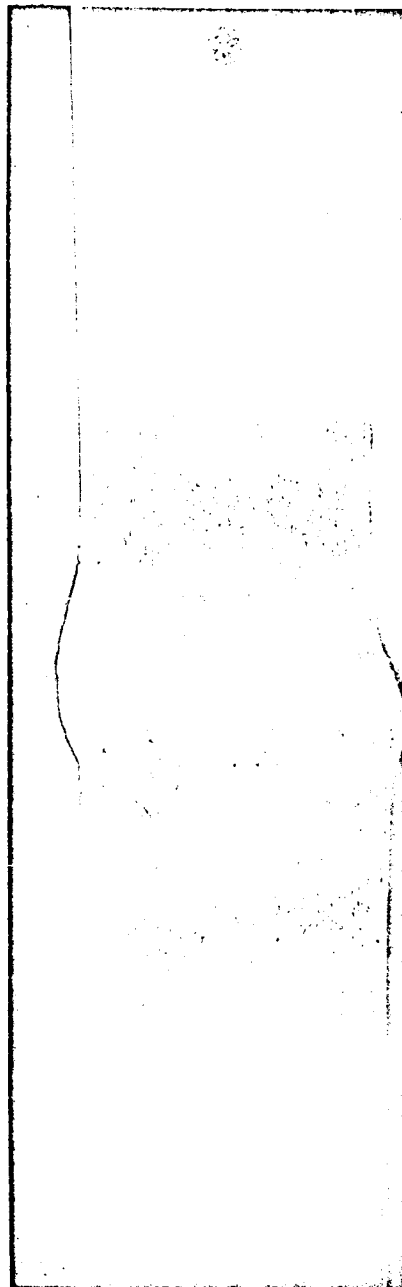
Unchilled
1AUW894

CO₂ Chilled
1ACFW893

Figure 28. Macrosections Showing Effect of Front Side Chilling of Welds
in 5/16-in. 2014-T6 Plate - Jet System No. 18

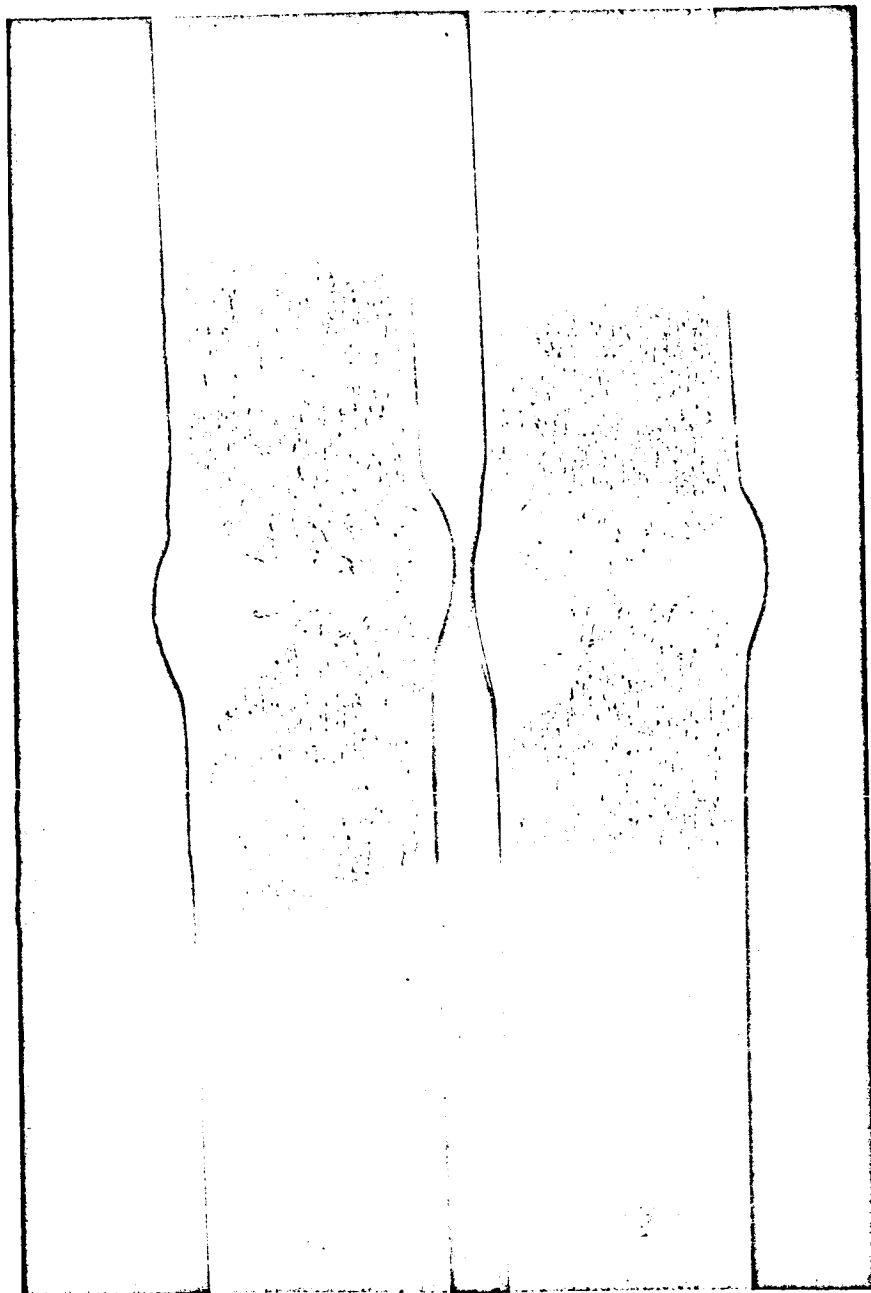


Unchilled
1BUW8254



CO₂ Chilled
1BCFW8253

Figure 29. Macrosections Showing Effect of Front Side Chilling of Welds
in 1/2-in. 2014-T6 Plate.- Jet System No. 19

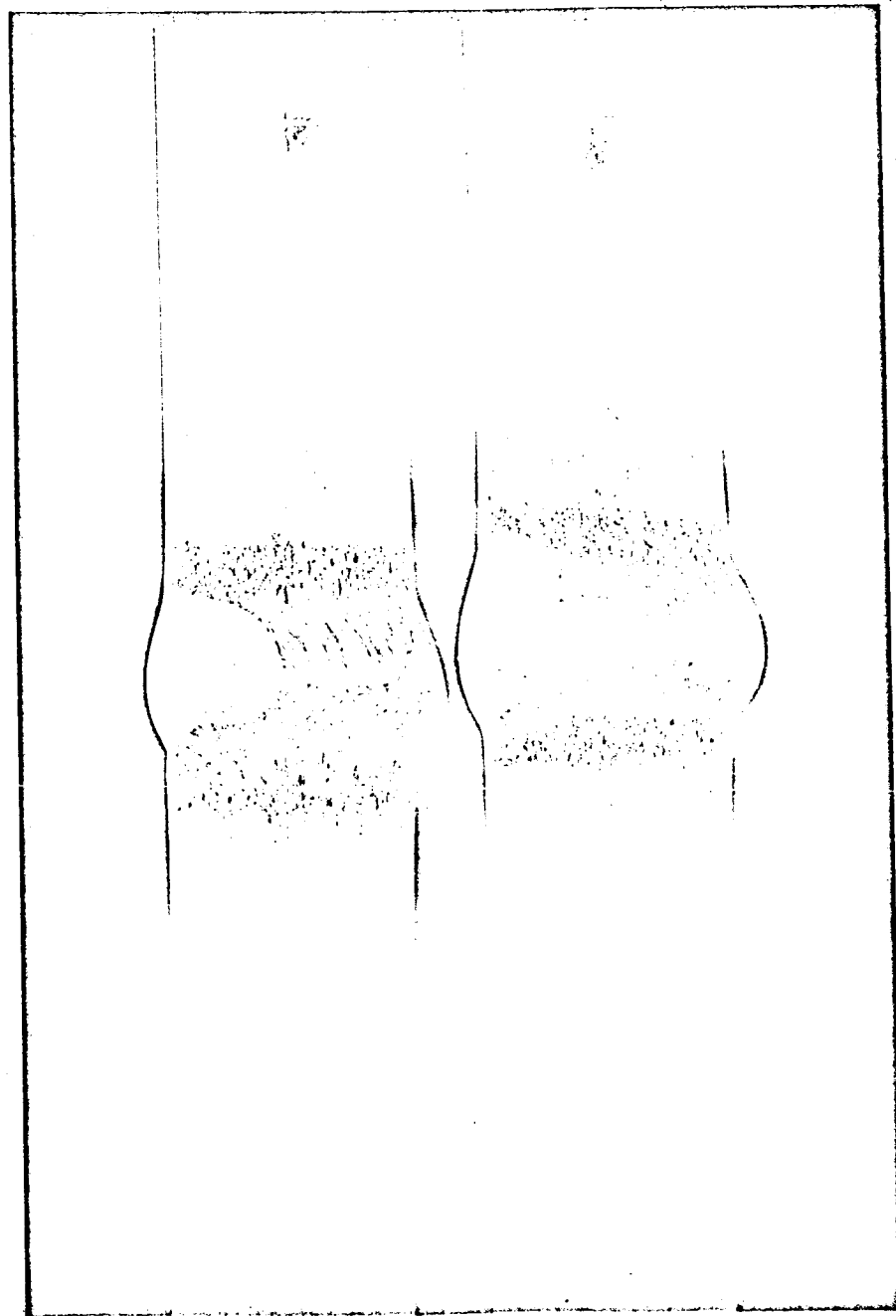


Unchilled
1BUW896

CO₂ Chilled
1BCFW895

Figure 30. Macrosections Showing Effect of Front Side Chilling of Welds
in 1/2-in. 2014-T6 Plate - Jet System No. 18

13165

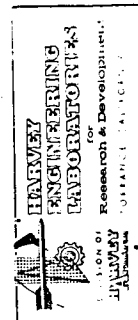


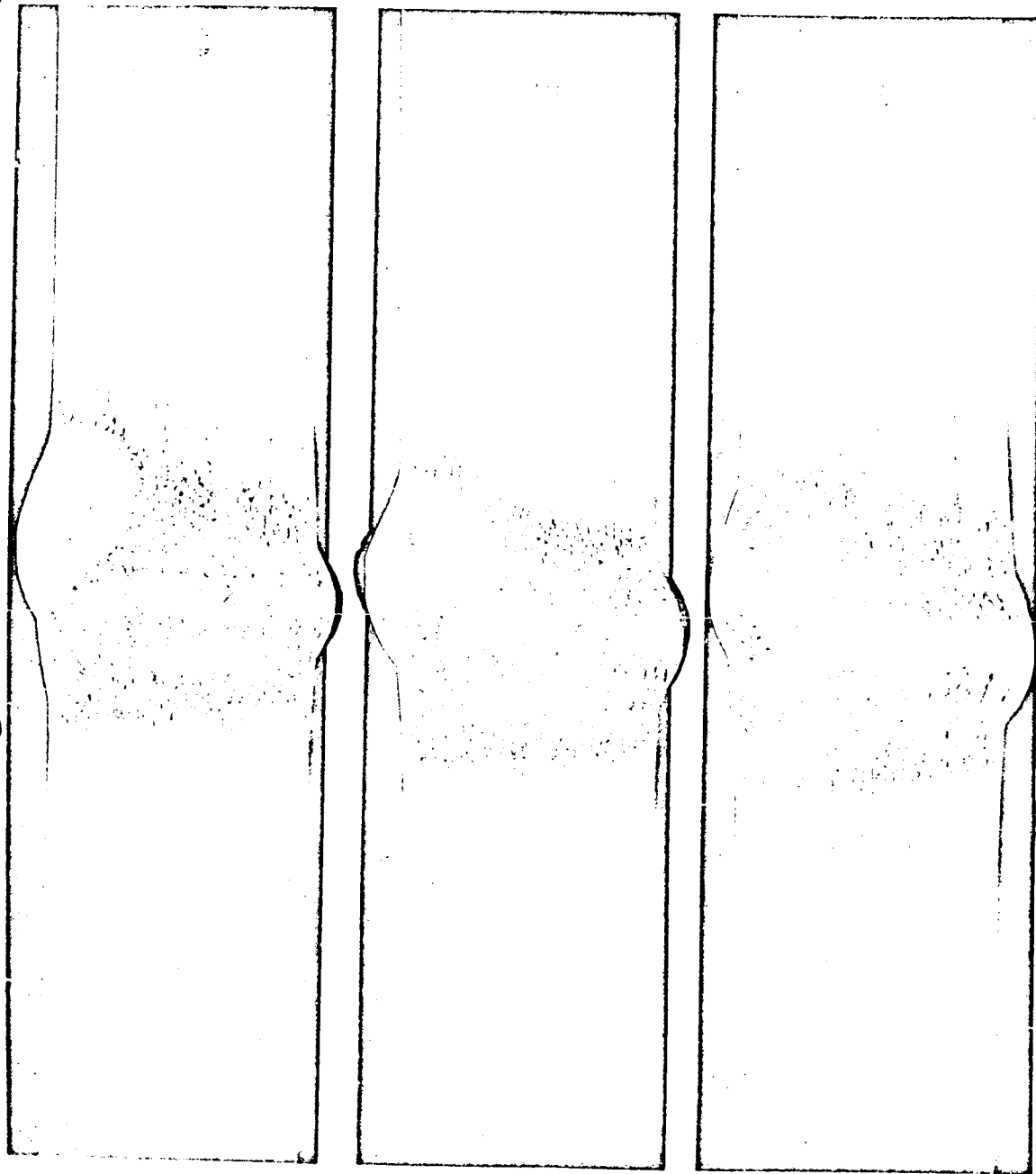
Unchilled
2BOW6151

Chilled
2BCFW751

Figure 31. Macrosections Showing Effect of Front Side Chilling of Welds
in 1/2-inch 2219-T87 Plate - Jet System No. 14

13070



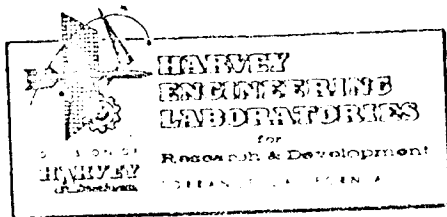


CO₂ Chilled
Jet System No. 18
2BCFW852A

CO₂ Chilled
Jet System No. 23
2BCFW8187

CO Chilled
Jet System No. 19
2BCFW8254

Figure 32. Macrosections Showing Comparison of the Effect of Three Jet Systems for Front Side of Chilling of Welds in 1/2-in. 2219-T87 Plate



Tensile Properties

Specimens were selected, from chilled and unchilled weld panels of each alloy and each thickness, for room temperature tensile tests. The selection was made on the basis of x-rays which indicated less than 1 percent porosity. The porosity content was verified by examination of fractures of specimens broken by bending. All specimens were cut to 3/4-in. wide straight-sided bars with the weld transverse and weld bead intact. One group of specimens from each panel was artificially aged to the -T6 condition after welding. All tests were performed at room temperature.

Table VI shows a summary of average tensile values obtained for artificially aged specimens, and Table VII shows such values for naturally aged specimens. Test results from which these tables are compiled are contained in Appendix V.

As indicated in Tables VIII and IX, yield strengths are substantially increased by chilling from the front side. The greatest increase in average values was 17.8% for artificially aged welds in 1/2-in. 2014-T6 plate. Individual maximum test values show increases as high as 20.3% for these welds. The greatest increase in average yield strength for welds in 2219-T87 plate was 8.8% (for welds in 5/16-in. artificially aged specimens) with increases in individual maximum test values as high as 16.6%.

Efforts were made to correlate strength with effective heat input by calculating a theoretical effective heat input value for the chilled welds using a formula based on a ratio of the cooling rates affected for each weldment. While a relationship between heat input and tensile strength appeared to follow a somewhat consistent pattern for unchilled welds, no such correlation could be obtained for chilled welds. Results of calculations are shown in Appendix VI. Undoubtedly some pattern exists, but sufficient testing has not been accomplished in this project to determine the relationship.

Table VI. Effect of Front Side Chilling on Tensile Properties of Weldments (Artificial Aging).

Weldment Material	Chill System	Tensile Strengths (KSI)					
		Average			Ultimate		
		Yield		Change	Unchilled	Chilled	Change
		Unchilled	Chilled				
5/16" 2014-T6	#18	33.9	36.9	+ 7.7%	45.9	41.3	-10.0%
	#18	37.1	39.9	+ 7.6%	49.0	48.3	- 1.4%
	#19	32.5	34.7	+ 6.8%	44.8	42.3	- 5.6%
	#23	36.3	39.0	+ 7.5%	48.5	47.5	+ 2.0%
1/2" 2014-T6	#18	30.9	36.4	+17.8%	47.0	47.3	+ 0.6%
	#19	34.4	38.9	+14.4%	47.2	47.6	+ 0.1%
	#19	34.0	38.7	+13.8%	47.2	48.7	+ 3.2%
5/16" 2219-T87	#19	31.9	33.2	+ 4.2%	38.4	39.0	+ 1.6%
	#19	35.4	38.5	+ 8.8%	40.4	44.7	+10.7%
	#23	35.1	36.0	+ 2.6%	42.5	40.7	- 4.2%
1/2" 2219-T87	#18	35.1	36.7	+ 4.6%	46.8	48.1	+ 3.4%
	#19	34.2	36.0	+ 6.4%	43.7	45.6	+ 4.3%
	#23	35.1	36.6	+ 4.3%	45.0	46.8	+ 4.0%

Table VII. Effect of Front Side Chilling on Tensile Properties of Weldments (Natural Aging).

Weldment Material	Chill System	Average Tensile Strengths (KSI)					
		Yield		Change		Ultimate	
		Unchilled	Chilled	Unchilled	Chilled	Unchilled	Chilled
5/16" 2014-T6	#18	32.7	34.5	+ 5.6%	49.5	45.2	- 0.6%
	#19	33.5	36.6	+ 9.3%	40.2	40.4	+ 0.5%
	#23	32.0	35.5	+ 7.6%	49.7	45.5	- 8.5%
1/2" 2014-T6	#19	28.8	32.1	+11.5%	47.4	48.3	+ 1.9%
	#19	28.8	35.2	+15.5%	47.4	49.0	+3.4%
5/16" 2219-T87	#23	24.2	26.8	+ 2.6%	37.3	40.5	+ 2.6%
	#19	25.5	25.7	+ 0.8%	36.1	37.3	+ 3.3%
1/2" 2219-T87	#18	20.9	22.5	+ 7.7%	40.4	41.5	+ 2.7%
	#19	19.7	20.2	+ 2.5%	38.7	40.1	+ 3.6%
	#23	21.7	21.6	- 0.5%	39.4	40.8	+ 3.6%

Table VIII. Maximum Increases in Tensile Strength
 Effected by Front Side Chilling.

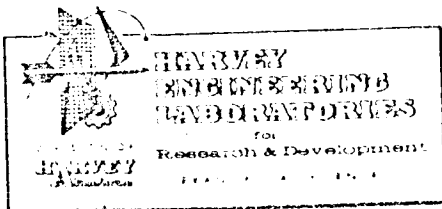
Weldment Material	Post-weld Aging	Yield Strength		Ultimate Strength	
		Increase in ave. values(1)	Increase in max. values(2)	Increase in ave. values(1)	Increase in max. values(2)
5/16" 2014-T6	Artificial Natural	7.7%	12.0%	2.0%	6.2%
		9.3%	11.8%	6.5%	3.1%
1/2" 2014-T6	Artificial Natural	17.8%	20.3%	3.2%	5.3%
		15.5%	22.5%	3.4%	2.9%
5/16" 2219-T87	Artificial Natural	8.8%	16.6%	10.7%	16.5%
		2.6%	4.8%	3.3%	4.1%
1/2" 2219-T87	Artificial Natural	6.4%	6.3%	4.3%	4.7%
		7.7%	8.5%	3.6%	12.5%

(1) Calculated from the average of test values from a series of specimens from comparable unchilled and chilled welds.

(2) Calculated from the highest test values from a series of specimens from comparable unchilled and chilled welds.

Table IX. Optimum Jet Systems for Improving
Tensile Strength - Front Side
Chilling.

Weldment Material	Post-weld Aging	Chill System	Increase in ave. yield strength	Increase in ave. ultimate strength
5/16" 2014-T6	Artificial Natural	#23 #19	7.5% 9.3%	2.0% 0.5%
1/2" 2014-T6	Artificial Natural	#18 #19	17.8% 15.5%	0.6% 3.4%
5/16" 2219-T87	Artificial Natural	#19 #23	8.8% 2.6%	10.7% 2.6%
1/2" 2219-T87	Artificial Natural	#19 #18	6.4% 7.7%	4.3% 2.7%



Porosity

Comparison of X-rays of the initial series of welds chilled from the front side (See note (4) Table X) with unchilled welds indicated a marked decrease in porosity for the chilled welds. A number of unchilled welds contained extensive areas of gross porosity, while none of the chilled welds contained more than small amounts of scattered porosity; and in most cases, porosity indications were entirely absent. These results were reasonably consistent for weld panels in both plate materials in each thickness (2014-T6 and 2219-T87 in 5/16 and 1/2-inch nominal). Approximately 60 percent of the unchilled weld samples contained porosity ranging from 1/2 to 20 percent of the cross sectional area, while more than 90 percent of the chilled welds were free of porosity.

Porosity in the unchilled welds in 2014-T6 was essentially spherical, while porosity in the unchilled welds in 2219-T87 was in the form of agglomerated oxide. Figure 33 shows photographic prints of portions of typical X-rays of unchilled and chilled welds in 1/2-inch 2014-T6 plate. X-rays of welds in 5/16-inch thick plate and in both thicknesses of 2219-T87 plate were similar.

In subsequent series of experiments, samples for determination of porosity by X-ray were taken from weld panels which had been welded so that half of the weld length was chilled by liquid CO₂ and the other half was welded without chilling. Specimens from each half were fractured by bending. The fractures of tensile specimens were examined for porosity.

Results indicate that the incidence of porosity is reduced by draw filing and by chilling (See Table X). Chilling also appears to reduce porosity size. In some cases CO₂ leaked into the arc while the chilled portion of the panel was being welded, which might account for the porosity in those welds. Causes for porosity in the other welds have not been determined. Although the results on this series of weldments are not entirely definitive, the indications combined with results on previous series would appear to warrant the conclusion that

Table X. Effect of Front Side Chilling
on Weld Porosity.

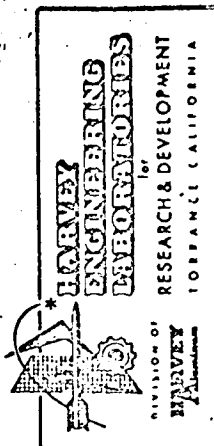
Weldment Material	Pre-Weld Preparation	Average Porosity			
		X-ray (1)		% Fracture (2)	
		Unchilled	Chilled	Unchilled	Chilled
3/8" 2014-T6	Wire Brushing ⁽⁴⁾ Draw Filing Draw Filing	G#3 SI None G#1 SI	G#1 SI None G#1 SI	2 0 0	1/2 0 0
1/2" 2014-T6	Wire Brushing ⁽⁴⁾ Draw Filing Draw Filing	G#3 LC G#1 SI G#1 SI	None G#1 SI G#1 SI	1 0 0	1/2 0 0
5/16" 2219-T87	Wire Brushing ⁽⁴⁾ Draw Filing Wire Brushing	D#3 LC D#3 LC D#3 LC	None D#1 LC D#3 LC	5 0 5	1/2 0 2
1/2" 2219-T87	Wire Brushing ⁽⁴⁾ Draw Filing Wire Brushing	D#2 LC D#1 SI None	D#1 LC None None	2 0 1	1/2 0 0

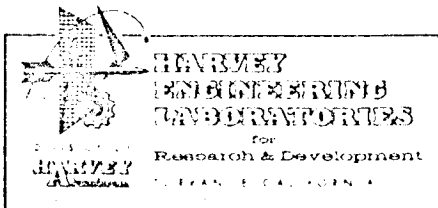
- (1) NAVORD CD 7574 - X-ray standards for shielded arc welds in aluminum.
- (2) Estimated percent of cross sectional area of fractured specimens.
- (3) D = dross, G = gas, S = scattered, I = intermittent, L = lineal, C = continuous.
- (4) Chilled and unchilled samples are not welded on the same panel.

Weld Chilled
from Front Side

Unchilled
Weld

Figure 33. Typical X-rays Showing Effect of Front Side Chilling on Porosity
in Welds in 1/2-inch 2014-T6 Plate





chilling appreciably reduces the incidence and severity of porosity. Further experimental work is needed to statistically substantiate these conclusions on a quantitative basis.

Warpage

Several panels fabricated by chilling from the front side remained essentially flat after welding, exhibiting almost no longitudinal bow or peaking. Unchilled weld panels have contained a longitudinal bow up to 1 1/2 inches and peaking to 10 degrees, depending upon the amount of heat input. Figure 34 shows a comparison of warpage in chilled and unchilled panels.

While no attempt has been made to develop optimum parameters for warpage control, the panels welded to date indicate clearly that the concept of chilling with cryogenic liquids during welding is amenable to elimination or reduction of warpage. It should also follow that if warpage problems can be alleviated by application of this concept, it might also be a solution to residual stress problems in welded structures.

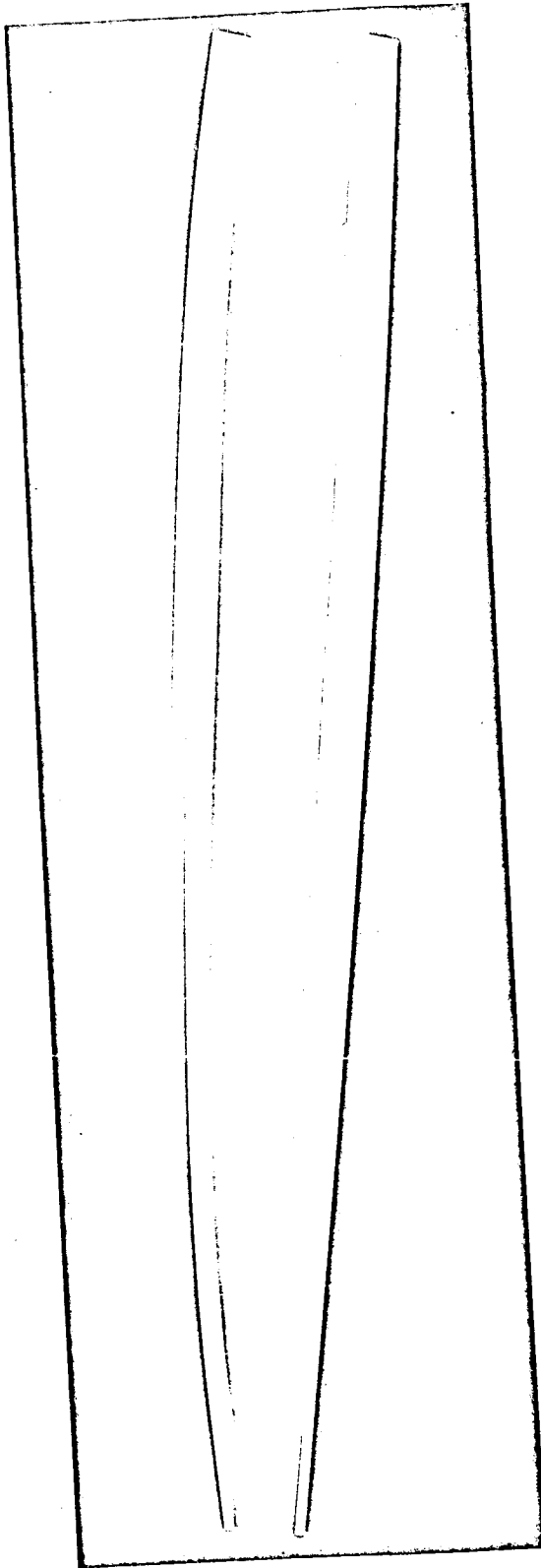
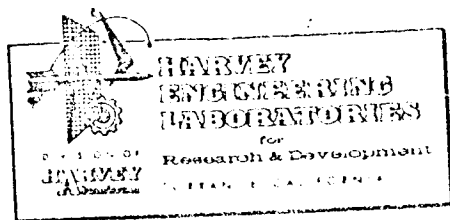


Figure 34. Effect of CO₂ Chilling on Warpage in Aluminum Weldments
(Top: Unchilled; Bottom: Chilled from Front Side)



V. DISCUSSION OF RESULTS

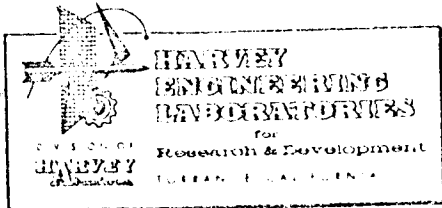
Chilling of weldments by means of cryogenic liquids offers advantages which may not be apparent from a cursory comparison of results of this program with welds made on other programs at different heat input levels. Although it might be possible to produce welds at lower levels of heat input than was used for the welds in this program and thus secure comparable strength improvements over high heat input welds, such low heat input welds can lead to such defects as intermittent lack of penetration or lack of fusion. In order to keep heat input low, such welds will have to be made by multiple passes and will require precise control which will increase the cost.

Chilled welds may be made at a much higher heat input, alleviating these problems, while achieving equal or better results.

While chilling did not eliminate porosity, there was a strong indication that the extent of the porosity was considerably reduced. In many cases such a reduction might mean the difference between acceptance of the weldment and scrapping an expensive part.

More nearly unidirectional solidification is promoted by chilling the weld from the back side and is therefore more conducive to reducing porosity and producing a better metallurgical structure. However, as experiments on chilling from the back side were discontinued on the basis of being difficult to apply to the majority of welded structure, the full potentials were not investigated.

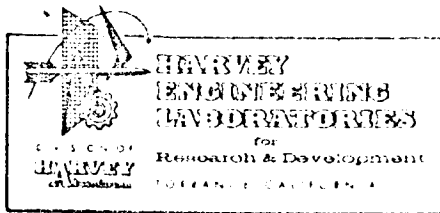
Chilling from the front side apparently also reduces porosity and does not adversely affect metallurgical structure. It is believed that the fast cooling rates are responsible for inhibiting nucleation and growth of porosity, as well as for reducing grain size so that adverse metallurgical structure is not produced.



VI. CONCLUSIONS

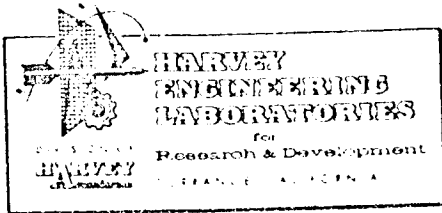
Tensile properties can be improved and porosity can be reduced by properly controlling time-temperature relationships during the welding process.

Use of cryogenic liquid jets as a means of accomplishing the required control is feasible. Limited experimental development performed in this program resulted in improvements in yield strength up to 20% for welds chilled by liquid carbon dioxide, with reductions in porosity over 100% and drastically reduced warpage. Further work is warranted to obtain statistical data and to refine the concept preparatory to its application to production welding.



VII. RECOMMENDATIONS

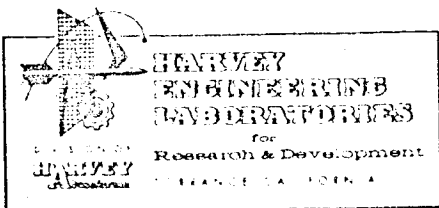
It is recommended that further experimental work be performed to establish the limits of the concepts for improvement in properties of welds on a statistical basis and to provide sufficient information for development of criteria for equipment, instrumentation, and procedures to be used in application of the concept of welding of production parts.



HA NO. 2283 PAGE A.I.

APPENDIX I

CALCULATION OF TARGET THERMAL PATTERNS

CALCULATION OF TARGET THERMAL PATTERNS

Preliminary work conducted by NASA, Huntsville (1) on time-temperature controls for welding 2219 aluminum indicated that it is desirable to achieve a peak temperature of 1500°F in the weld, and to limit the time at which the weld is above 450°F to a maximum of 16 seconds. These criteria are undoubtedly closely related to values which will promote partial solution treatment and prevent gross overaging in critical portions of the weldment. For proper solution treatment and aging response, the quench rate from 1000°F should be on the order of 100°F/sec. At temperatures above 450°F, overaging becomes increasingly rapid as the annealing temperature (775°F) is approached.

The first step in this program was to determine whether these criteria are within limits which can be practically accomplished, using special methods of heat extraction.

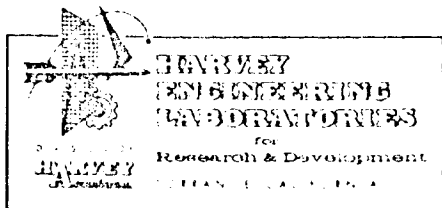
A considerable amount of work has been performed by various researchers to develop precise formulae to calculate heat flow and thermal patterns produced by fusion welding. Due to the number of inter-dependent variables, it has become expedient to use approximations which have been verified experimentally.

In the following paragraphs, these formulae have been utilized to calculate approximate peak temperatures and tentative target thermal patterns for the experimental portion of this program.

$$\frac{1}{T_p - T_o} = \frac{4.13 \text{ PCYt}}{(q/\bar{V})} + \frac{1}{T_m - T_o} \quad (1) \text{ Ref. 2}$$

$$R = 2 \text{ KPC} \left(\frac{V_t}{q} \right)^2 (T^1 - T_o)^3 \quad (2) \text{ Ref. 2}$$

(1) "Analysis of Time-Temperature Effects in 2219 Aluminum Welding," F. J. Jackson, Welding Journal, April, 1966, pages 1885-1925.



R = cooling rate on the welded centerline (and immediate heat-affected zones at temperature T^1) in $^{\circ}\text{F}/\text{sec}$.

K = thermal conductivity in $\text{Btu}/\text{in}.\text{sec } ^{\circ}\text{F}$.

P = density in $\text{lb.}/\text{in}^3$

C = specific heat in $\text{Btu}/\text{lb}^{\circ}\text{F}$

V = arc travel speed in inches/sec.

t = plate thickness in inches

q = strength of heat source in Btu/sec . (amps x volts x 3.413 x efficiency/3600).

T^1 = temperature at which the cooling rate is to be determined in $^{\circ}\text{F}$.

T_o = the initial temperature of the plate in $^{\circ}\text{F}$.

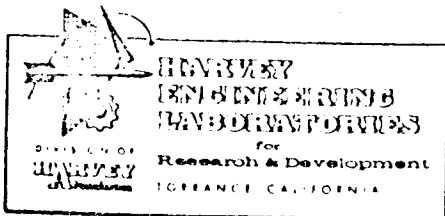
T_p = peak temperature at a distance Y from the fusion weld boundary in $^{\circ}\text{F}$.

T_m = melting point of the metal in $^{\circ}\text{F}$.

Y = the distance from the weld fusion boundary in inches.

The following assumptions are included in the derivation of equations (1) and (2):

- (a) the heat flow is two dimensional,
- (b) the heat losses through the plate surfaces are neglected,
- (c) the heat source is a point,
- (d) the temperature at a great distance from the point is unchanged, and
- (e) the physical properties of the material are constant.



Using equation (2) and assuming that the optimum parameters for welding 0.50 inch thick plate are 400 amps, 12.5 volts and arc travel speed of 10 inches per minute, the approximate time for cooling through a 500 degree temperature range is calculated as follows:

$$K = 100 \text{ Btu/ft. hr.}^{\circ}\text{F} = 100/12 \times 60 \times 60 \text{ }^{\circ}\text{F} = 2.3 \times 10^{-3} \text{ Btu/in. sec.}^{\circ}\text{F.}$$

$$P = 0.090 \text{ lb/in.}^3 = 9.0 \times 10^{-2} \text{ lb/in.}^3$$

$$C = 0.25 \text{ Btu/lb.}^{\circ}\text{F} = 2.5 \times 10^{-1} \text{ Btu/lb.}^{\circ}\text{F}$$

$$\begin{aligned} 2 \text{ KPC} &= 2 \times 3.1416 \times 2.3 \times 10^{-3} \times 90 \times 10^{-2} \times 2.5 \times 10^{-1} \\ &= 3.25 \times 10^{-4} \left(\frac{\text{Btu}}{\text{in.}^4 \text{ sec.}} \frac{\text{lb.}}{\text{sec.}^{\circ}\text{F}} \right) \end{aligned}$$

$$q = 400 \times 12.5 \times 3.413 \times .75/3600 = 3.55 \text{ Btu/sec.}$$

$$v = 10 \text{ in./min.} = 1.65 \times 10^{-1} \text{ in./sec.}$$

$$t = 0.50 \text{ in.} = 5 \times 10^{-1} \text{ in.}$$

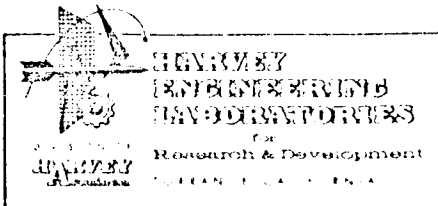
$$\left(\frac{Vt}{q} \right)^2 = \left(\frac{1.65 \times 10^{-1} \times 5 \times 10^{-1}}{3.55} \right)^2 = 10.75 \times 10^{-4} (\text{in}^4/\text{Btu}^2)$$

$$(T^1 - T_o)^3 = (1000 - 500)^3 = 0.125 \times 10^9 (\text{ }^{\circ}\text{F}^3)$$

$$\begin{aligned} R &= 2 \text{ KPC} \left(\frac{Vt}{q} \right)^2 (T^1 - T_o)^3 = 3.25 \times 10^{-4} \times 10.75 \times 10^{-4} \times \\ &0.125 \times 10^9 = 43.7 \text{ }^{\circ}\text{F/sec.} \end{aligned}$$

Since this cooling rate is less than one-half of the optimum rate, the additional heat extraction accomplished by the liquid cryogenic material must approximately equal the heat extraction provided by the plate itself, which in turn is equal to the net heat input from the welding torch.

$$q = \frac{60 \text{ E I}}{vt} = \frac{60 \times 400 \times 12.5}{10 \times .50} = 60,000 \text{ joules/in./in.}$$



The latent heat of liquid CO_2 plus the sensible heat to 70°F is approximately 149.1 Btu/lb. or 157,500 joules/lb. At 25% efficiency, the amount of liquid CO_2 required to accomplish the required chilling would be:

$$\frac{60,000}{157,500 \times .25} = 1.52 \text{ lb./in./in.}$$

or .76 lb./in. for 1/2" material

At welding speeds of 10 inches per minute, this delivery of liquid CO_2 can easily be accomplished.

On the basis of these equations, calculations were made for peak temperatures and schematic thermal patterns were drawn.

The equation for peak temperature (equation (1)) has been verified by experimental work (Ref. 3) and restated for welds in 1/2" thick aluminum plate as follows:

$$\frac{1000}{T_p - T_o} = 1.68 \left(\frac{1000 \text{ } t r v}{E I} \right) + 0.82$$

t = plate thickness in inches

r = distance from the weld centerline in inches

v = arc travel speed in inches per minute

I = arc current in amperes

E = arc voltage

Substituting some selected values for welding parameters, Figure 35 was drawn to indicate peak temperatures which might be expected in the weldment in 1/2" thick aluminum plate; schematic target thermal pattern sketches are shown in Figures 36 and 37.

Ref. (3) C.M. Adams, Jr., MIT, (Weld Journal, May 1958)

$$\frac{1000}{T_p - T_o} = 1.68 \left(\frac{1000 t r v}{EI} \right) + 0.82$$

- T_p = Peak temperature of plate
 T_o = Initial temp of plate (-200 to 600F)
 t = Plate thickness (1/2 in.)
 r = Distance from weld centerline (0-6")
 v = Welding speed (20 ipm)
 E = Welding amperage (400 amp)
 I = Welding current (125 volt)

For values indicated in parentheses above

$$r = \frac{300}{T_p - T_o} - .25; T_p = \frac{300}{r + .25} + T_o$$

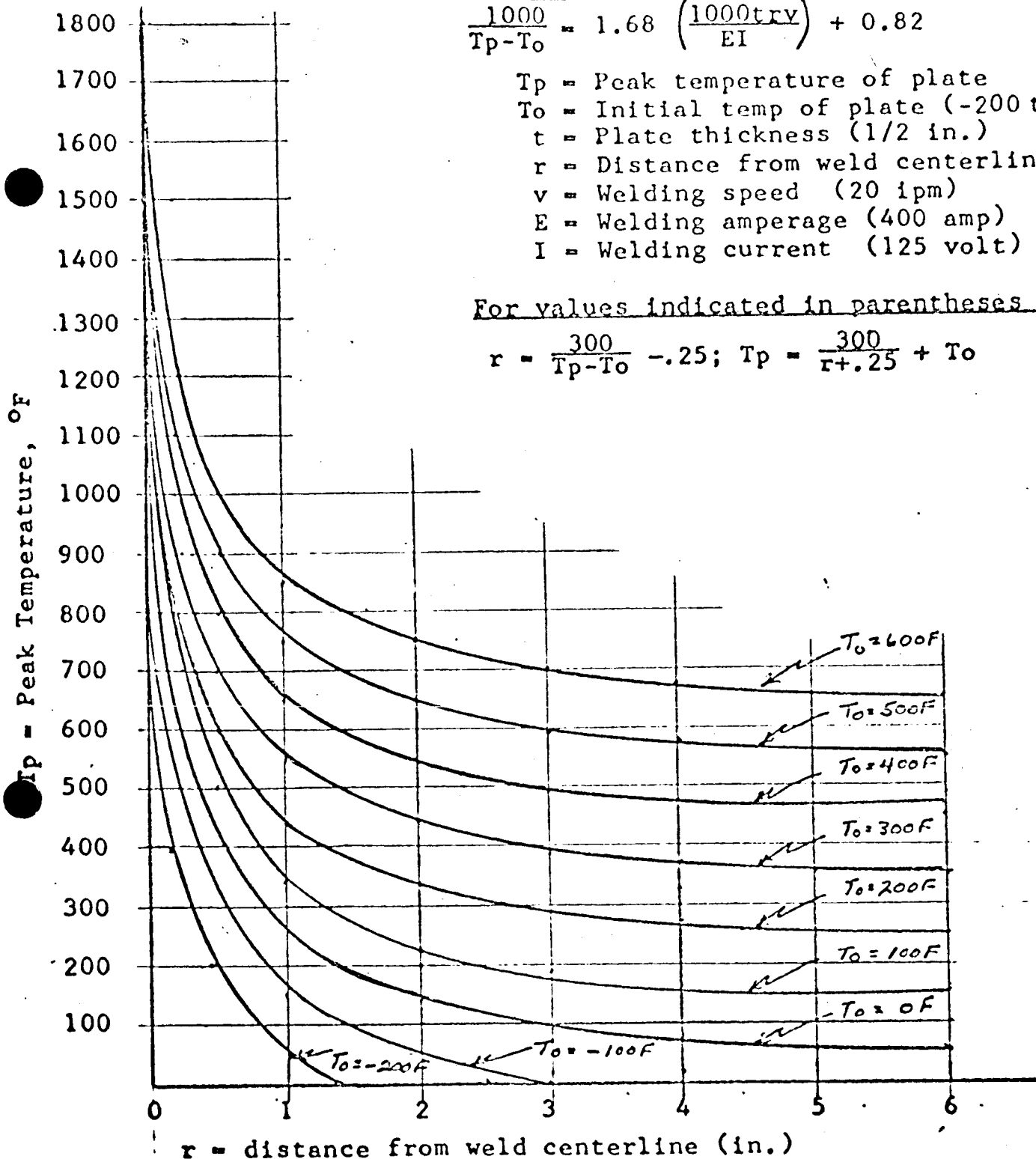
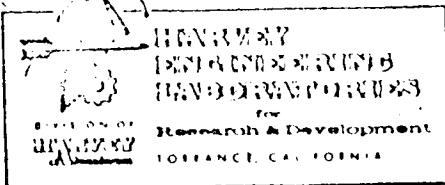


FIGURE 35 CALCULATED PEAK TEMPERATURES

SCHEMATIC FOR TARGET THERMAL PATTERNS DURING WELDING 1/2" THICK ALUMINUM PLATE (LONGITUDINAL SECTION VIEWS)



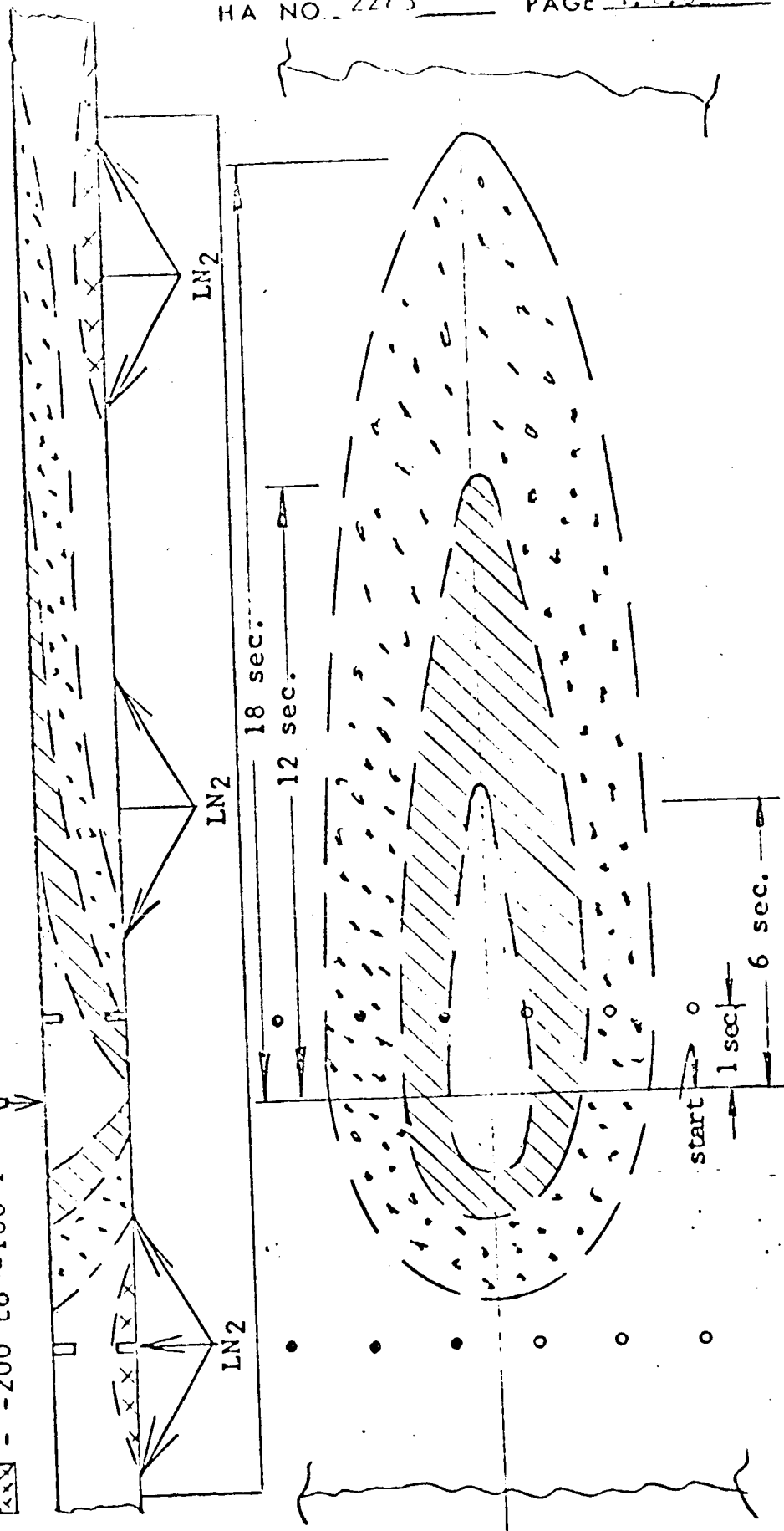
HA NO. 2283

PAGE 1.05

• } thermocouple locations,
 backside
 □ } thermocouple locations,
 top-side

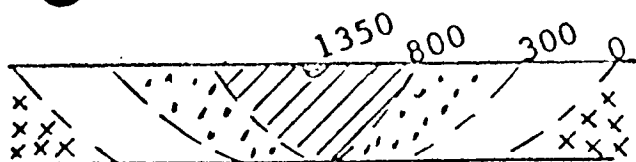
WELDING ELECTRODE
 (400 amp, 12.5 V,
 approx.)
 (carriage = 10 ipm)

- ▬ - 1200 to 1500 F
- ▨ - 500 to 1200 F
- ▧ - 100 to 500 F
- ▩ - -100 to +100 F
- - -200 to -100 F

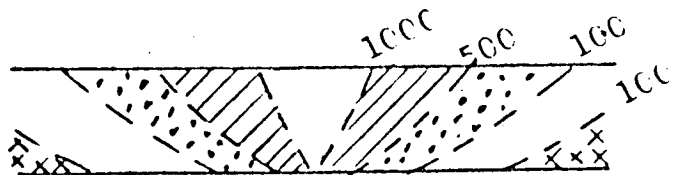


SCHEMATIC FOR TARGET THERMAL PATTERNS DURING WELDING
1/2" THICK ALUMINUM PLATE (TRANSVERSE SECTION VIEWS)

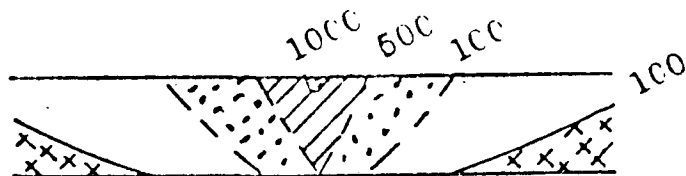
Temperature Distribution at Various Time Intervals
After Start of Welding



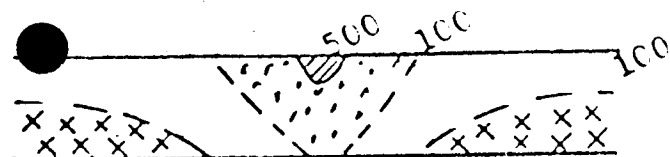
1/2" ahead of arc - start



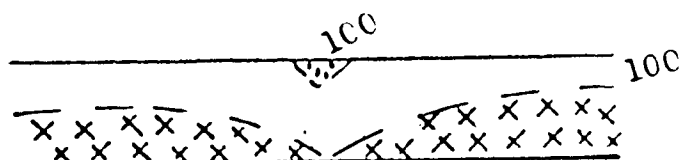
at center of arc - 1 sec.



2" behind arc - 6 sec.

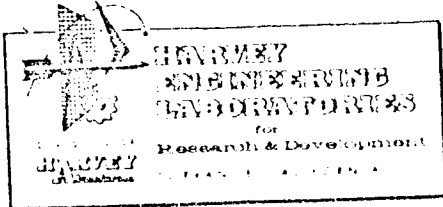


4" behind arc - 12 sec.



6" behind arc - 18 sec.

FIGURE 37 - SCHEMATIC FOR TARGET THERMAL PATTERNS (2)



HA NO. 2283

PAGE 0. II.

APPENDIX II

EXAMPLES OF

EXPERIMENTAL THERMAL PATTERNS

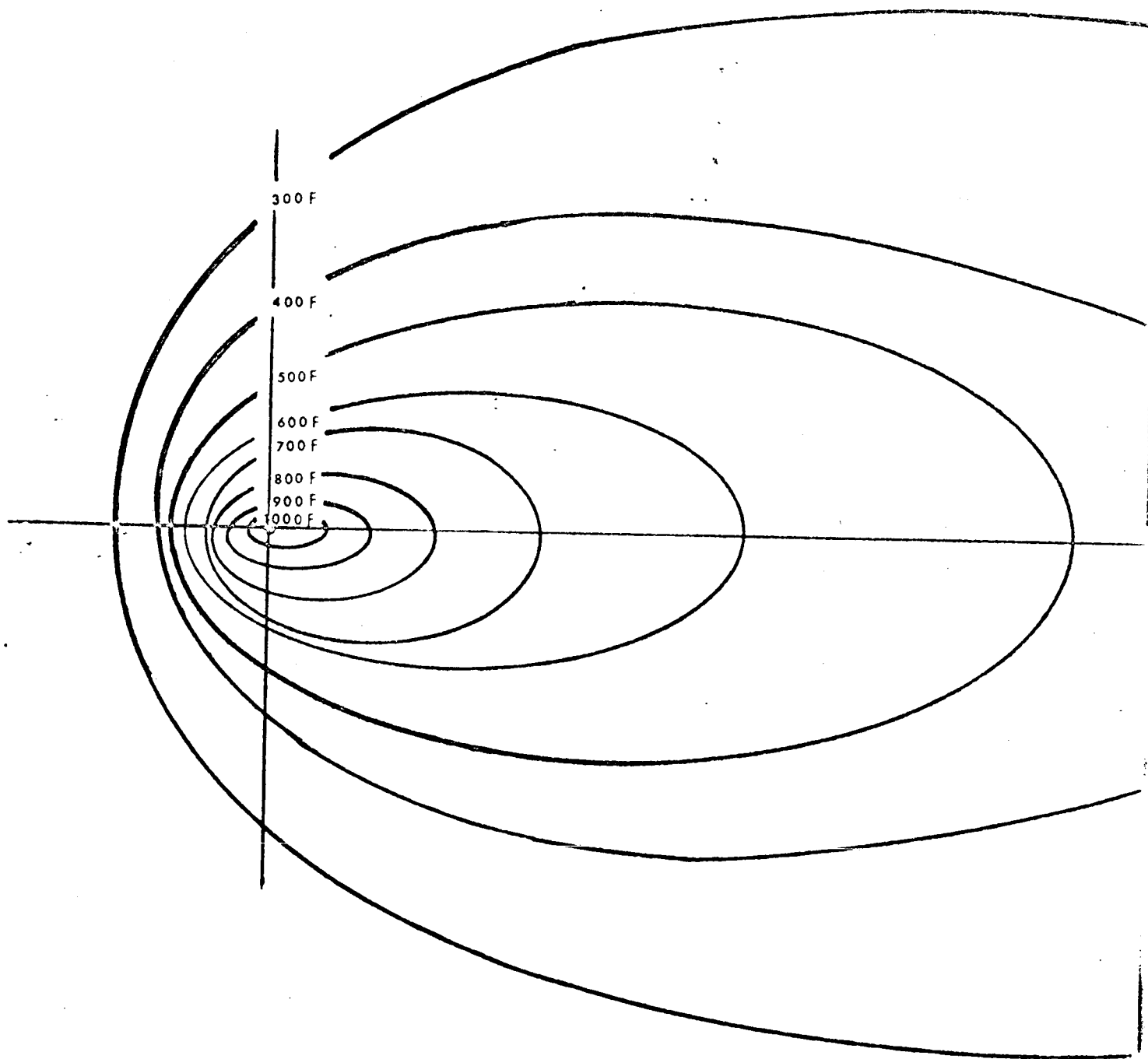
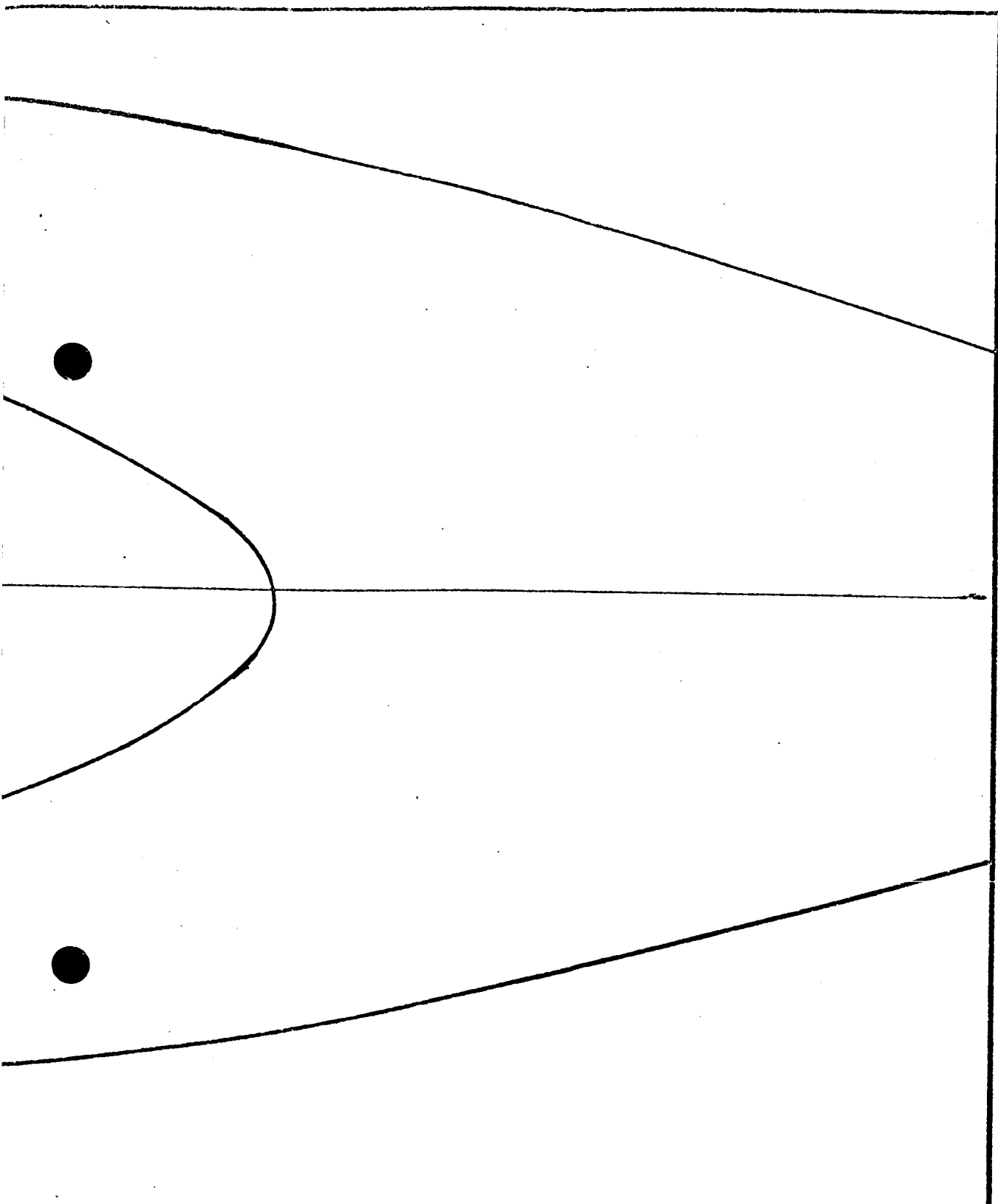


FIGURE 38 THERMAL PATTERN FOR WELD PANEL 1A1

THERMAL P/



CHILLING, 5/16" 2014-T6, PENETRATION PASS.

ERN

FULL SCALE

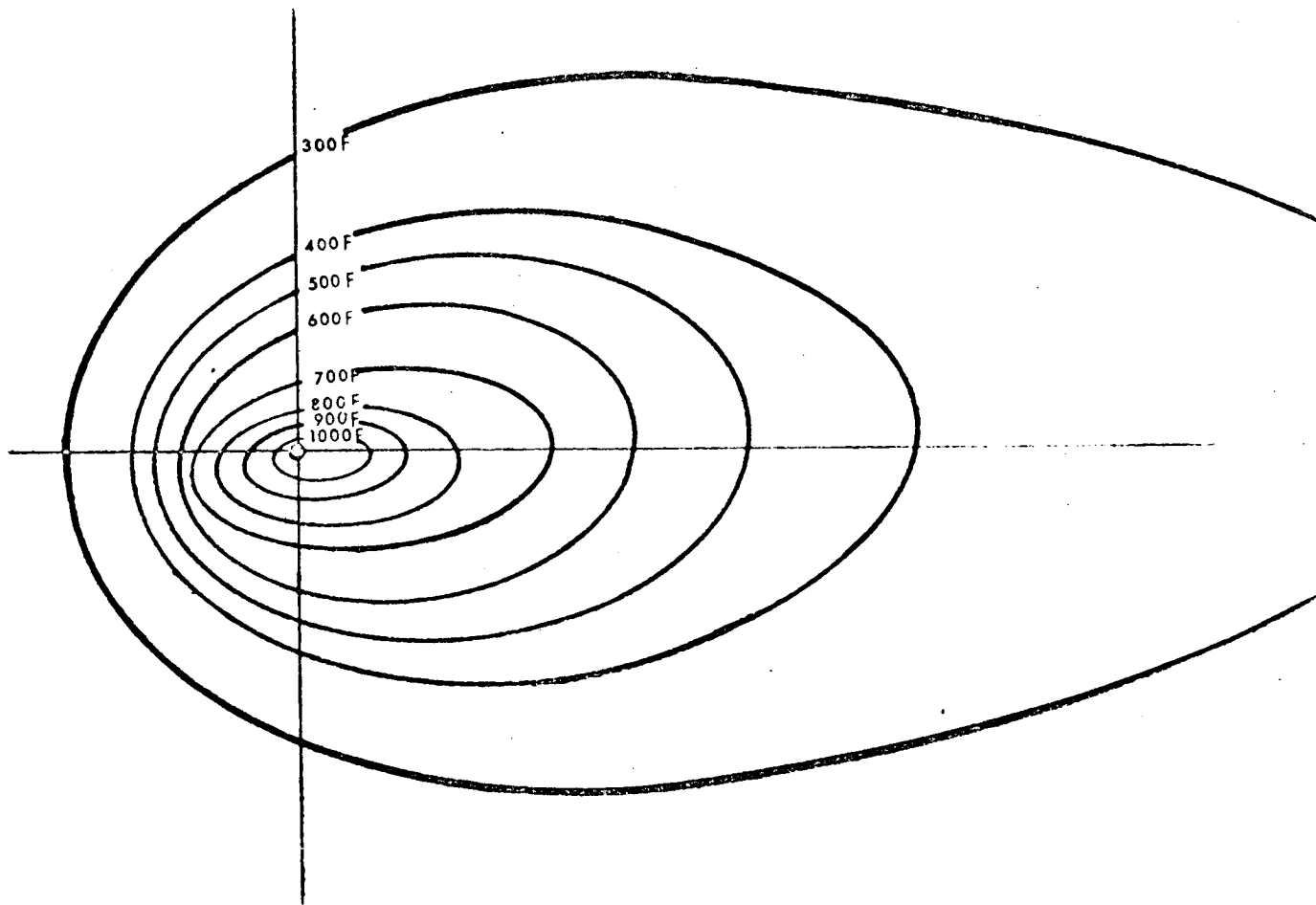


FIGURE 39 THERMAL PATTERN FOR WELD PANEL IE

THERMAL P

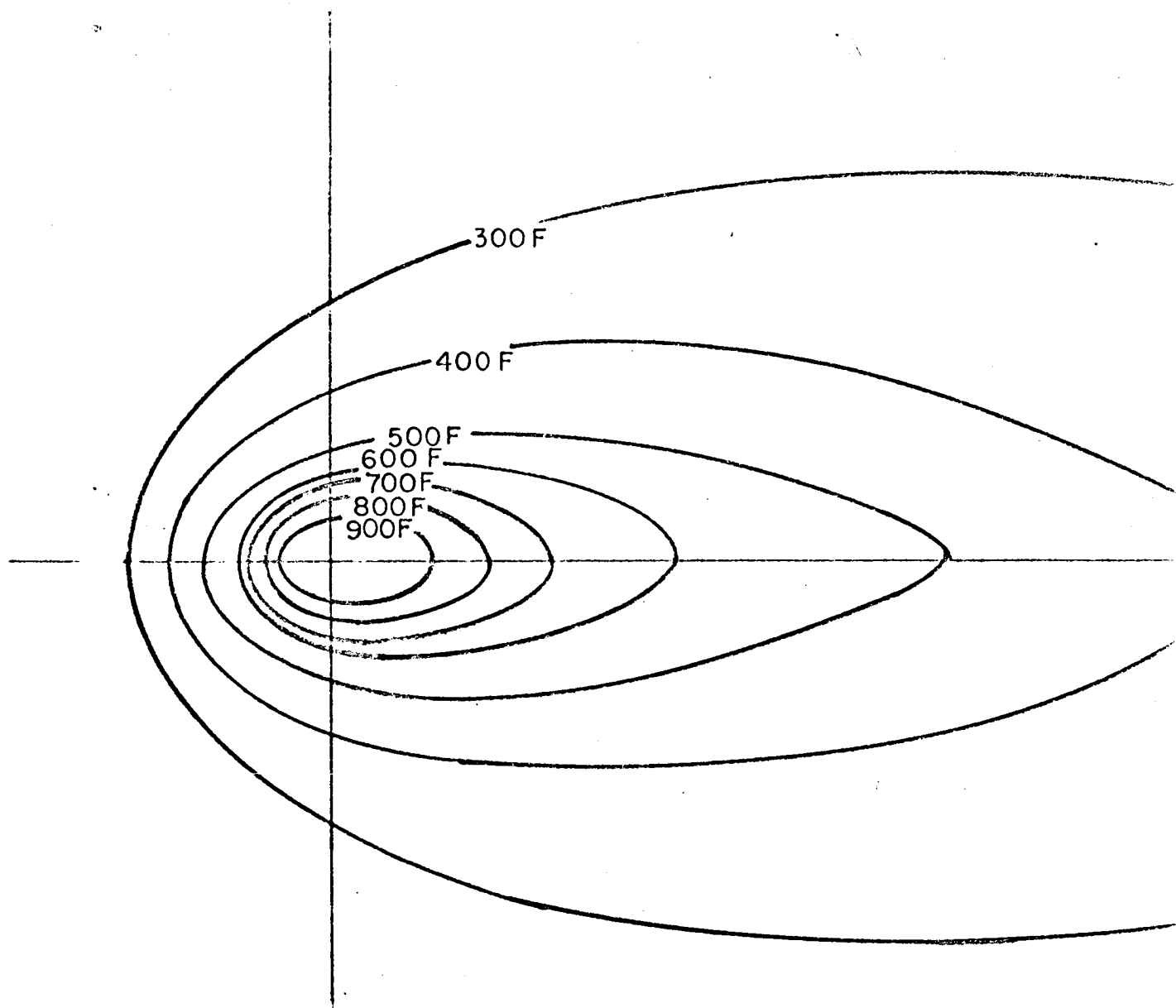
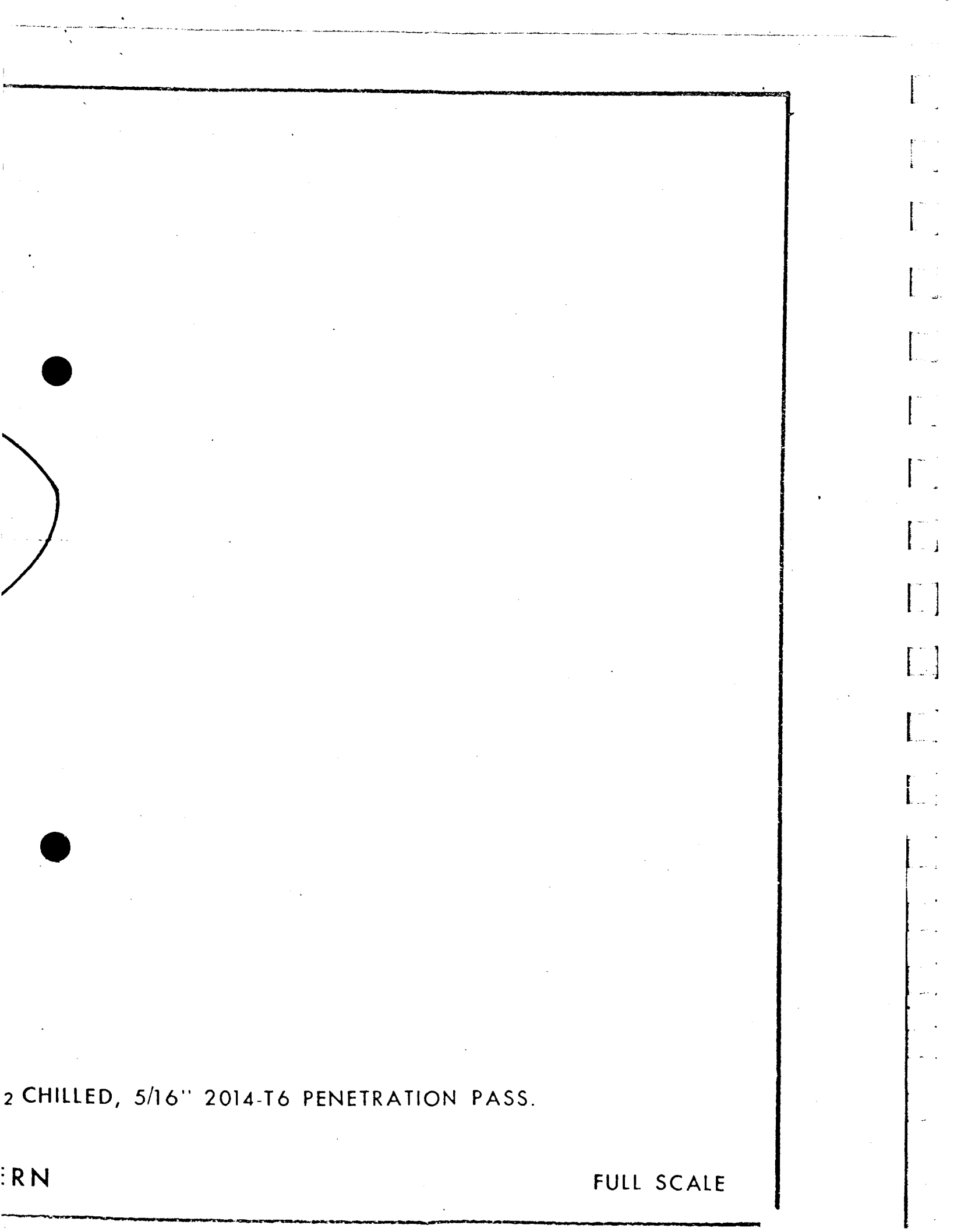


Figure 42 . Thermal Pattern for Weld Panel
No Chilling, $\frac{1}{2}$ Inch 2219-T87



2 CHILLED, 5/16" 2014-T6 PENETRATION PASS.

ERN

FULL SCALE

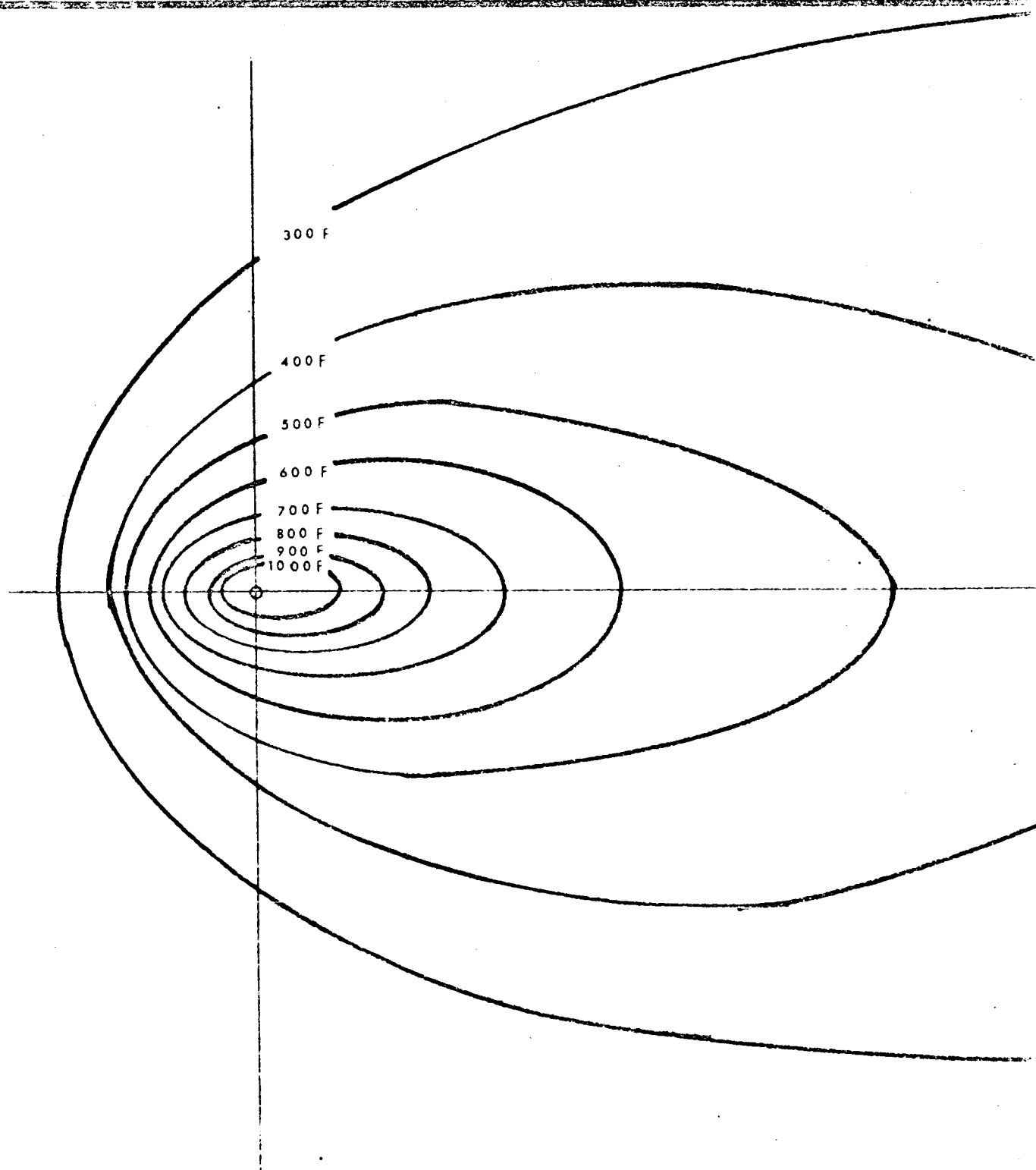
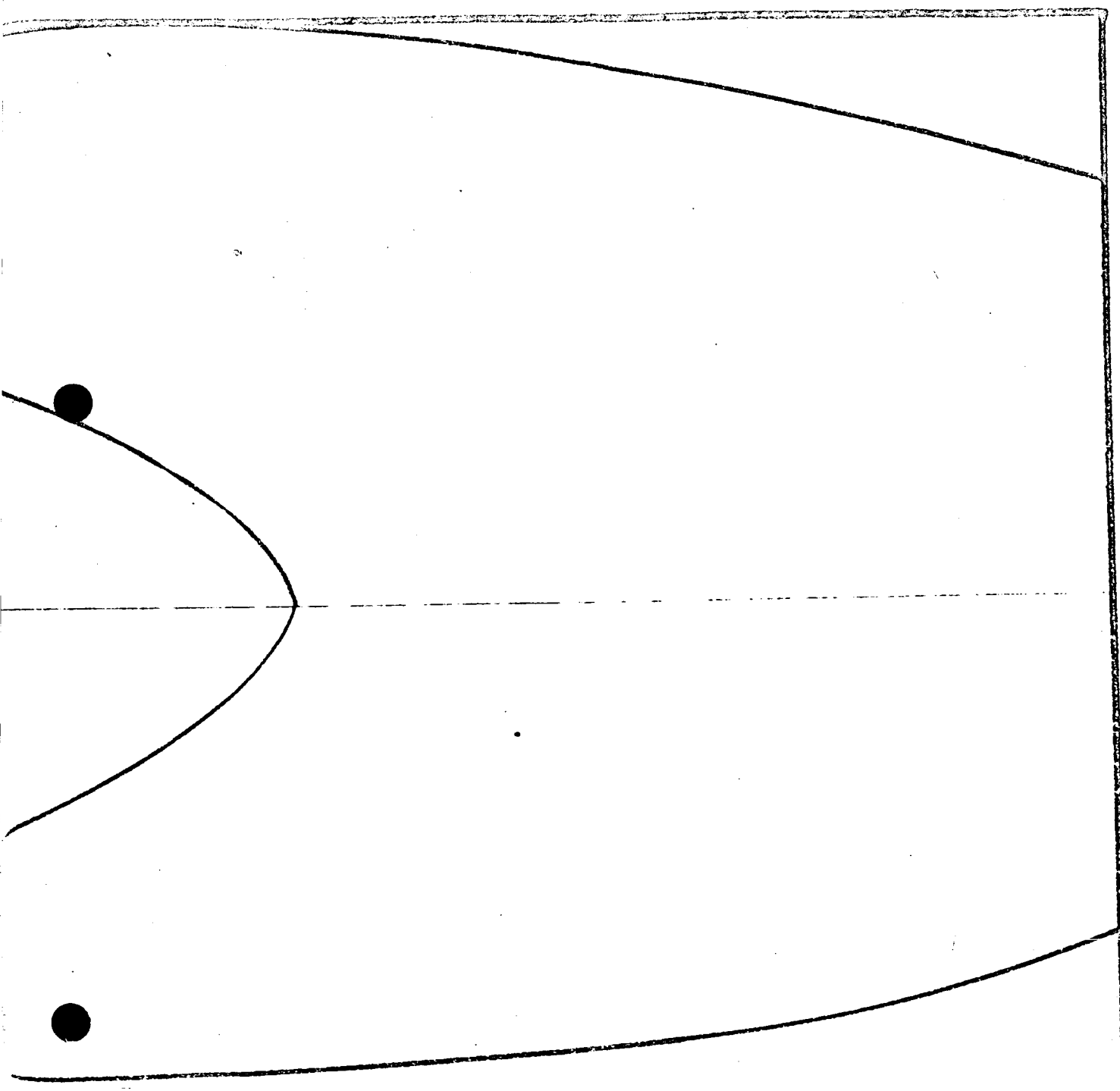


FIGURE 40.-THERMAL PATTERN FOR WELD PANE

THERMAL



2 NO CHILLING, 1/2" 2014-T6, PENETRATION PASS

PATTERN

FULL SCALE

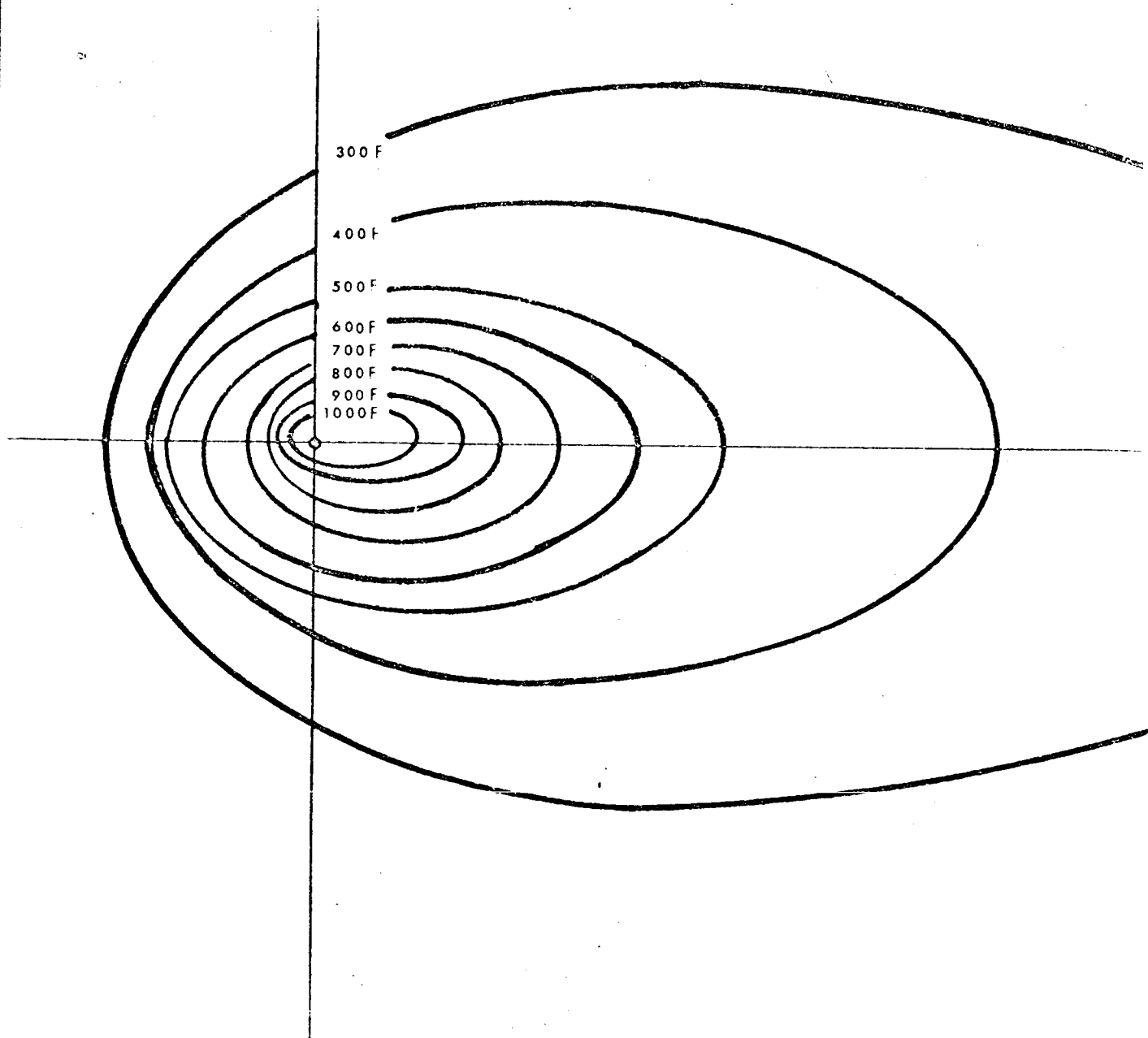
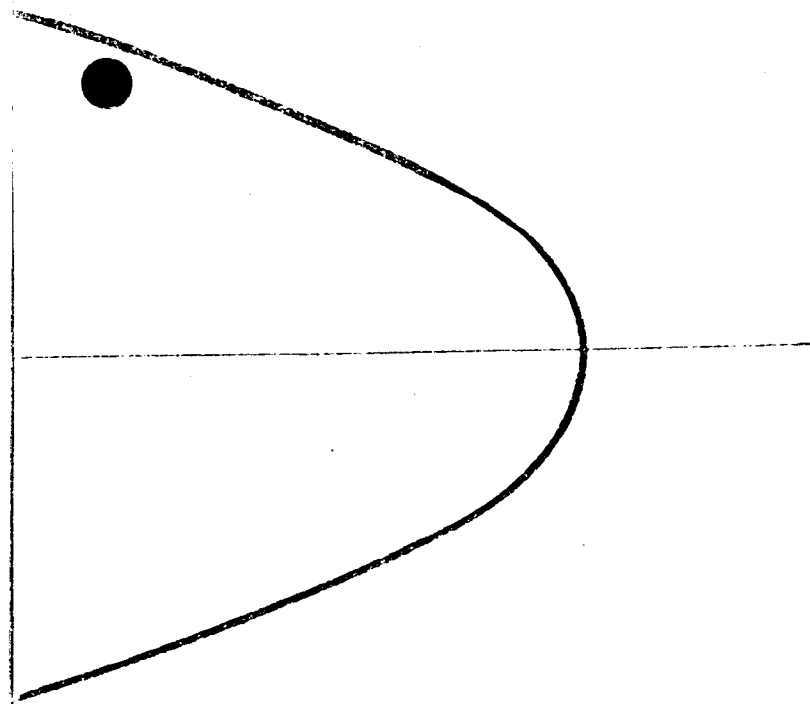


FIGURE 41 - THERMAL PATTERN FOR WELD PANEL I

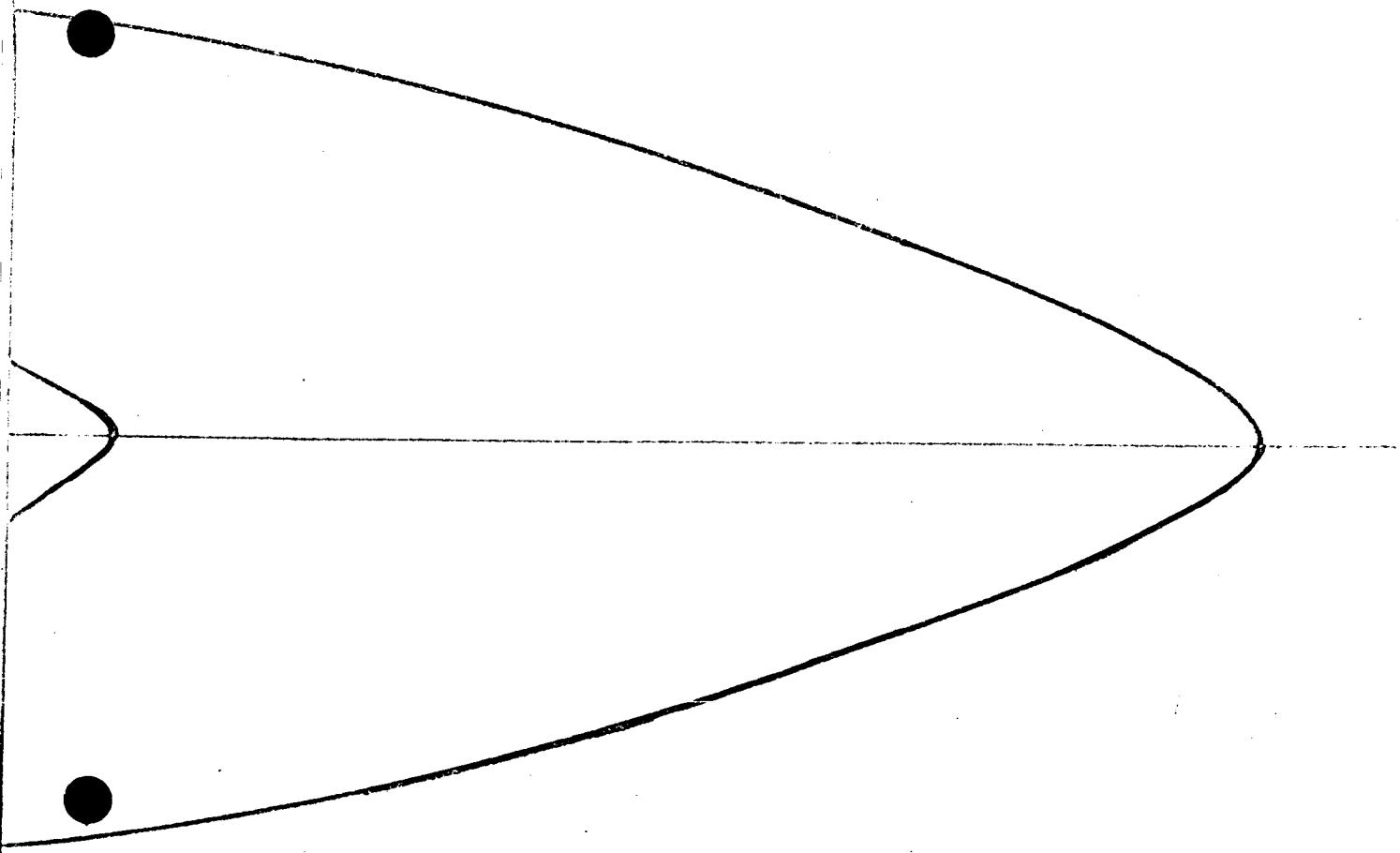
THERMAL



DC3 CO₂ CHILLED, 1/2" 2014-T6, PENETRATION PASS

PATTERN

.ULL SCALE



B2-20

Full Scale

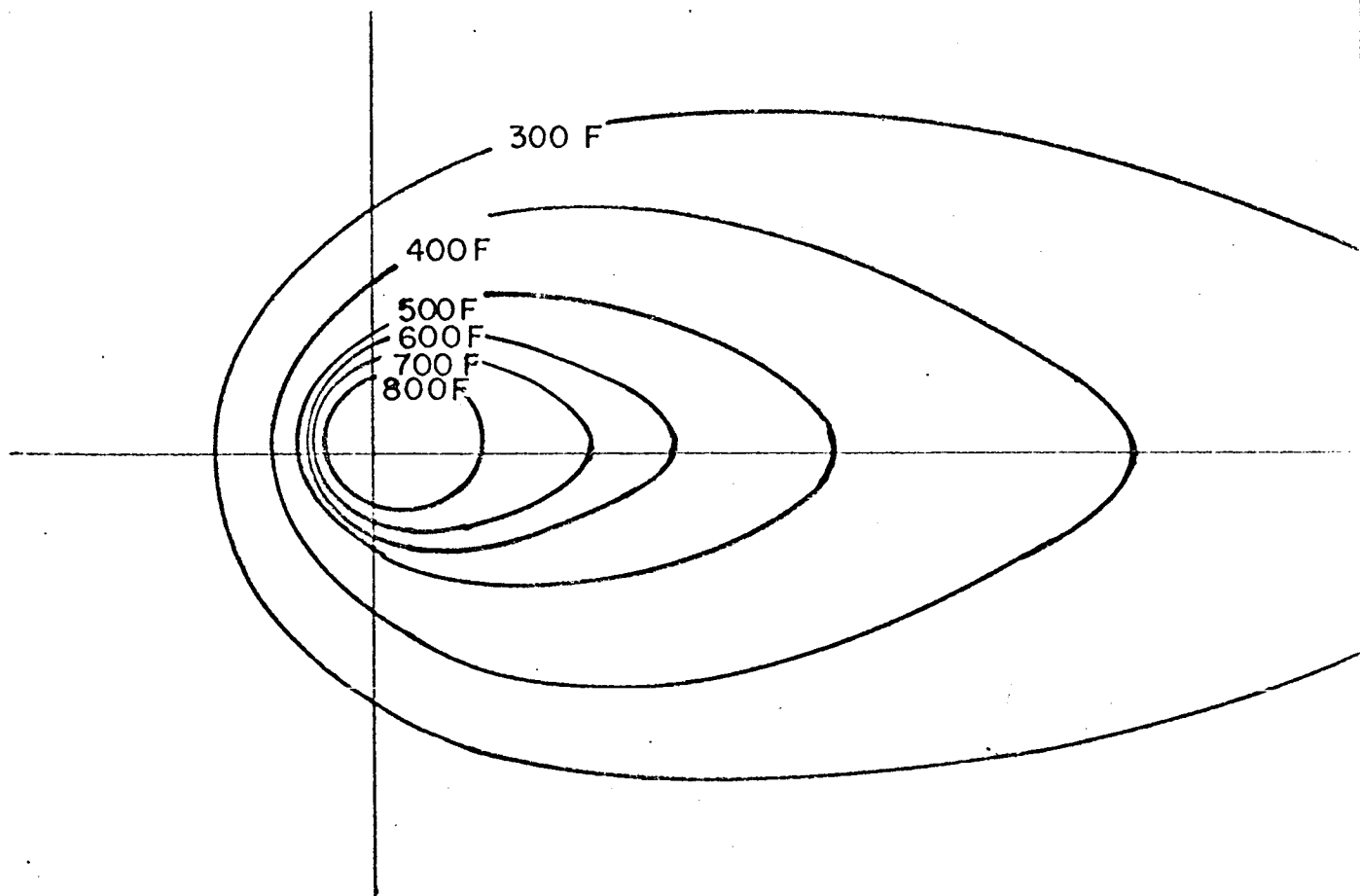
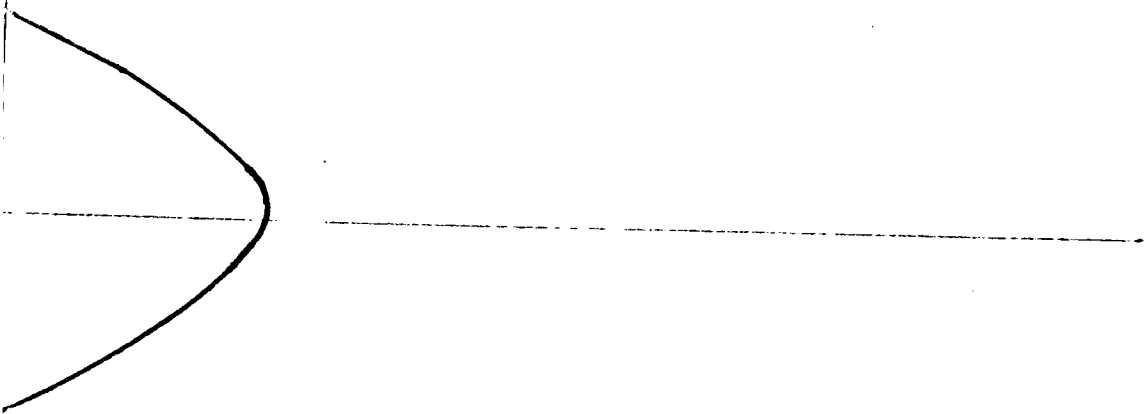


Figure 43 . Thermal Pattern for Weld Panel 2
CO₂ Chilled, $\frac{1}{2}$ Inch 2219-T87



C3-1

Full Scale

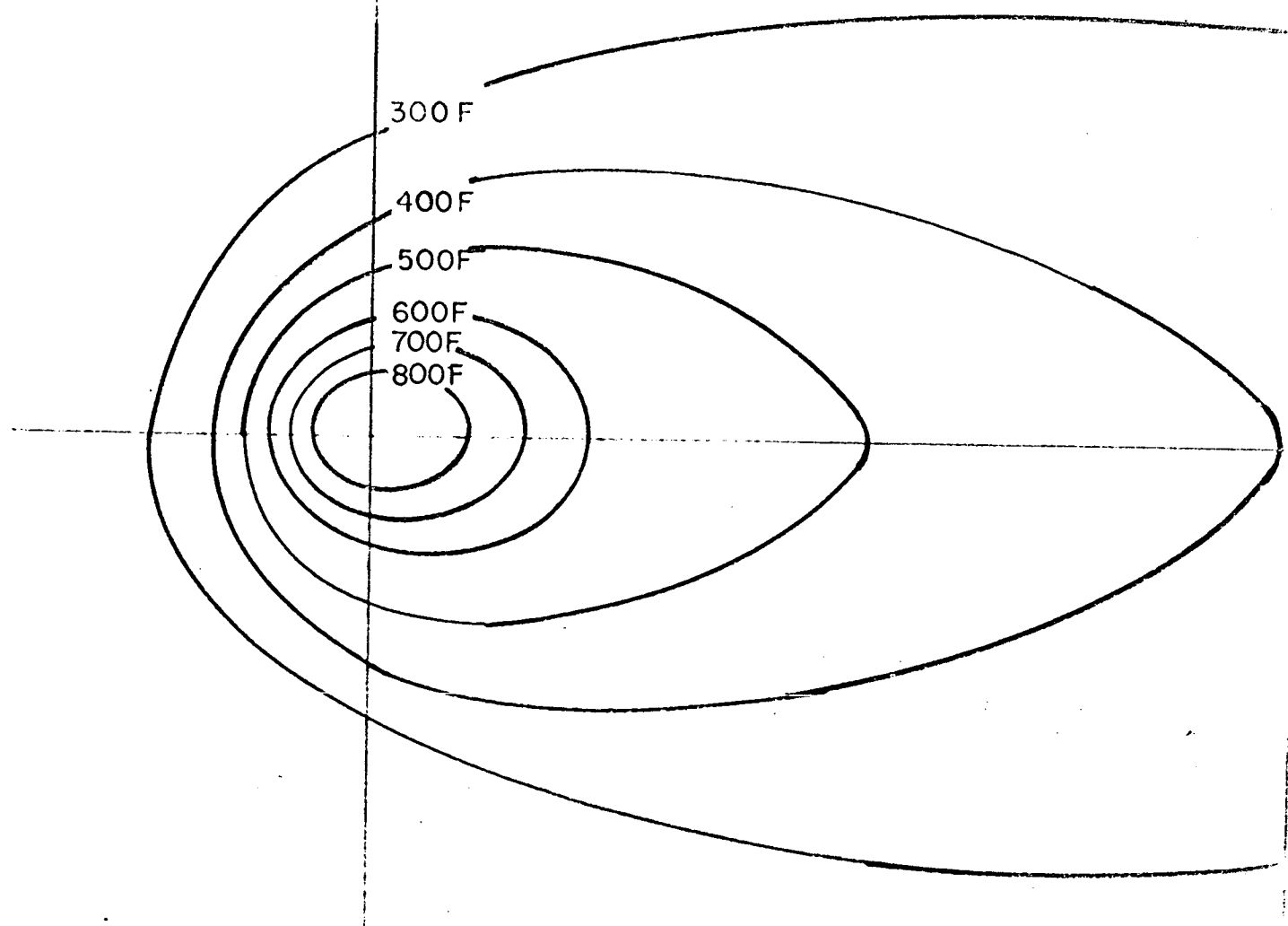
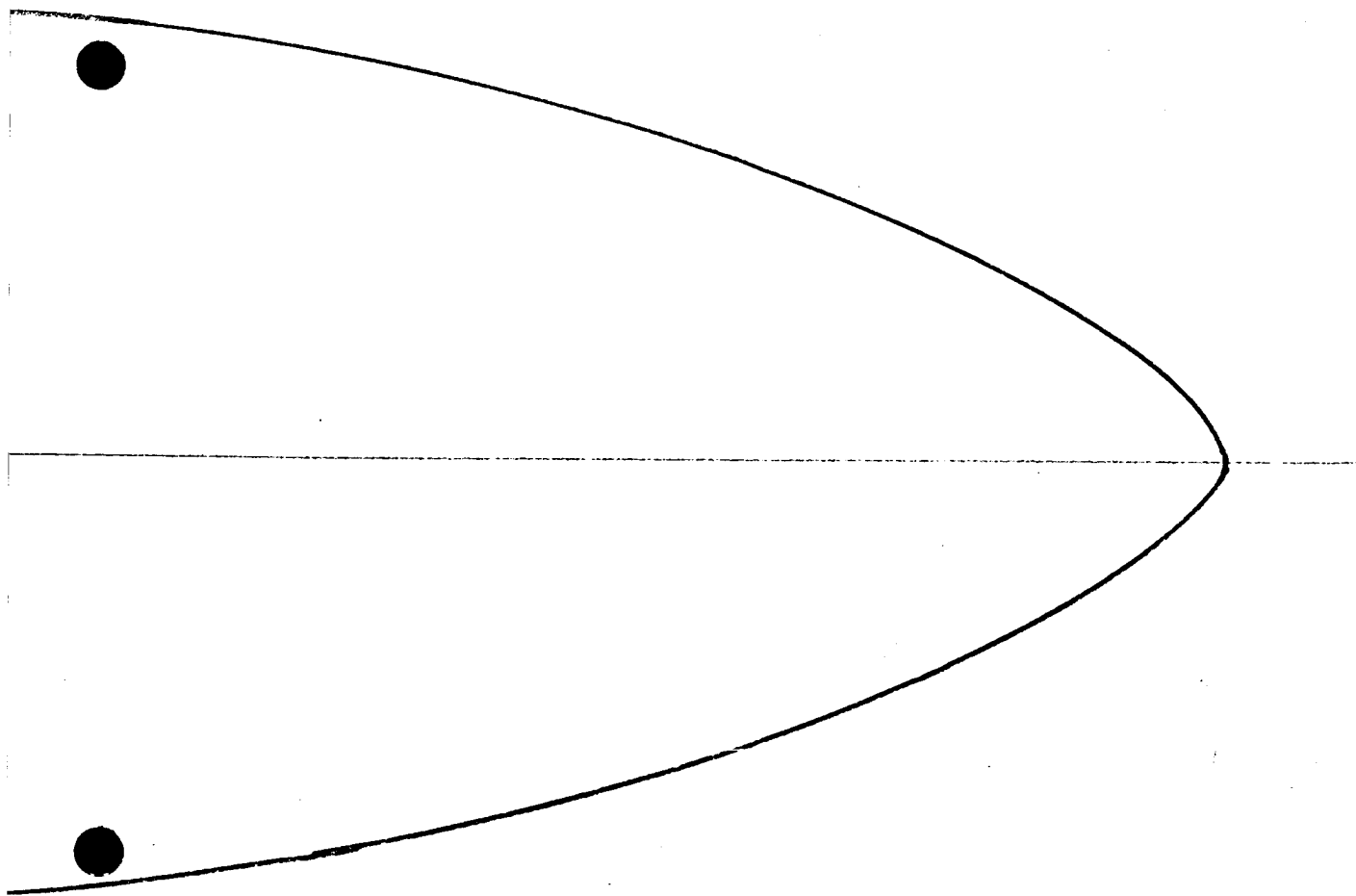


Figure 44. Thermal Pattern for Weld Panel 2
No Chilling, $\frac{5}{16}$ Inch, 2219-T87



-X

Full Scale

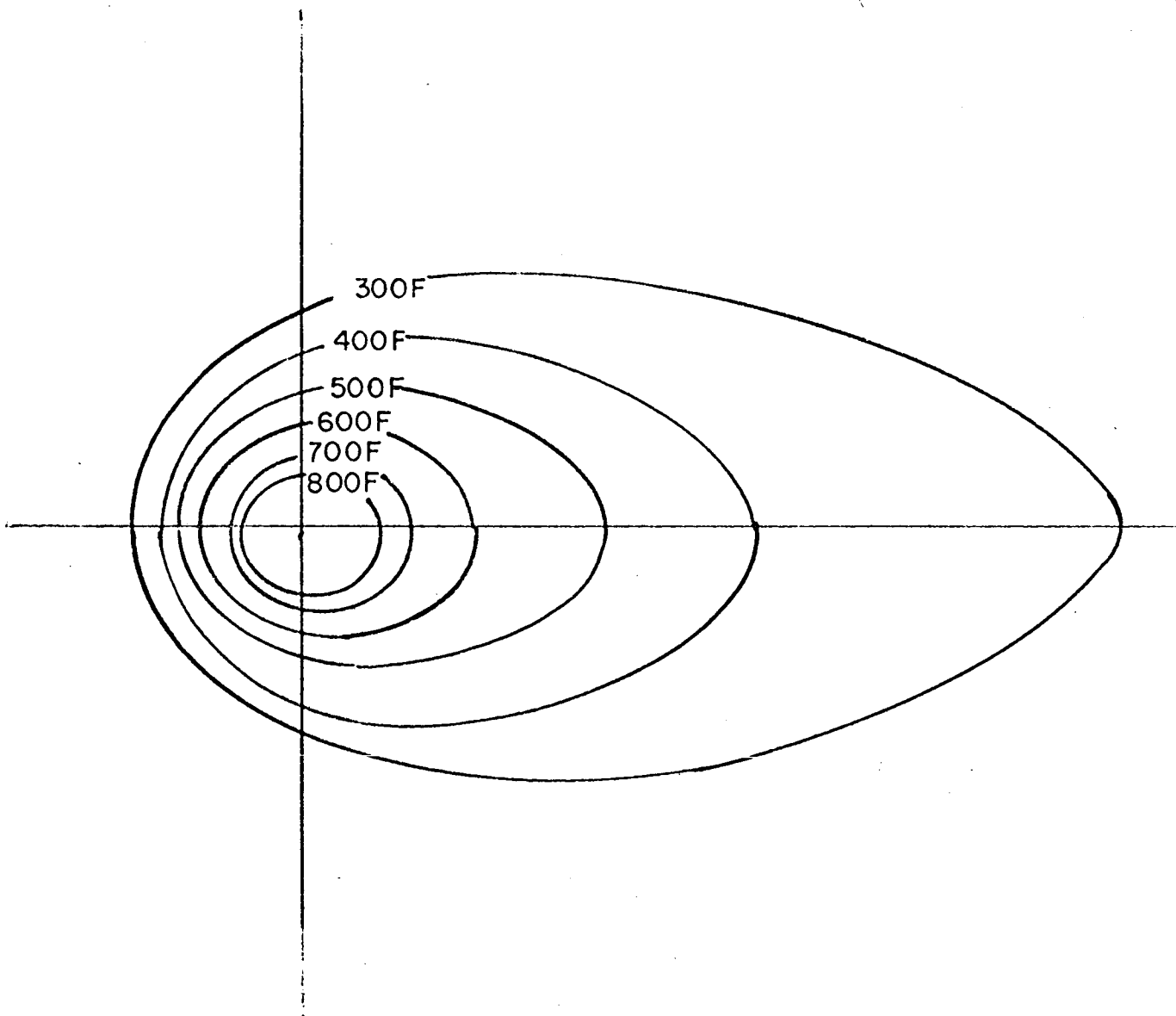
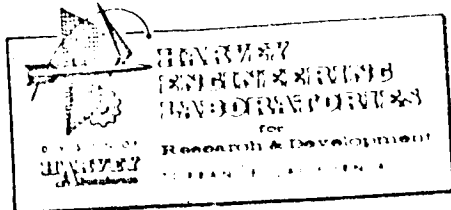


Figure 45. Thermal Pattern for Weld Panel 2AC
CO₂ Chilled, $\frac{5}{16}$ Inch 2219-T87

Full Scale



HA NO. 2283 PAGE A.III.

APPENDIX III

CALCULATION OF THERMAL BALANCE

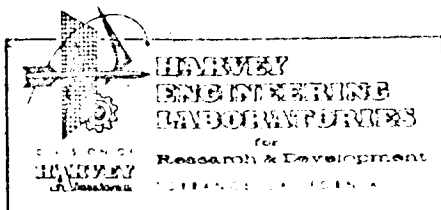
CALCULATION OF THERMAL BALANCE

Table XI shows a calculated estimate of cooling available for altering the thermal pattern of welds chilled by liquid CO₂, using the heat inputs shown in Table XII and the first jet arrangement investigated with a double layer of glass tape on the back side of the welds (Table XIII). From these figures, it appears that a substantial amount of cooling is available for quenching. For the 5/16" plate, 5.6 Btu/in. is available. This would be sufficient to reduce the temperature of a one-inch square portion of the plate approximately 800°F (using a specific heat of 0.25 Btu/lb/°F and neglecting all other heat transfer); for the 1/2-inch plate the available cooling (9.0 Btu/in.) could reduce the temperature 825°F.

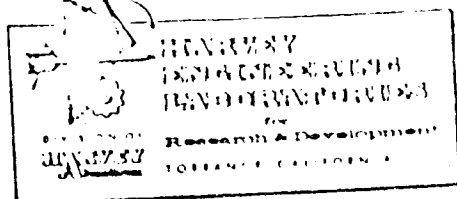


TABLE X1

Cooling Available for Altering the Thermal Pattern of Weld Panels Chilled by Liquid CO₂

Weld Panel	Thickness (inches)	Heat Input (1) (BTU/in.)	Cooling Provided by Liquid CO ₂ (BTU/in) ⁽²⁾		
			Total Provided (50% effc.) ⁽³⁾	Absorbed in Forming Bead ⁽⁴⁾	Available for Quenching ⁽⁵⁾
1A1	5/16	22.2	none	---	---
1EC1	5/16	31.1	14.5	8.9	5.6
1F2	1/2	36.4	none	---	---
1DC3	1/2	44.1	16.7	7.7	9.0

(1) Heat input = $\frac{60 \times E \times I}{V} \times 9.48 \times 10^{-4}$ (See Table 12)

(2) Calculated from vendors data (See Table 13)

(3) Estimated from temperature measurements through backing tape.

(4) Calculated by subtracting the heat input required to effect penetration in an unchilled weld panel from that required to penetrate a chilled panel.

(5) Calculated by subtracting the cooling absorbed in forming the weld bead from the total cooling provided.

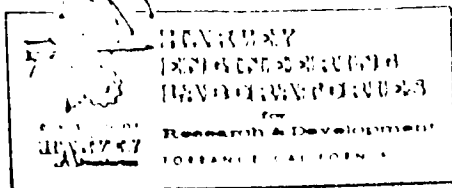
HA NO 2283PAGE A.III.03

TABLE XII

Heat Input for the Penetration Pass in
Unchilled and Liquid CO₂ Chilled Weld Panels;
5/16" and 1/2" 2014-T6 Plates

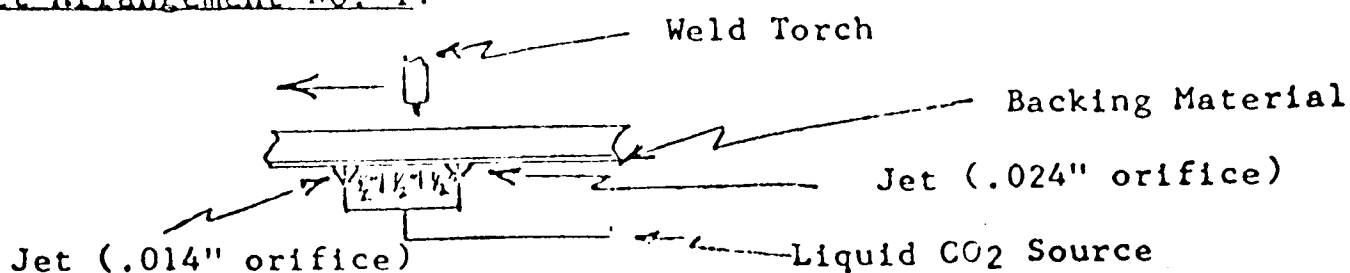
Weld Panel Number	Thickness (inches)	Chilled	Weld Parameters	Heat Input ⁽¹⁾ (BTU/in)
1A1	5/16	no	250 amps 14 volts 9.0 ipm	22.2
1EC1	5/16	yes	235 amps 16 volts 6.9 ipm	31.1
1F2	1/2	no	300 amps 16 volts 7.5 ipm	36.4
1DC3	1/2	yes	310 amps 15 volts 6.0 ipm	44.1

(1) Heat input = $\frac{60 \times E \times I}{V} \times 9.48 \times 10^{-4}$ BTU/in.

TABLE XIII

Heat Extraction Expected by Liquid CO₂ Chilling
During Penetration Pass of Weld Panels in
in 5/16" and 1/2" 2014-T6 Plate

Jet Arrangement No. 1:



Backing Material No. 1: Adhesive glass tape over non-adhesive glass tape.

Liquid CO₂ at 300 psig:

Latent heat of vaporization plus sensible heat at 70°F = 150 BTU/lb. (Approx.)

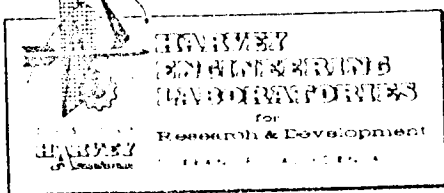
Delivery Rate: .014" orifice = 22 #/hr. = .0061#/sec. = .918 BTU/sec.

.024" orifice = 58 #/hr. = .0161#/sec. = 2.425 BTU/sec.

Total = 80 #/hr. = .0222#/sec. = 3.343 BTU/sec.

Total (at estimated 50% effic.) = 1.674 BTU/sec.

Weld Panel No.	Travel		Chilling Available at 50% effic. (BTU/in)
	(ipm)	(sec/in.)	
1EC1	6.9	8.7	14.5
1DC3	6.0	10	16.7

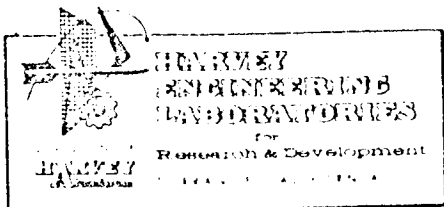


HA NO. 2283 PAGE A.III.

APPENDIX IV

DEVELOPMENT OF CO₂ SHIELDS FOR

FRONT SIDE CHILLING



DEVELOPMENT OF CO₂ SHIELDS FOR FRONT SIDE CHILLING

Stationary Shields for Front Side Chilling

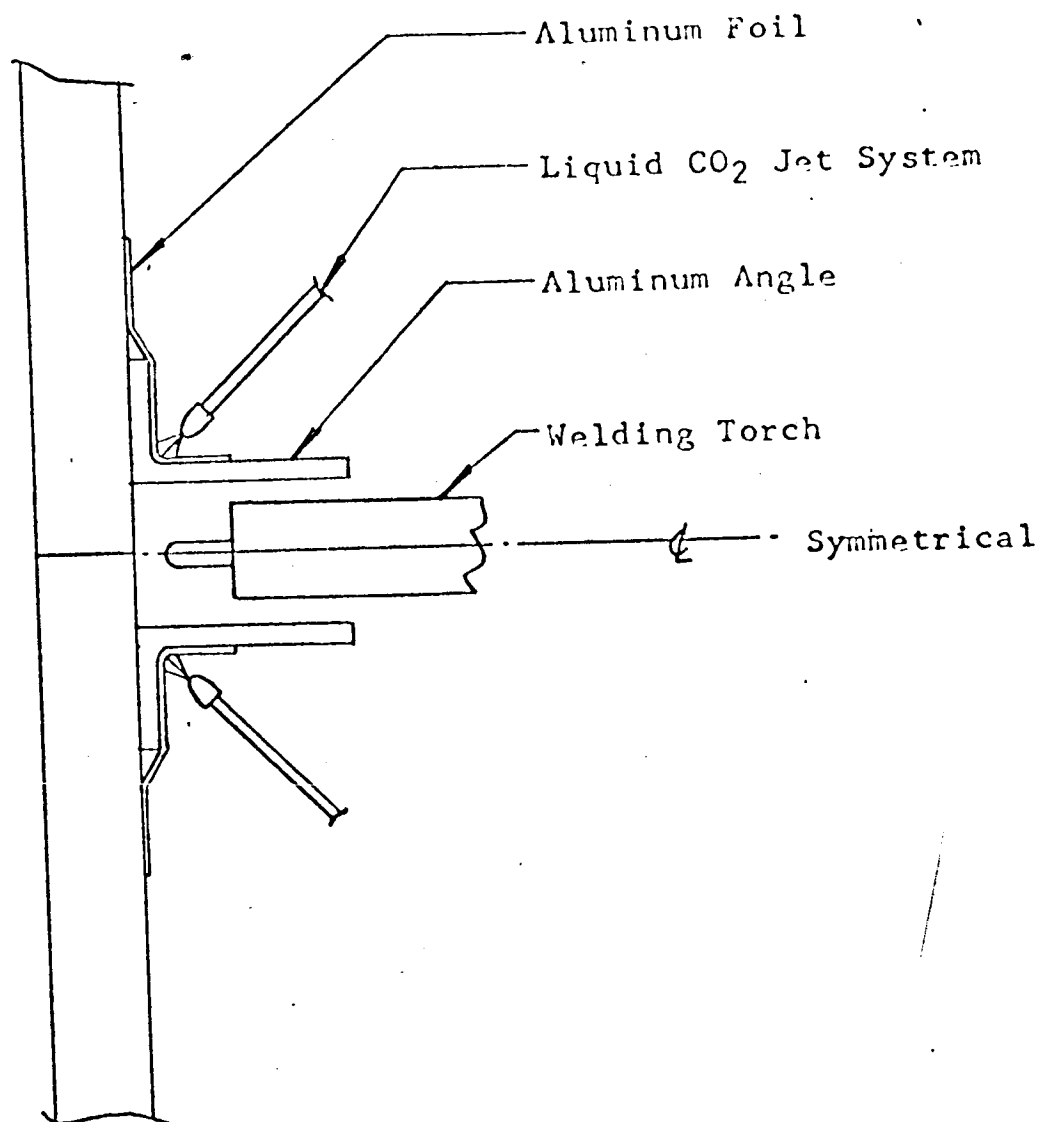
The first concept tried for applying liquid CO₂ chilling to the front side of the weldment, consisted of two aluminum divider strips fixed in place on each side of the welding torch parallel to the weld seam as shown in Figure 46. A metallic foil, fastened to the dividers, was used as a seal to prevent CO₂ from leaking into the arc area. The liquid CO₂ jets were positioned on the outer side of each divider, and travelled with the welding torch. This concept proved effective for preventing interference with the welding arc, but did not result in adequate chilling of the weld.

Traveling Shield with Foil Shoe

In order to permit positioning of liquid CO₂ jets on or near the weld bead immediately after welding, a shielding device such as shown in Figure 47 was fabricated. The aluminum foil seal to prevent the CO₂ from entering the arc area was fastened to the aluminum shield with adhesive tape to form a "shoe" which was dragged behind the shield and into which the liquid CO₂ jets were directed. Although increased chilling was obtained using this concept, it was still extremely inefficient due to insulation produced by the foil and air layer between the CO₂ jets and the weldment. A further disadvantage was that aluminum foil was not sufficiently strong, and tears developed when traveling over rough portions of the weld bead, causing leaking of CO₂ into the welding arc.

Traveling Shield with Skirt

Best heat transfer is obtained, of course, when the liquid CO₂ jets impinge directly on the weldment surface. In order to accomplish direct impingement, the shielding device shown in Figure 48 was fabricated. This system consists of an aluminum shield with a liquid CO₂ jet manifold on the side opposite the torch. In order to prevent CO₂



Sketch of Jet System Arrangement
for Chilling Weldments from Front Side
using a Stationary Shield.

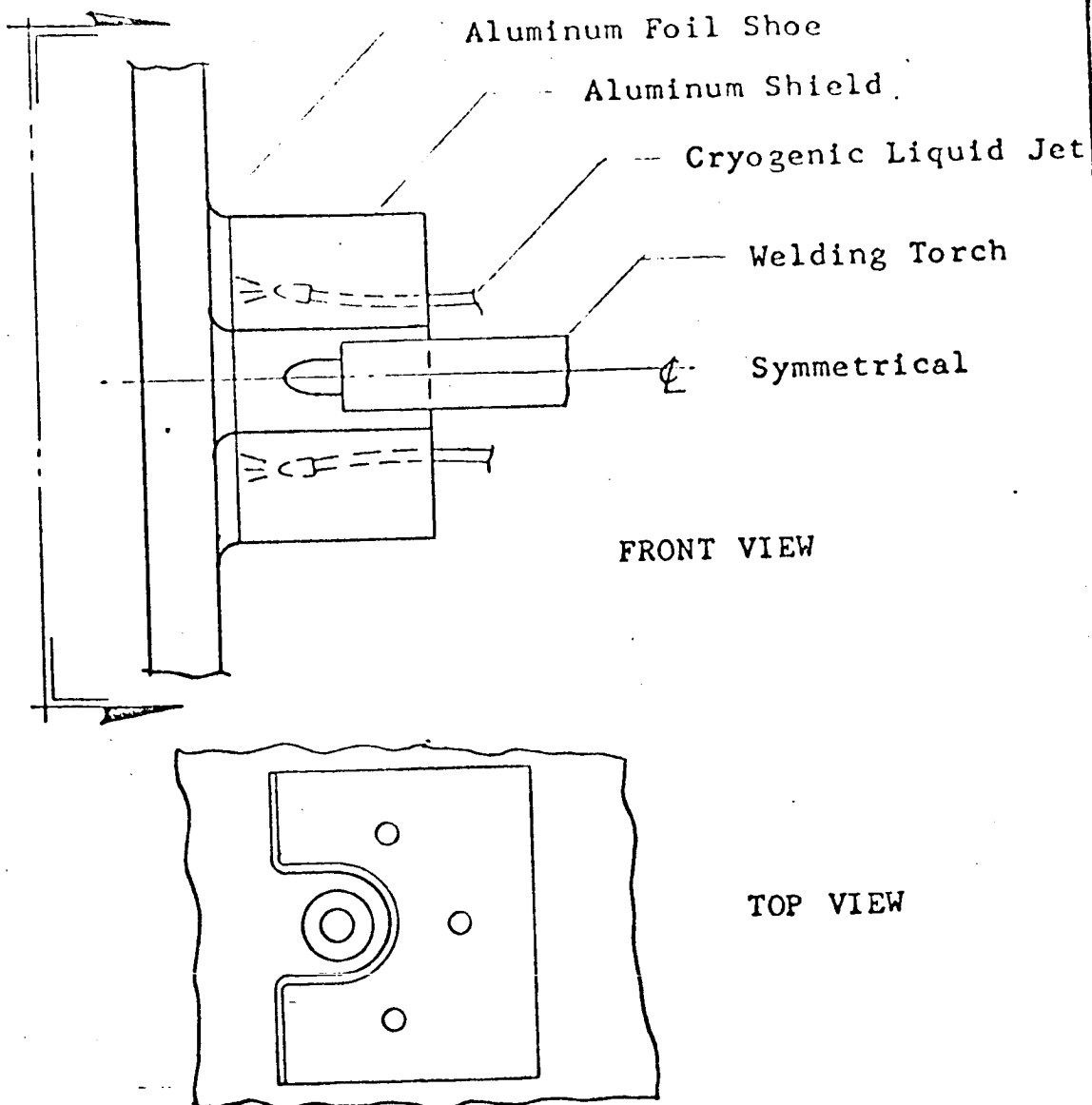


Figure 47. Jet System No. 2 for Front Side Chilling of Weldments using a Cryogenic Liquid — Traveling Shield with Metal Foil Shoe

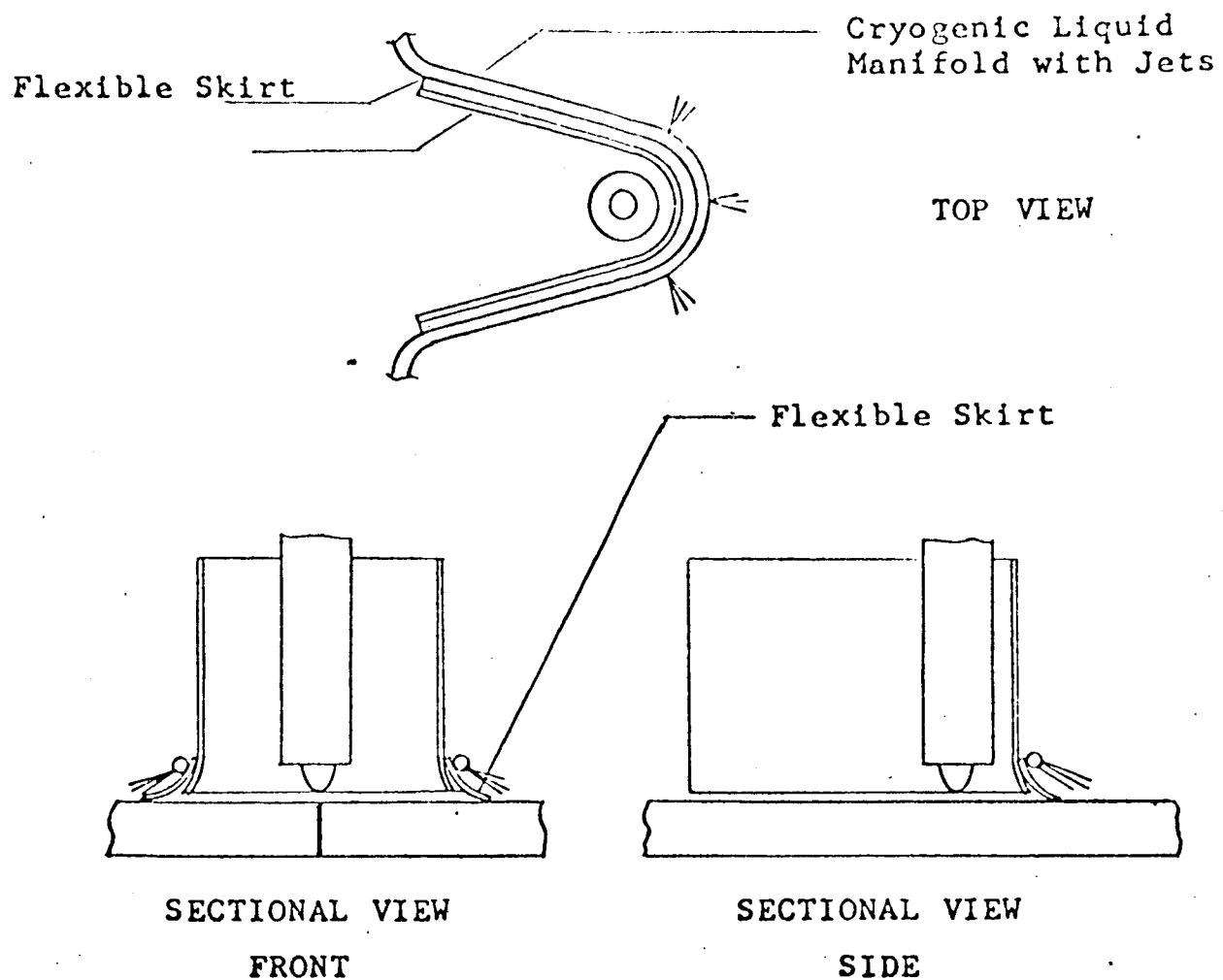
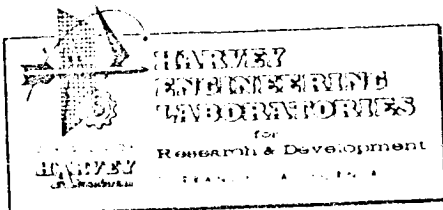


Figure 48. Jet System No. 3 for Front Side Chilling of Weldments using a Cryogenic Liquid — Traveling Shield with Flexible Skirt Seal



from leaking into the arc area, a skirt which dragged on the surface of the weldment was attached to the aluminum shield. Several materials were tried for the skirt, including glass tape, mylar strip, thin steel strip and thin copper strip. Glass tape and mylar strip did not successfully withstand the service conditions of extreme heat and cold along with abrasion. The metal strips possessed sufficient properties to withstand the environment, but were not sufficiently flexible to conform to small irregularities in the surface of the weldment, permitting CO_2 to leak into the arc.

Traveling Shield with Skirt and Helium Purge

Systems for purging CO_2 from the arc area were devised, as shown in Figures 49, 50, and 51. The first concept (shown in Figure 49) purged only the back end of the shield. It was noted that a draft was created in this system, which caused air to be drawn into the arc. A ring-type helium purge manifold (shown in Figure 50) was then fabricated to prevent introduction of air, but also resulted in arc disturbances. It was thought that the individual purge jets caused eddy currents and turbulence, and the bell-type purge (shown in Figure 51) was used. While this system appeared to purge the CO_2 from the weld area, extreme arc instability occurred. The reasons for this instability were not determined, and rather than devote an extended study period to develop a detailed analysis of gas flow, the helium purge technique has been set aside in favor of developing a metallic wool seal.

Traveling Shield with Metallic Wool Seal

The shield used for helium purge technique was modified by removing the helium manifold and adding a flange (half tube) around the lower edge of the shield to contain a roll of metallic wool as shown in Figure 52. Steel wool performed quite well but had a tendency to "burn" and "mat down" behind the arc. Fine bronze wool indicated better resistance to this tendency. Satisfactory bead on plate welds were made with this system, but the need for increased chilling was indicated by the thermal cycle curves and macrosections of bead on plate

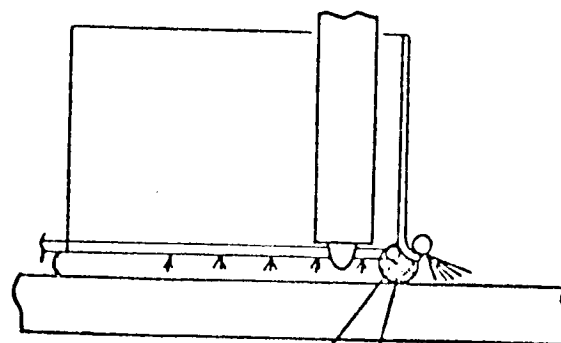
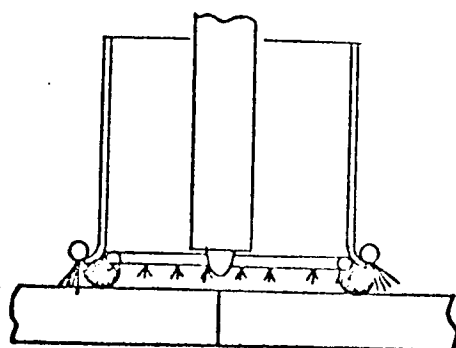
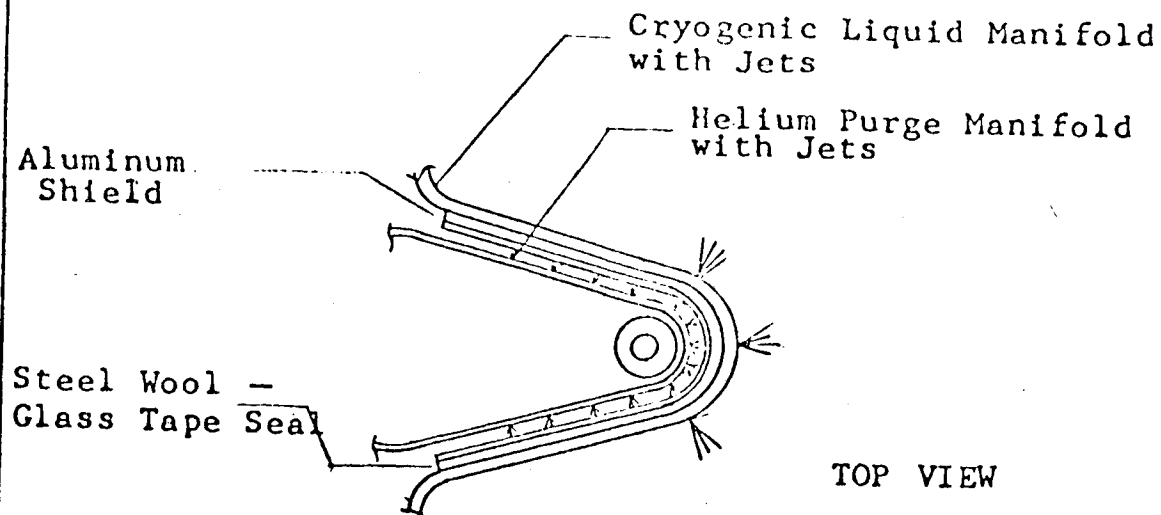


Figure 49. Jet System No. 4 for Front Side Chilling of Weldments using a Cryogenic Liquid — Traveling Shield with Helium Purge Manifold

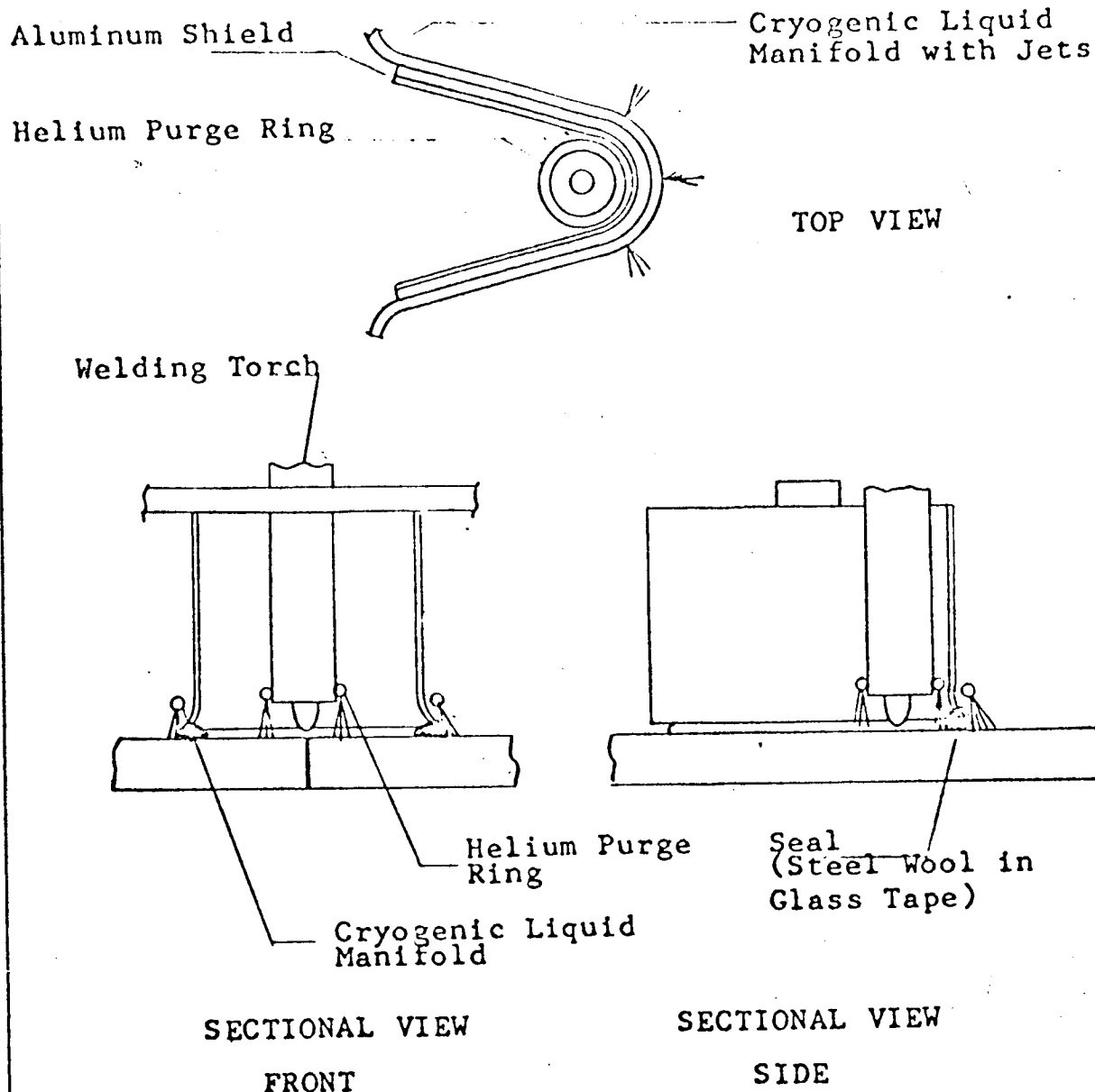


Figure 50. Jet System No. 5 for Front Side Chilling of Weldments using a Cryogenic Liquid — Traveling Shield with Helium Purge Ring

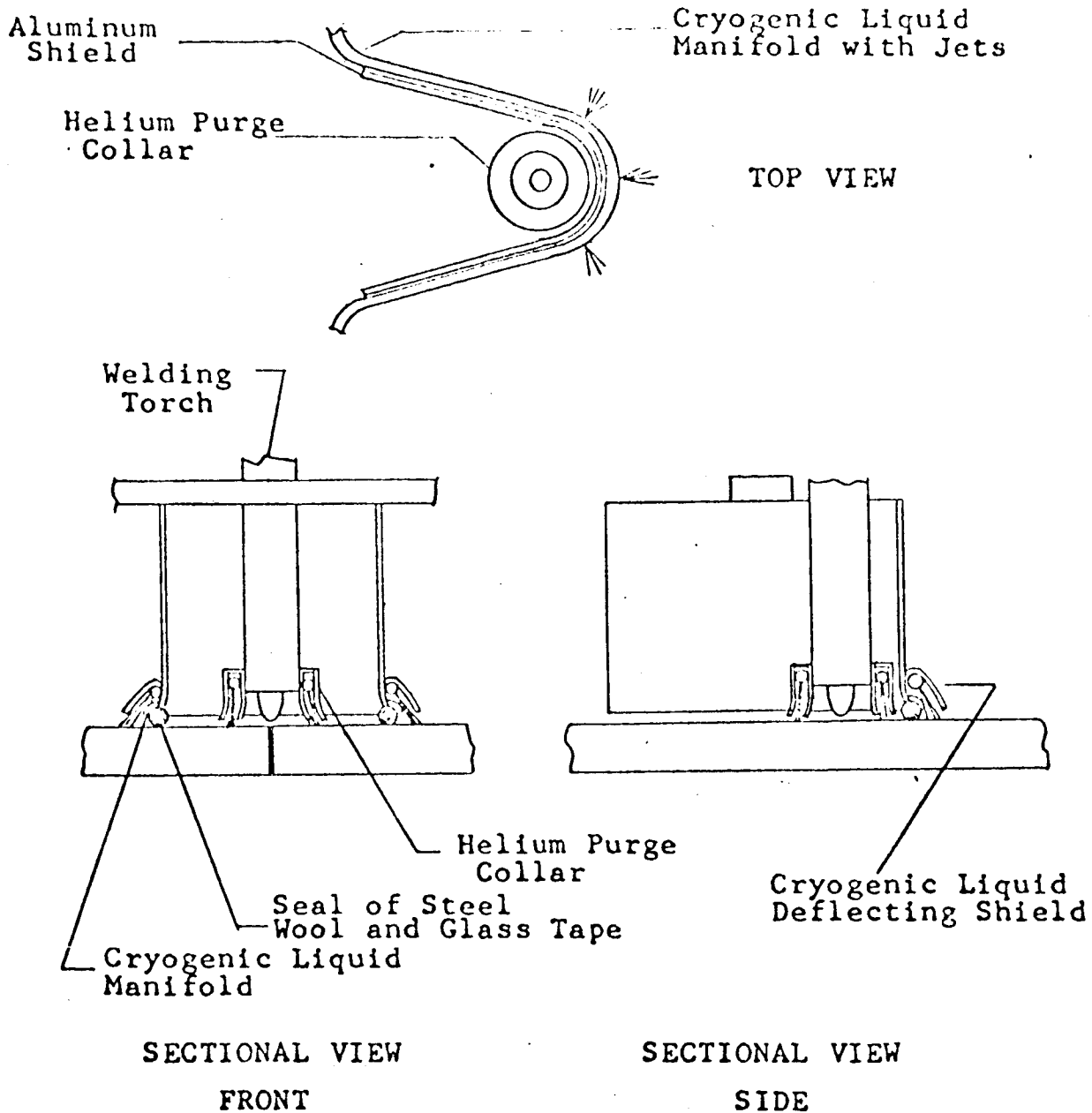


Figure 51. Jet System No. 6 for Front Side Chilling of Weldments using a Cryogenic Liquid — Traveling Shield with Helium Purge Collar

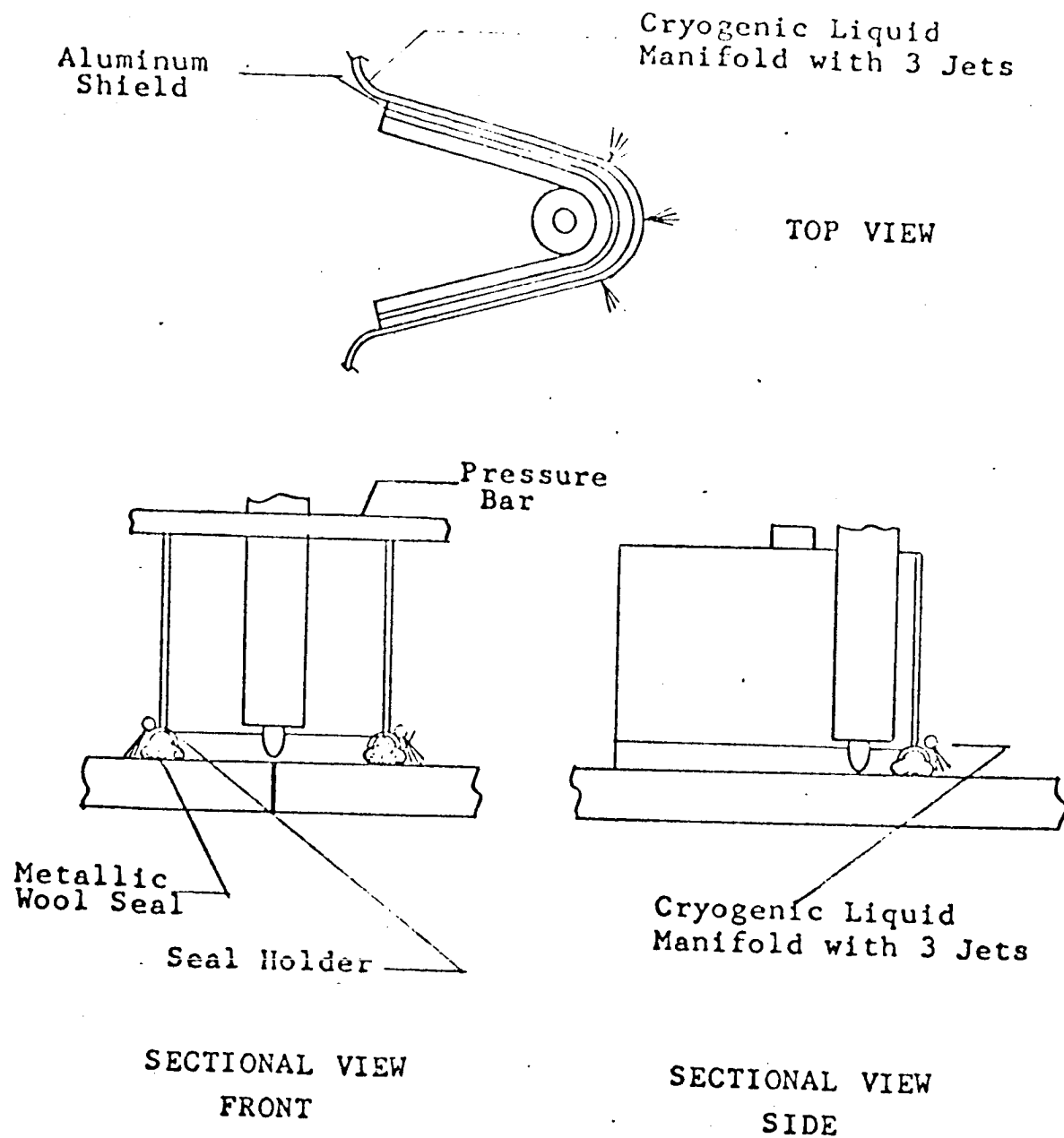
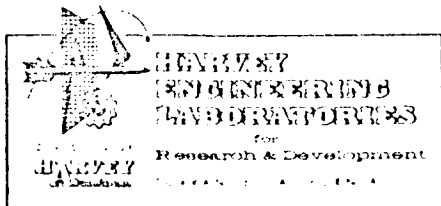


Figure 52. Jet System No. 7 for Front Side Chilling of Weldments using a Cryogenic Liquid — Traveling Shield with Metallic Wool Seal - 3 Jet Manifold



welds. In an attempt to obtain a higher order of chilling, the liquid CO_2 manifold was then modified by adding two additional orifices (Jet System No. 8) as shown in Figure 53. Comparison of typical cooling curves and macrosections shows that modification of Jet System No. 7 by adding two more jet orifices did not appreciably affect the chilling. It was determined that addition of these orifices resulted in a pressure drop in the liquid CO_2 line below the inlet solenoid which, in combination with² the pressure drop between the tank outlet and the manifold solenoid, effectively delivered approximately the same amount of liquid CO_2 to the weld area as Jet System No. 7. It was found that by by-passing the solenoid too much pressure was delivered to the chilling jets. This pressure was reduced by changing the outlet orifice of the liquid CO_2 tank from $3/8"$ to $3/64"$. At the same time, two additional orifices were added to the jet manifold in a position slightly ahead of the arc in an effort to increase the weld cooling gradient. These modifications resulted in Jet System No. 9 which is shown in Figure 54. This system produced greatly increased chilling as shown by typical thermal cycle curves. Macrosections of bead on plate welds in $1/2"$ plate verified the increased cooling.

Although Jet System No. 9 was capable of producing acceptable welds with a high degree of chilling, it was quite sensitive to sharp surface irregularities on the plate or weld bead.

In order to provide a seal which would conform to such irregularities, the concept of a fine wire brush to back up the metallic wool over the weld seam area was developed. Organic bristles would not withstand the heat from the weld bead, and suitable metal bristle brushes were not available. It was, therefore, necessary to fabricate a semi-circular metal backed brush approximately $1\ 1/2$ inches long and containing .005-inch stainless steel bristles approximately one inch long. This brush, when inserted in the back end of the trailing shield as shown in Figure 55, was flexible enough and sufficiently dense to conform to irregular weld bead contours and prevent gross leakage of CO_2 into the arc area. There was some evidence, however, of minor leaks, and these were thought to be due to non-uniform pressure of the steel wool seal against the weldment surface resulting from local variation in the density of the steel wool "roll".

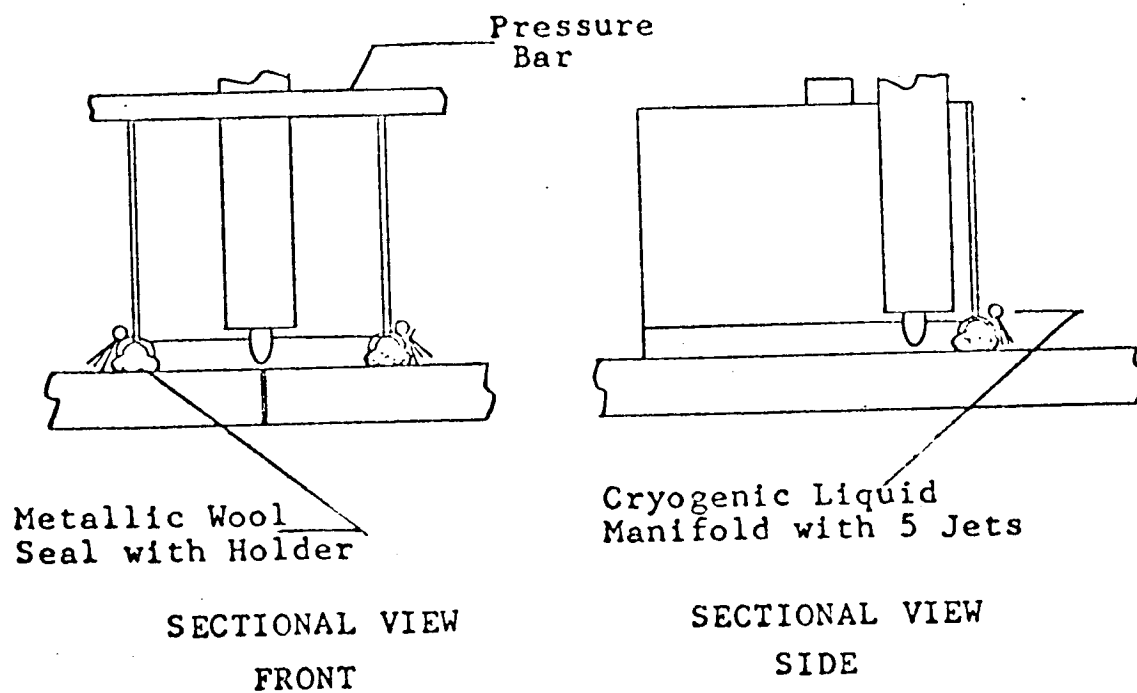
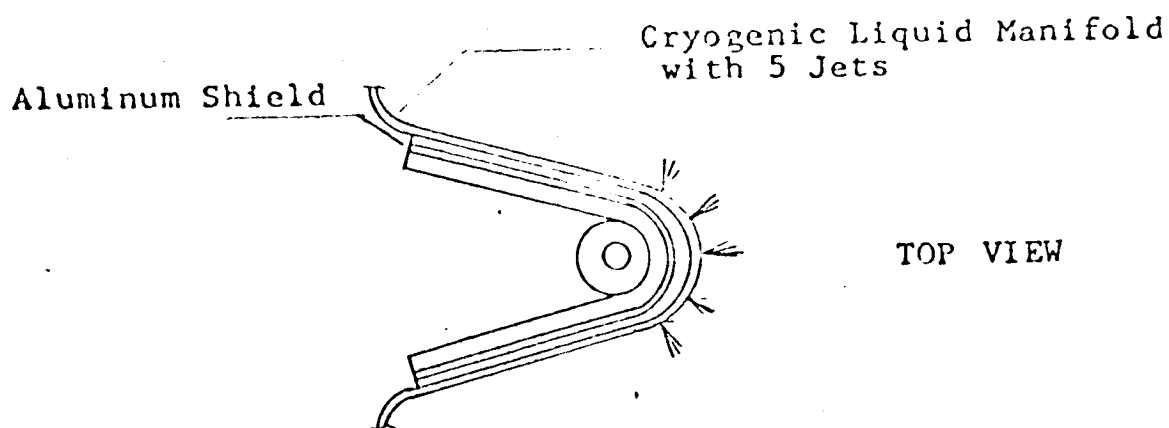


Figure 53 . Jet System No. 8 for Front Side Chilling of Weldments using a Cryogenic Liquid — Traveling Shield with Metallic Wool Seal - 5 Jet Manifold

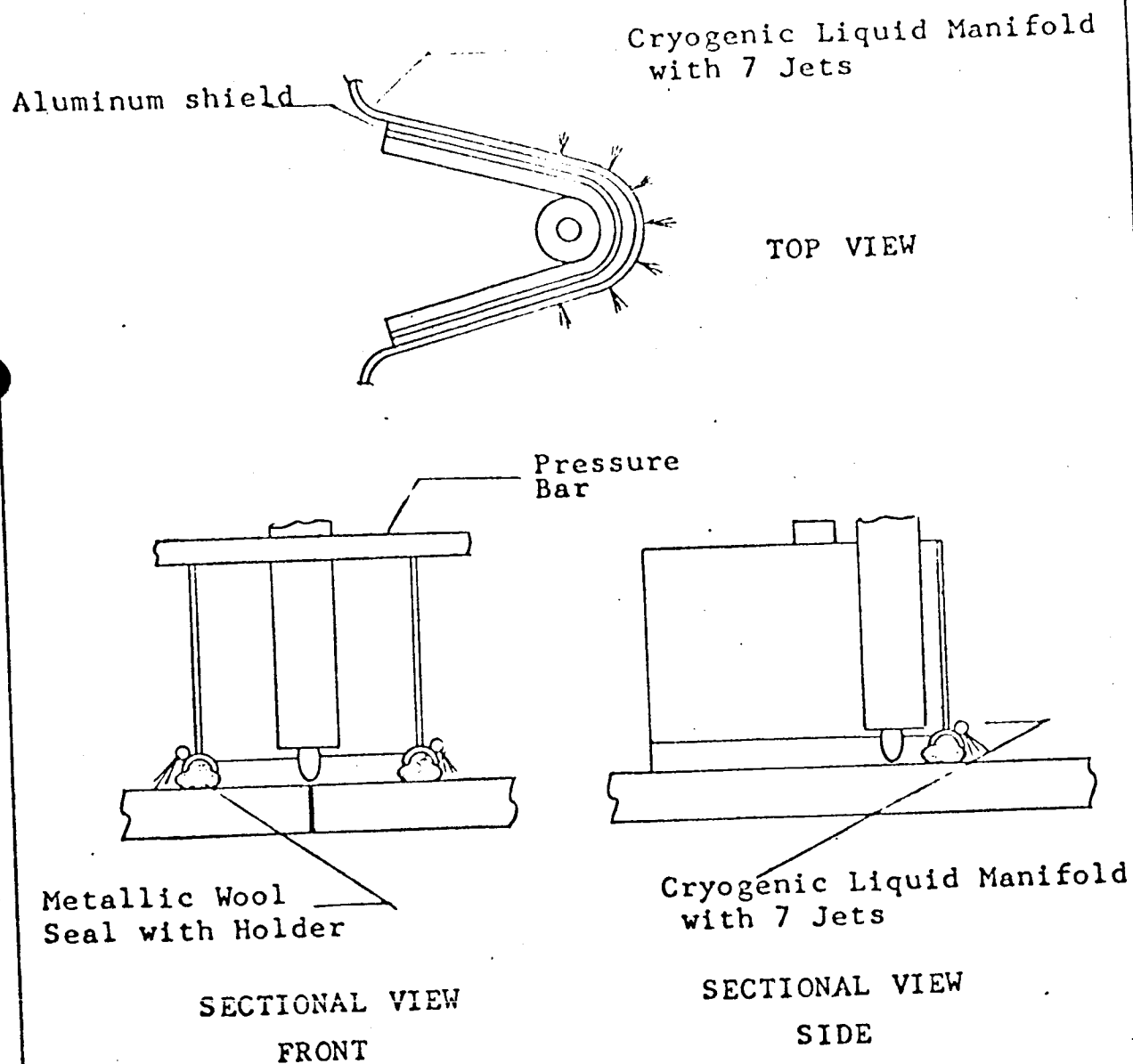


Figure 54. Jet System No. 9 for Front Side Chilling of Weldments using a Cryogenic Liquid — Traveling Shield with Metallic Wool Seal - 7 Jet Manifold

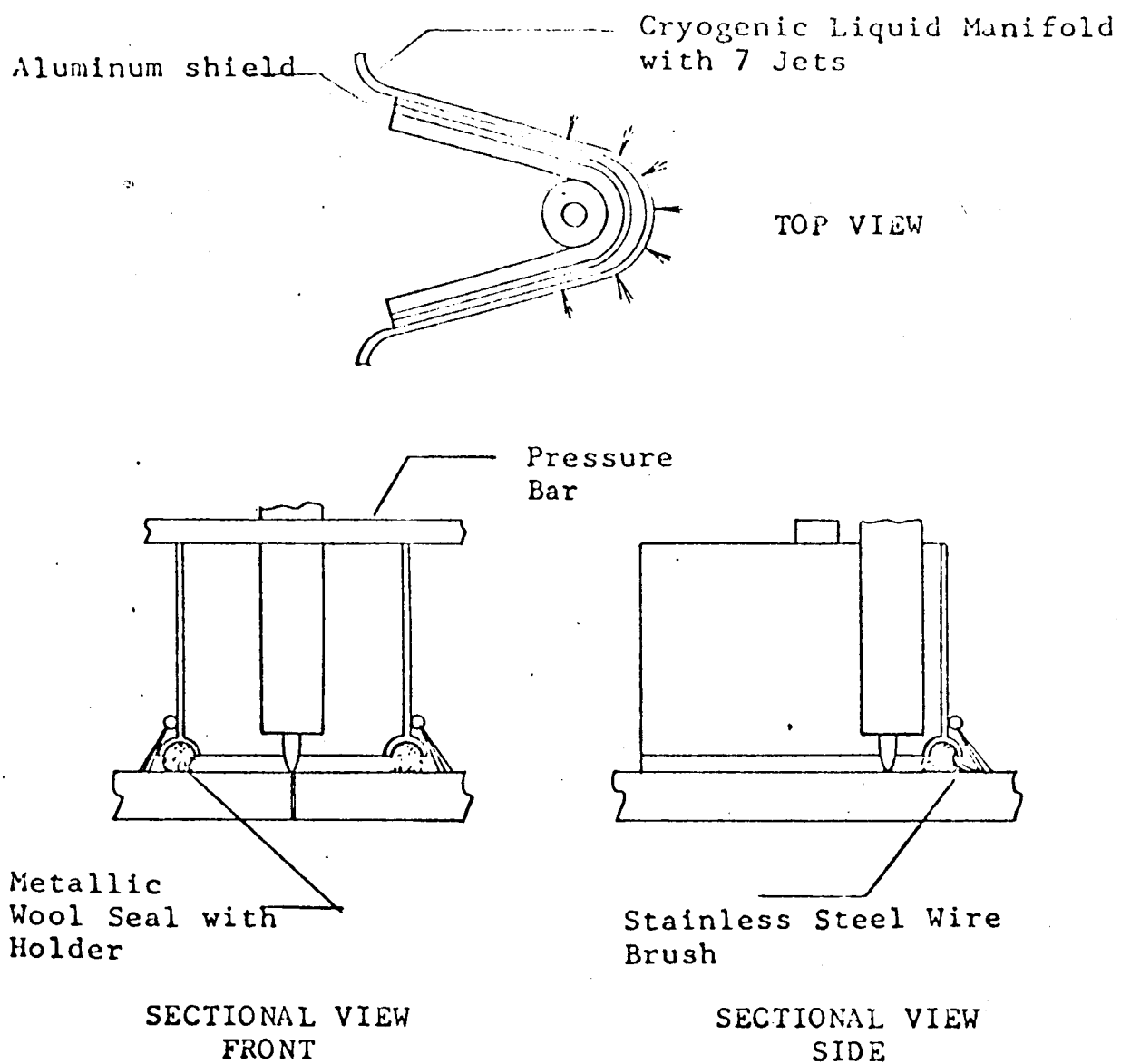
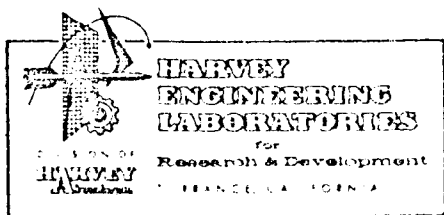


Figure 55. Jet System No. 10 for Front Side Chilling of Weldments using a Cryogenic Liquid -- Traveling Shield with Metallic Wool and Wire Brush Seal - 7 Jet Manifold



To overcome the variations in density of the hand-rolled steel wool seal, a concept for spring loading the seal at intervals of 1/2-inch was devised. The half tube holder was removed from Jet System No. 10 and replaced with a one-inch deep channel into which 1/2" and 5/8" No. 4 springs were fastened as shown in Figure 56.

While spring loading of the steel wool appeared to provide a seal of more uniform density, it did not have the required flexibility to fill in depressions and sharp discontinuities on the surface of the weld bead. Therefore, the wire brush used in Jet System No. 10 was adapted for use on the new system as shown in Figure 57.

On a high percentage of the trial runs, this shield performed satisfactorily. In order to attain increased assurance of completely eliminating CO₂ from the arc area, a helium purge was provided through the steel wool shield as shown in Figure 58.

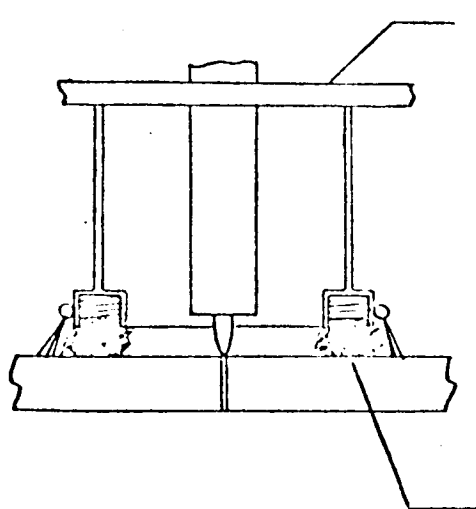
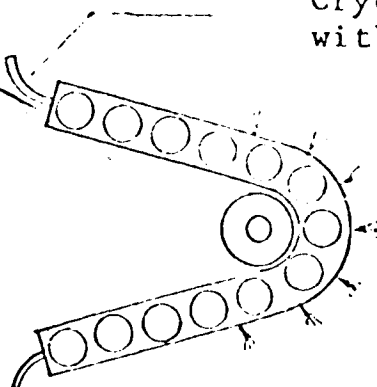
To provide more abrasion resistance for the steel wool seal and to direct the flow of the helium purge away from the arc, a copper skirt was inserted in the shield between the arc and the steel wool, as shown in Figure 12 in the body of this report. This jet system performed satisfactorily on repeated trial runs, and was, therefore, used to fabricate CO₂ chilled welded panels for mechanical property determinations.

Figures 59 through 63 show typical thermal cycle curves for 1/2" plate, illustrating the charges effected by five of the jet systems.

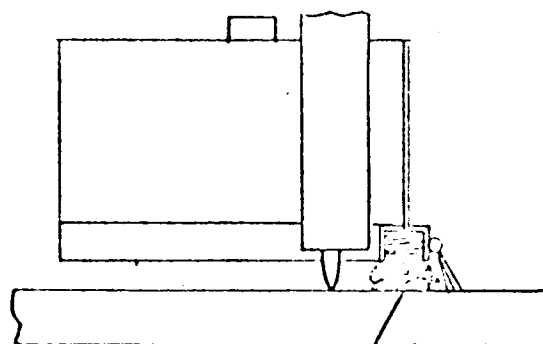
Aluminum Shield
with
Multiple Spring
Hold-down Channel

Cryogenic Liquid Manifold
with 7 Jets

TOP VIEW



Pressure
Bar



Spring Loaded
Metallic Wool Seal

SECTIONAL VIEW
FRONT

SECTIONAL VIEW
SIDE

Figure 55. Jet System No. 11 for Front Side Chilling
of Weldments using a Cryogenic Liquid--
Traveling Shield with Spring Loaded Metallic
Wool 7 Jet Manifold

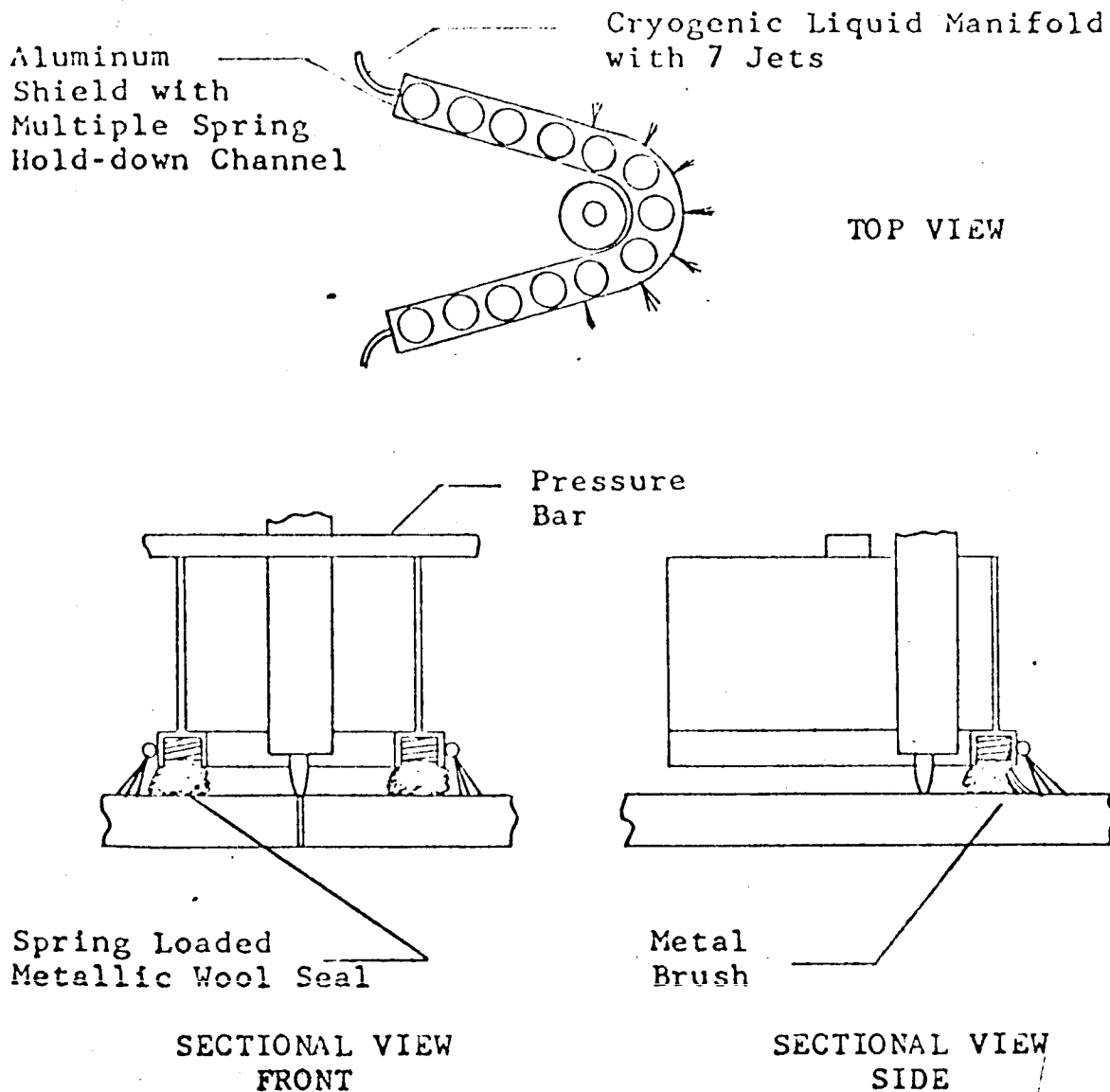


Figure 57. Jet System No. 12 for Front Side Chilling using a Cryogenic Liquid--Traveling Shield with Spring Loaded Metallic Wool and Wire Brush Seal - 7 Jet Manifold

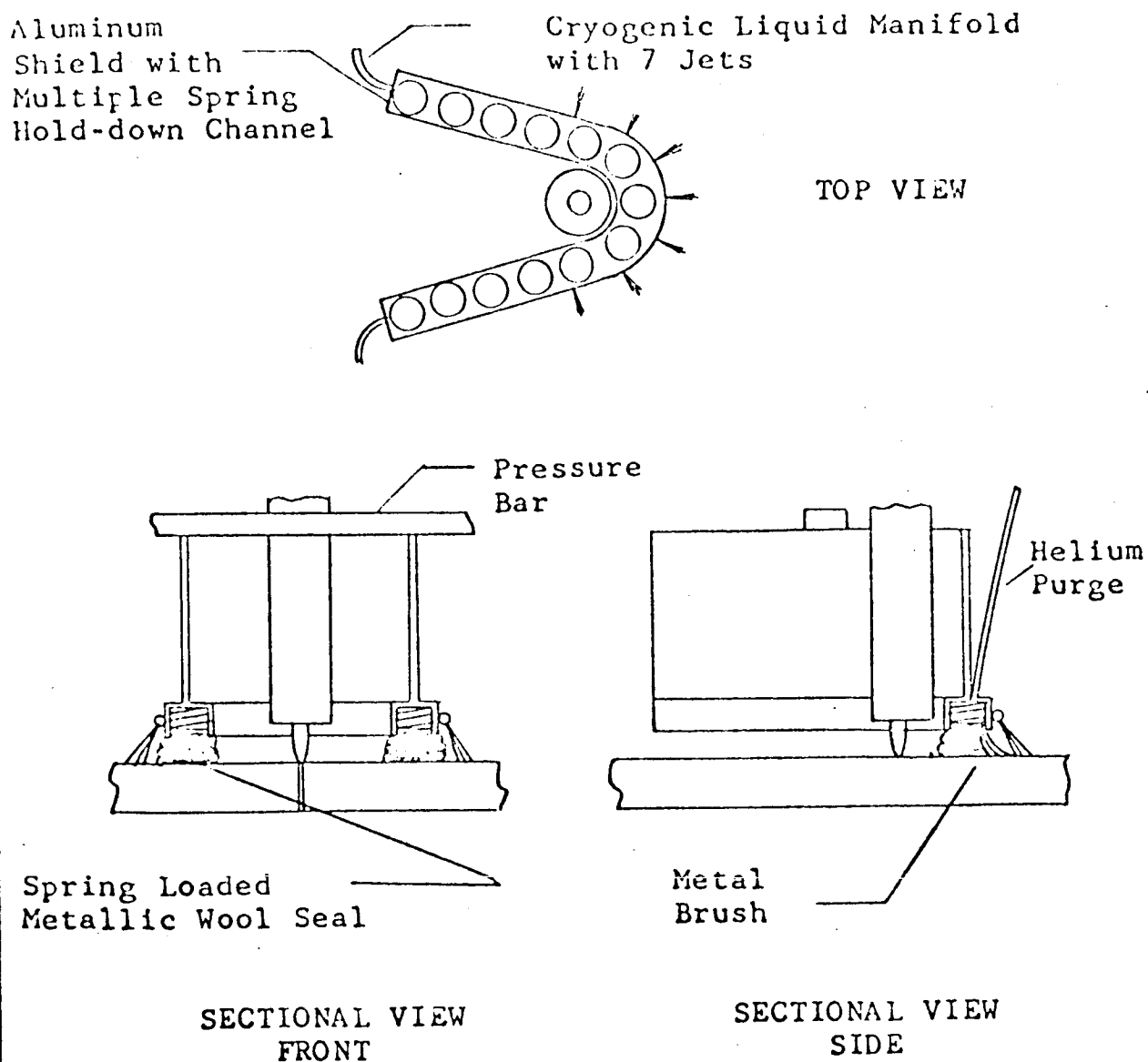


Figure 58.. Jet System No. 13 for Front Side Chilling using a Cryogenic Liquid--Traveling Shield with Spring Loaded Metallic Wool and Wire Brush Seal, Helium Purged - 7 Jet Manifold

TYPICAL THERMAL CYCLE CURVES FOR A
POINT 3/8" FROM WELD CENTERLINE OF
BEAD ON PLATE WELDS IN 1/2" ALUMINUM
PLATE. BOTH CHILLED AND UNCHILLED
WELDS WERE MADE WITH THE SAME HEAT
INPUT.

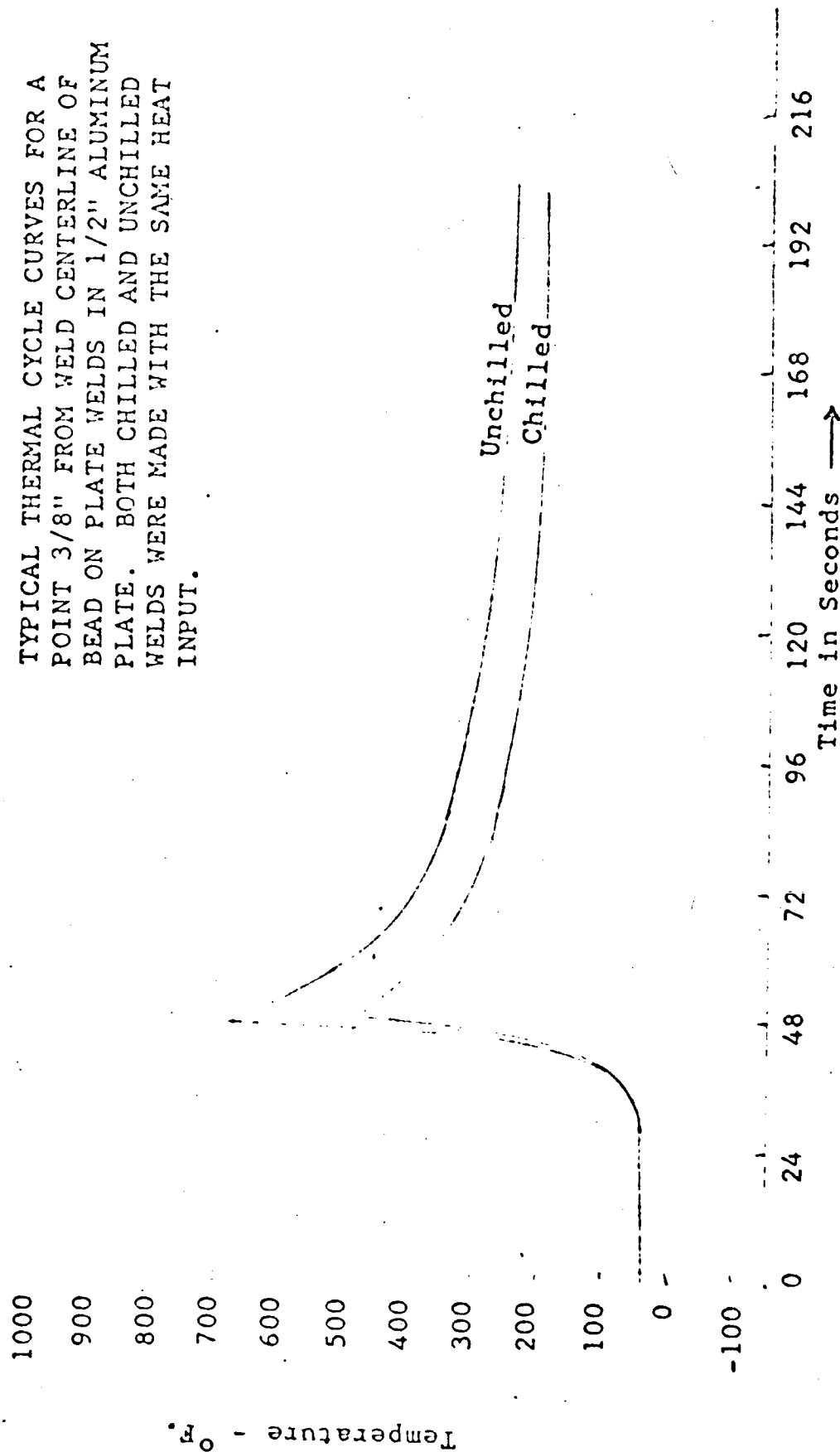


Figure 59. Effect of Front Side Chilling on Thermal Cycle Curves
Jet System No. 1

TYPICAL THERMAL CYCLE CURVES FOR A
POINT 3/8" FROM WELD CENTERLINE OF
BEAD ON PLATE WELDS IN 1/2" ALUMINUM
PLATE. BOTH CHILLED AND UNCHILLED
WELDS WERE MADE WITH THE SAME HEAT
INPUT.

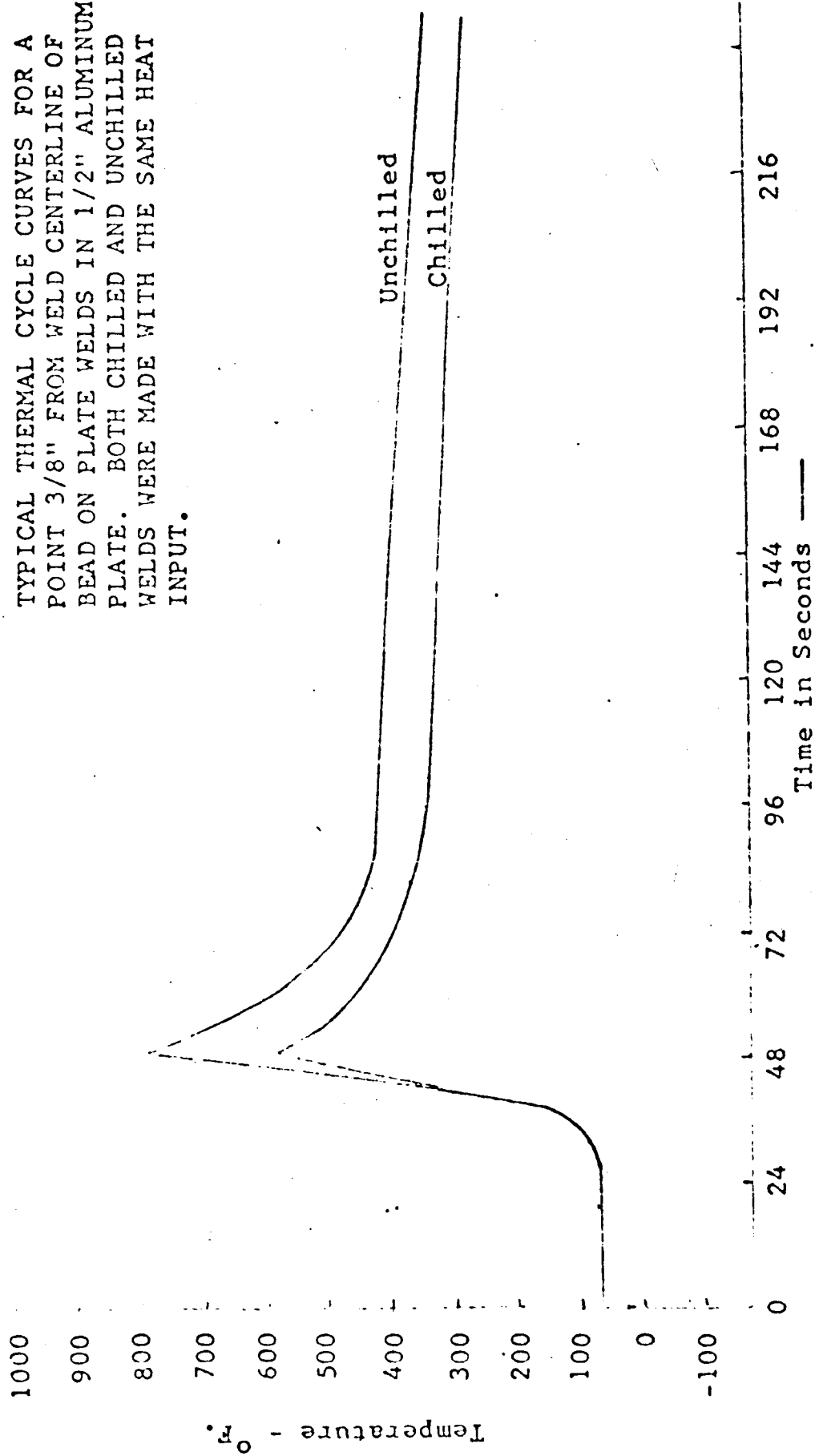


Figure 60. Effect of Front Side Chilling on Thermal Cycle Curves -
Jet System No. 2.

TYPICAL THERMAL CYCLE CURVES FOR
A POINT 3/8" FROM WELD CENTERLINE
OF BEAD ON PLATE WELDS IN 1/2"
ALUMINUM PLATE. BOTH CHILLED AND
UNCHILLED WELDS WERE MADE WITH
THE SAME HEAT INPUT.

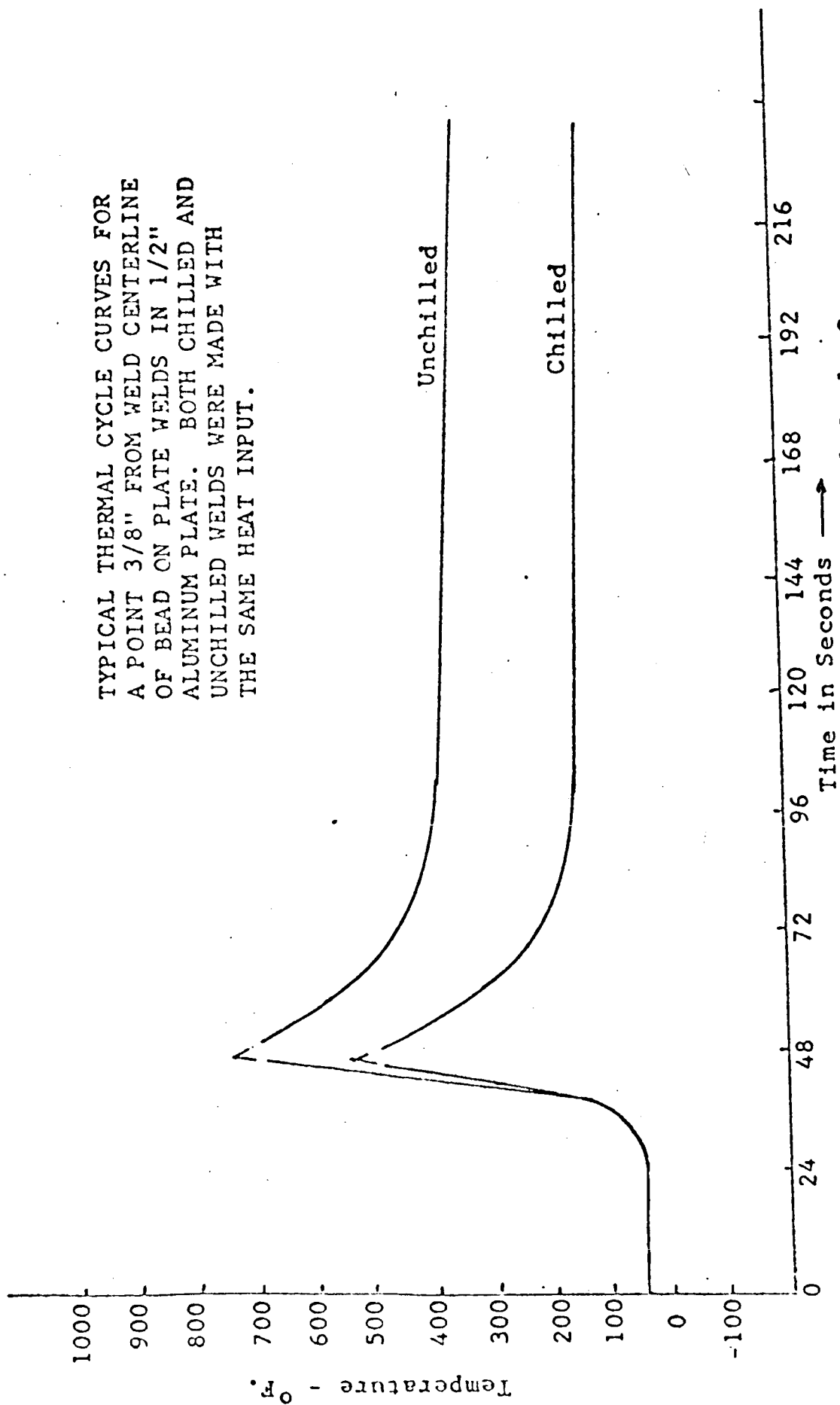


Figure 61. Effect of Front Side Chilling on Thermal Cycle Curves -
Jet System No. 7

TYPICAL THERMAL CYCLE CURVES FOR A POINT
 3/8" FROM WELD CENTERLINE OF BEAD ON PLATE
 WELDS IN 1/2" ALUMINUM PLATE. BOTH CHILLED
 AND UNCHILLED WELDS WERE MADE WITH THE SAME
 HEAT INPUT.

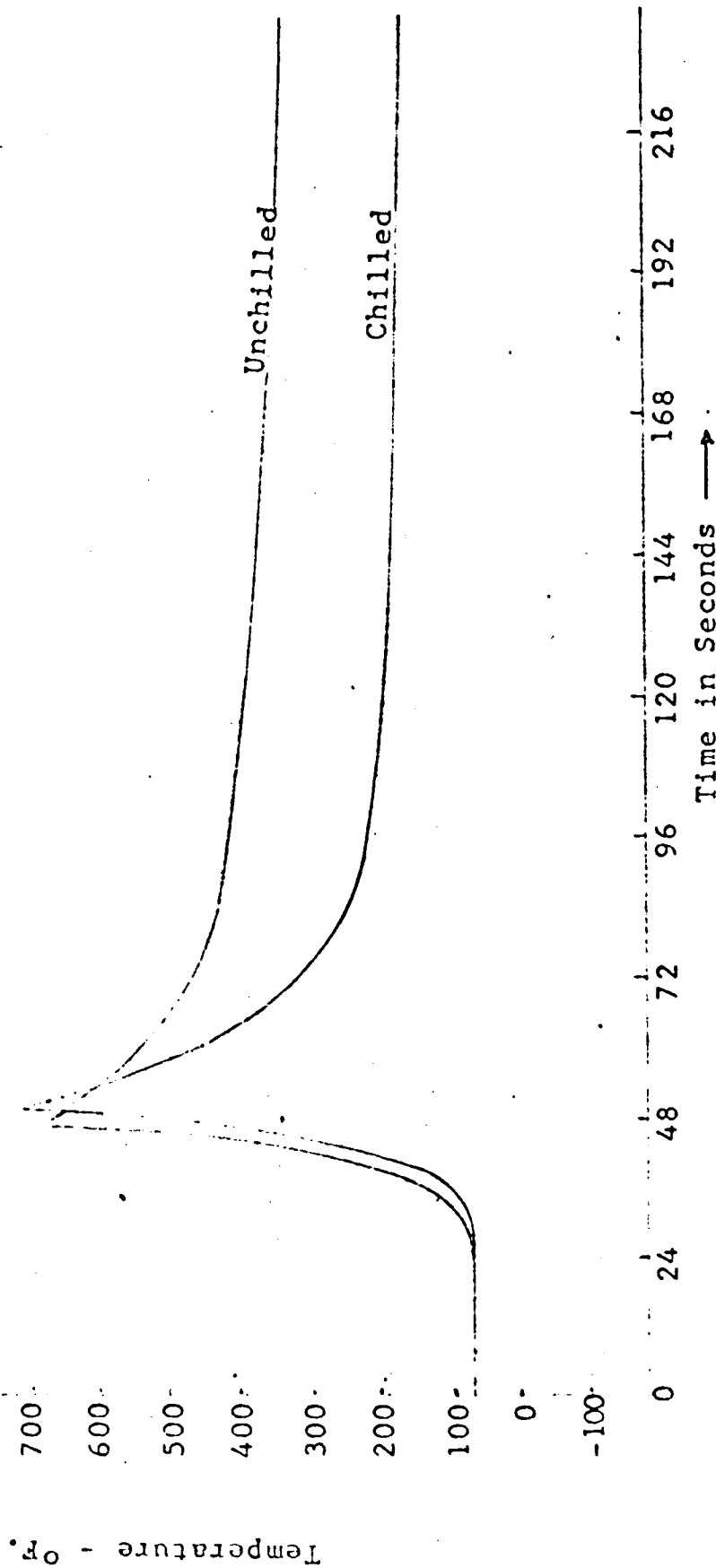


Figure 62. Effect of Front Side Chilling on Thermal Cycle Curves -
 Jet System No. 8 (1/2" Plate).

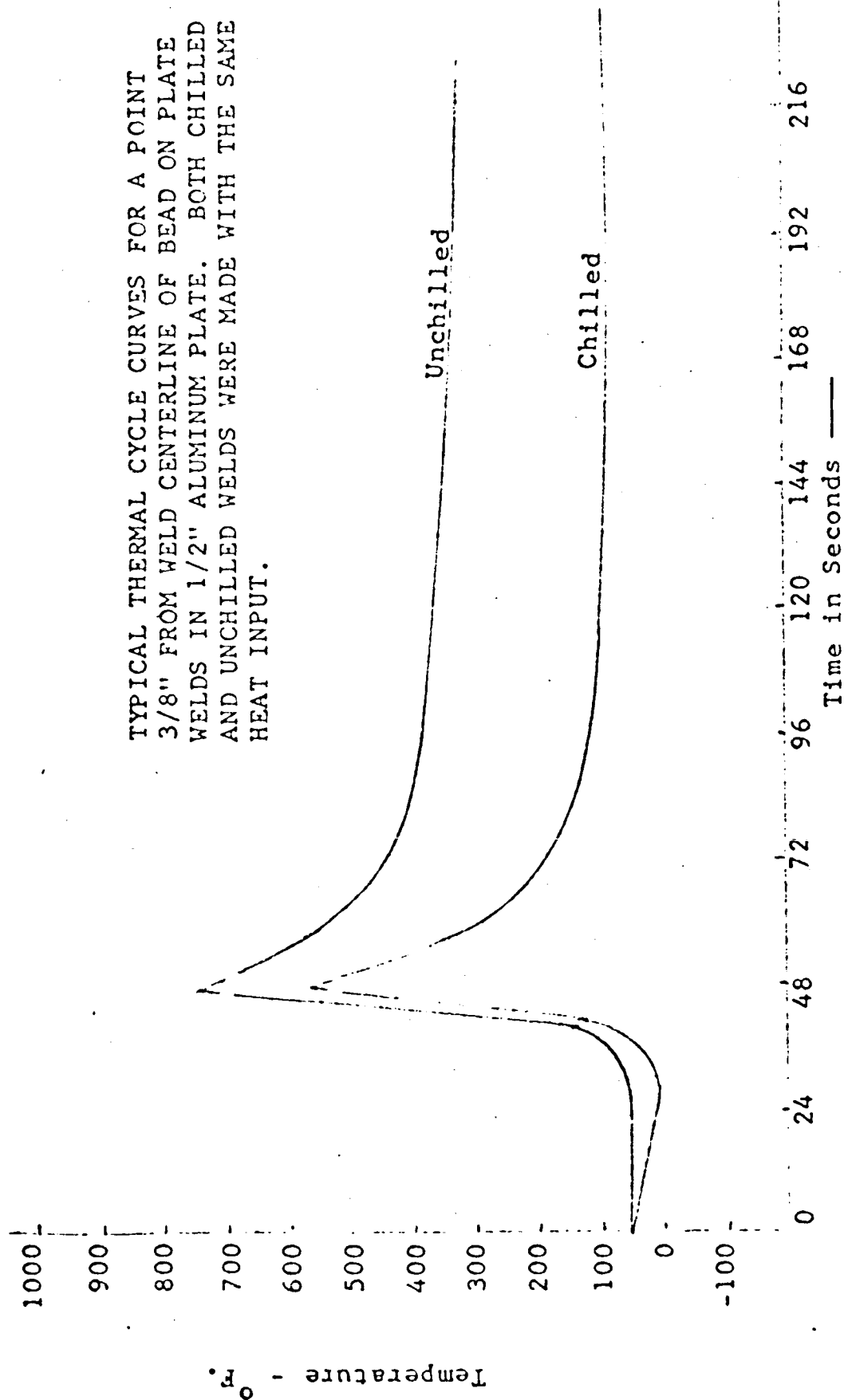
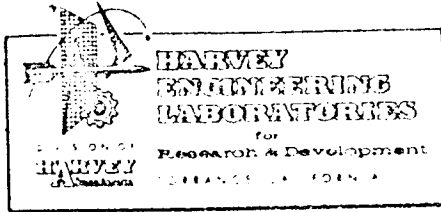


Figure 63 - Effect of Front Side Chilling on Thermal Cycle Curves —
Jet System No. 9



HA NO. 2283 PAGE A.V.

APPENDIX V

TENSILE TEST RESULTS

Table I. Effect of Front Side Chilling on Tensile Properties of Welds in 5/16" 2014-T6 Plate. Artificially Aged After Welding.

Weld Sample No.(1) and Change in Properties (2)	Chill System	T e n s i l e V a l u e s							
		Yield (ksi)		Ultimate (ksi)		Elongation in 2" Average %			
		Max.	Min.	Avg.	Max.	Min.	Avg.		
1AUW 892 1ACFW 891 Change Change (%)	None #18	34.4	33.6	33.9	46.6	45.5	45.9	4.0	
		36.9	35.8	36.5	43.1	40.8	41.3	2.7	
		+2.5	+2.2	+2.6	-3.5	-4.7	-4.6	-1.3	
		+7.3	+6.6	+7.7	-7.5	-10.4	-10.0	-32.5	
1AUW 894 1ACFW 893 Change Change (%)	None #18	37.5	36.6	37.1	49.5	48.4	49.0	3.1	
		41.5	38.3	39.9	48.6	48.0	48.3	2.0	
		+4.0	+1.7	+2.8	-0.9	-0.4	-0.7	-1.1	
		+10.7	+4.6	+7.6	-1.8	-0.8	-1.4	-35.5	
1AUW 8106 1ACFW 8105 Change Change (%)	None #19	32.9	32.2	32.5	46.0	42.0	44.8	2.7	
		35.4	34.1	34.7	42.0	42.1	42.3	2.3	
		+2.5	+1.9	+2.2	-4.0	+0.1	-2.5	-0.4	
		+6.4	+5.9	+6.8	-8.7	+0.2	-5.6	-14.8	
1AUW 8186 1ACFW 8185 Change Change (%)	None #23	36.6	35.4	36.3	49.0	47.5	48.5	3.7	
		41.0	35.3	39.0	48.7	46.5	47.5	2.0	
		+4.4	-0.1	+2.7	-0.3	-1.0	-1.0	-1.7	
		+12.0	-0.3	+7.5	-0.6	-2.1	-2.0	-45.8	

(1) Chilled and unchilled samples were welded on the same panel.

(2) Plus sign indicates improvement effected by chilling; Minus sign indicates decrease.

Table II. Effect of Front Side Chilling on Tensile Properties of Welds in 1/2" 2014-T6 Plate. Artificially Aged After Welding.

Weld Sample No. (1) and Change in Properties (2)	Chill System	T e n s i l e V a l u e s							Elongation in 2" Average %
		Yield (ksi)			Ultimate (ksi)				
		Max.	Min.	Avg.	Max.	Min.	Avg.		
1BUW 896 1BCFW 895 Change Change (%)	None #18	31.0 37.3 +6.3 +20.3	29.7 34.5 +4.8 +16.2	30.9 36.4 +5.5 +17.8	47.5 47.5 0 0	46.0 47.2 +1.2 +2.5	47.0 47.3 +0.3 +0.6	4.0 4.0 0 0	
1BUW 8254 1BCFW 8253 Change Change (%)	None #19	35.0 40.0 +5.0 +14.3	33.4 38.2 +4.8 +14.4	34.0 38.9 +4.9 +14.4	47.0 48.2 +1.2 +2.6	46.6 45.4 -1.2 -2.6	47.2 47.6 +0.4 +0.1	5.0 4.7 -0.3 -6.0	
1BUW 8254 1BCFW 8235 Change Change (%)	None #19	35.0 39.0 +4.0 +11.4	33.4 38.0 +3.6 +10.8	34.0 38.7 +4.7 +13.8	47.0 49.5 +2.5 +5.3	46.6 48.2 +1.6 +3.4	47.2 48.7 +1.5 +3.2	5.0 4.3 -0.7 -14.0	

(1) Chilled and unchilled samples were welded on the same panel.

(2) Plus sign indicates improvement effected by chilling; minus sign indicates decrease.

Table III. Effect of Front Side Chilling on Tensile Properties of Welds in 5/16" 2219-T87 Plate. Artificially Aged After Welding.

Weld Sample No.(1) and Change in Properties (2)	Chill System	T e n s i l e V a l u e s						
		Yield (ksi)			Ultimate (ksi)		Elongation in 2" Average %	
		Max.	Min.	Avg.	Max.	Min.		Avg.
2AUW 8104	None #19	32.6	31.4	31.9	38.8	38.1	38.4	4.0
2AUW 8103		35.0	30.6	33.2	41.6	37.0	39.0	3.7
Change		+3.6	-0.8	+1.3	+2.8	-1.1	+0.6	-0.3
Change (%)		+11.1	-2.5	+4.2	+7.4	-2.9	+1.6	-7.5
2AUW 8232	None #19	35.6	35.1	35.4	40.8	40.4	40.4	3.3
2ACFW 8231		41.5	36.9	38.5	47.5	43.2	44.7	5.0
Change		+5.9	+1.8	+3.1	+6.7	+2.8	+4.3	+1.7
Change (%)		+16.6	+5.1	+8.8	+16.5	+6.9	+10.7	+51.6
2AUW 8162	None #23	35.5	34.6	35.1	43.0	42.0	42.5	4.0
2ACFW8181(3)		36.1	35.9	36.0	40.8	40.7	40.7	4.3
Change		+0.6	+1.3	+0.9	-2.2	-1.3	-1.8	+0.3
Change (%)		+1.7	+3.8	+2.6	-5.1	-3.1	-4.2	+7.5

(1) Chilled and unchilled samples were welded on the same panel.

(2) Plus sign indicates improvement effected by chilling; minus sign indicates decrease.

(3) CO₂ leaked into arc area during welding.

Table IV. Effect of Front Side Chilling on Tensile Properties of Welds in 1/2" 2219-T87 Plate. Artificially Aged After Welding.

Weld Sample No.(1) and Change in Properties(2)	Chill System	Tensile Values							
		Yield (ksi)		Ultimate (ksi)				Elongation in 2 in. Average %	
		Max.	Min.	Avg.	Max.	Min.	Avg.		
2BUW 851A 2BCFW 852A Change Change (%)	none #18	35.5	34.4	35.1	46.6	46.0	46.5		6.0
		37.4	36.2	36.7	48.8	47.2	48.1		5.7
		+1.9	+1.8	+1.6	+2.2	+1.2	+1.6		-0.3
		+5.4	+5.2	+4.6	+4.7	+2.6	+3.4		-5.0
2BUW 8255 2BCFW 8254 Change Change (%)	none #19	34.6	33.5	34.2	44.0	43.0	43.7		6.0
		36.5	35.6	36.0	46.0	44.7	45.6		5.7
		+1.9	+2.1	+2.2	+2.0	+1.7	+1.9		-0.3
		+5.5	+6.3	+6.4	+4.5	+4.0	+4.3		-5.0
2BUW 8188 2BCFW 8187 Change Change (%)	none #23	35.4	34.6	35.1	45.6	44.5	45.0		6.7
		37.5	36.4	36.6	47.4	46.0	46.8		6.0
		+2.1	+1.8	+1.5	+1.8	+1.5	+1.8		-0.7
		+5.9	+5.2	+4.3	+3.9	+3.4	+4.0		-10.5

(1) Chilled and unchilled samples were welded on the same panel.

(2) Plus sign indicates improvement effected by chilling; minus sign indicates decrease.

Table V. Effect of Front Side Chilling on Tensile Properties of Welds in 5/16" 2014-T6 Plate. Naturally Aged 30 Days After Welding.

Weld Sample No.(2) and Change in Properties(2)	Chill System	T e n s i l e V a l u e s								Elongation in 2" Average %
		Yield (ksi)			Ultimate (ksi)			Avg.		
		Max.	Min.	Avg.	Max.	Min.				
1 AUW 894 1ACFW 893 Change Change (%)	None #18	32.8 34.7 +1.9 +5.8	32.6 34.4 +1.8 +5.5	32.7 34.5 +1.8 +5.6	44.7 46.1 +1.4 +3.1	44.0 43.4 -0.6 -1.3	45.5 45.2 -0.3 -0.6	3.8 3.8 0 0		
1AUW 8106 1ACFW 8105 Change Change (%)	None #19	38.3 36.9 -1.4 -3.7	29.9 31.4 +1.5 +5.0	33.5 36.6 +3.1 +9.3	40.6 41.3 +0.7 +1.7	39.6 39.5 -0.1 -0.3	40.2 40.4 +0.2 +0.5	4.0 4.0 0 0		
1AUW 8186 1ACFW 8185 Change Change (%)	None #23	33.1 35.8 +2.7 +8.2	32.9 35.0 +3.9 +11.8	33.0 35.5 +2.5 +7.6	49.9 46.6 -3.3 -6.6	49.6 44.0 -5.6 -11.3	49.7 45.5 -4.2 -8.5	3.5 4.0 +0.5 -14.2		

(1) Chilled and unchilled samples were welded on the same panel.

(2) Plus sign indicates improvement effected by chilling; minus sign indicates decrease.

Table VI. Effect of Front Side Chilling on Tensile Properties of Welds in 1/2" 2014-T6 Plate. Naturally Aged After Welding.

Weld Sample No.(1) and Change in Properties(2)	Chill System	T e n s i l e V a l u e s							Elongation in 2" Average %
		Yield (ksi)			Ultimate (ksi)				
		Max.	Min.	Avg.	Max.	Min.	Avg.		
1 BUW 8254	None	29.5	27.1	28.8	47.7	47.6	47.4	6.3	
1 BCFW 8253	#19	33.1	31.4	32.1	48.2	47.5	48.3	6.0	
Change		+3.6	+4.3	+3.3	+0.5	-0.1	+0.9	-0.3	
Change (%)		+12.2	+15.8	+11.5	+1.0	-0.2	+1.9	-4.8	
1 BUW 8254	None	29.5	27.1	28.8	47.7	47.6	47.4	6.3	
1 BCFW 8235	#19	33.4	33.2	33.2	49.1	46.4	49.0	6.3	
Change		+3.9	+6.1	+4.4	+1.4	-1.2	+1.6	0	
Change (%)		+13.2	+22.5	+15.5	+2.9	-2.5	+3.4	0	

(1) Chilled and unchilled samples were welded on the same panel.

(2) Plus sign indicates improvement effected by chilling; minus sign indicates decrease.

Table VII. Effect of Front Side Chilling on Tensile Properties of Welds in 5/16" 2219-T87 Plate. Naturally Aged After Welding.

Weld Sample No. (1) and Change in Properties (2)	Chill System	Tensile Values							
		Yield (ksi)			Ultimate (ksi)		Elongation in 2" Average %		
		Max.	Min.	Avg.	Max.	Min.		Avg.	
2 AUW 8182	none	24.3	24.0	24.2	38.2	37.4	37.8	5.3	
2ACFW 8181	#23	29.1	25.2	26.8	41.8	39.2	40.5	5.0	
Change		+4.8	+1.2	+2.6	+3.6	+1.8	+2.6	-0.3	
Change %									
2 AUW 8232 (3)	none	26.9	24.7	25.5	36.6	35.8	36.1	4.0	
2ACFW 8231 (3)	#19	25.8	25.6	25.7	38.1	36.5	37.3	4.3	
Change		-0.9	+0.9	+0.2	+1.5	+0.7	+1.2	+0.3	
Change %		-3.3	+3.6	+0.8	+4.1	+0.2	+3.3	+7.5	

(1) Chilled and unchilled samples were welded on the same panel.

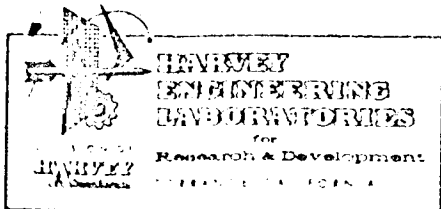
(2) Plus sign indicates improvement effected by chilling; minus sign indicates decrease.

(3) Specimens contained approximately 3% porosity. Panel wire brushed prior to welding.

Table VIII. Effect of Front Side Chilling on Tensile Properties of Welds in 1/2" 2219-T87 Plate. Naturally Aged After Welding.

Weld Sample No. (1) and Change in Properties (2)	Chill System	T e n s i l e V A l u e s							
		Yield (ksi)			Ultimate (ksi)			Elongation in 2" Average %	
		Max.	Min.	Avg.	Max.	Min.	Avg.		
2 BUW 851A 2BCFW 851A Change Change (%)	none #18	21.2 23.0 +1.8 +8.5	20.6 22.3 +1.7 +8.3	20.9 22.5 +1.6 +7.7	40.6 42.2 +1.6 +3.9	40.2 41.0 +0.8 +0.2	40.4 41.5 +1.1 +2.7	8.0 7.3 -0.7 -8.8	
2 BUW 8255 2BCFW 8254 Change Change (%)	none #19	19.9 20.5 +0.6 +3.0	19.6 19.3 -0.3 -1.5	19.7 20.2 +0.5 +2.5	39.0 40.8 +1.8 +4.6	38.4 39.9 +1.4 +3.9	38.8 40.2 +1.4 +3.6	8.3 7.8 -0.5 -6.0	
2 BUW 8188 2BCFW 8187 (3) Change Change (%)	none #23	23.2 21.8 -1.4 -6.0	19.7 21.1 +1.5 +7.6	21.7 21.6 -0.1 -0.5	42.6 40.9 -1.7 -4.0	36.1 40.6 +4.5 +12.5	39.4 40.8 +1.4 +3.6	7.3 8.3 +1.0 +13.7	

- (1) Chilled and unchilled samples were welded on the same panel.
 (2) Plus sign indicates improvement effected by chilling; minus sign indicates decrease.
 (3) Cr2 leaked into the arc during welding.



HA NO. 2283 PAGE A.VI.

APPENDIX VI

SUMMARY OF DATA ON HEAT INPUT,
HEAT EXTRACTION, TENSILE STRENGTH, AND POROSITY
FOR FRONT SIDE CHILLING
OF WELDS

Plate Material		Weld Sample Number	Heat Input ⁽¹⁾				Heat Extraction (by Liquid CO ₂)			
Alloy	Thick-ness (inch)		A	V	T	Q ₁	System	CO ₂ ⁽²⁾	Q ₂ ⁽³⁾	Ma
2014-T6	5/16	1AUW8186	220	12.0	9.6	52.7	-	-	-	36
"	"	1ACFW8185	220	12.0	6.9	73.6	#23	1.5	10.0	41
"	"	1AUW892	230	12.0	7.9	67.0	-	-	-	34
"	"	1ACFW891	230	12.0	7.7	68.7	#18	1.67	42.7	36
2014-T6	5/16	1AUW894	230	11.5	9.6	52.8	-	-	-	37
"	"	1ACFW893	230	11.5	8.2	61.9	#18	1.44	28.0	41
"	"	1AUW8106	220	12.0	8.4	60.3	-	-	-	32
"	"	1ACFW8105	220	12.0	6.2	81.6	#19	1.62	34.5	35
2014-T6	1/2	1BUW8254	315	12.0	6.3	72.1	-	-	-	35
"	"	1BCFW8253	315	12.0	5.4	84.1	#19	2.2	50.6	40
"	"	1BCFW8235	325	12.5	6.7	72.8	#19	1.85	52.8	39
"	"	1BUW896	335	11.5	7.9	58.6	-	-	-	31
"	"	1BCFW895	335	11.5	7.2	64.3	#18	1.5	34.0	37
2219-T87	5/16	2AUW8182	220	12.5	10.9	48.4	-	-	-	35
"	"	2ACFW8181	220	12.5	9.6	54.9	#23	1.48	16.6	36
"	"	2AUW8104	210	12.5	8.4	60.0	-	-	-	32
"	"	2ACFW8103	210	12.5	7.7	65.6	#19	1.36	38.4	35
2219-T87	5/16	2AUW8232	220	12.0	10.4	48.7	-	-	-	35
"	"	2ACFW8231	220	12.0	9.6	52.8	#19	1.38	30.5	41
2219-T87	1/2	2BUW851A	330	11.5	9.6	47.4	-	-	-	35
"	"	2BCFW852A	320	11.8	7.6	59.7	#18	1.4	24.7	37
2219-T87	1/2	2BUW8188	335	11.5	8.7	53.2	-	-	-	35
"	"	2BCFW8187	335	11.5	7.6	60.9	#23	1.39	34.3	37
2219-T87	1/2	2BUW8255	315	12.5	7.1	66.8	-	-	-	34
"	"	2BCFW8254	315	12.5	6.0	78.7	#19	2.24	41.8	36

(1) For single pass weld in 5/16" samples and for penetration pass only

(2) lb. of liquid CO₂ delivery per inch of weld (chilling available for)

(3) Theoretical heat input for chilled welds -

calculated from the change in cooling rate (peak to 450°F.) between

(4) S = Scattered; L = Lineal; I = Intermittent; C = Continuous. X

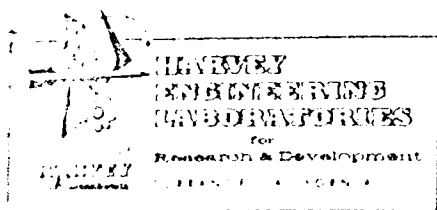
TABLE XIV

Artificially Aged After Welding							T E N S I L E P R O P E R T I E S						
Yield (ksi)			Ultimate (ksi)			Elongation in 2" (%)	Solution H.T. and Aged After Welding			Yield (ksi)			Elongation in 2" (%)
Max.	Min.	Avg.	Max.	Min.	Avg.		Max.	Min.	Avg.	Max.	Min.	Avg.	
6	35.4	36.3	49.0	47.5	48.7	3.7	55.7	52.0	54.1	65.5	62.8	64.2	4.0
0	35.3	39.0	48.7	46.5	47.5	2.0	-	-	-	65.3	-	-	6.0
4	33.6	33.9	46.6	45.5	45.9	4.0	63.6	62.0	62.8	70.5	69.9	70.0	4.0
5	35.8	36.5	43.1	40.8	41.3	2.7	65.3	62.4	63.9	73.4	71.0	72.2	6.3
5	36.6	37.1	49.5	48.4	49.0	3.1	-	-	-	-	-	-	-
5	38.3	39.9	48.6	48.0	48.3	2.0	-	-	-	-	-	-	-
9	32.2	32.5	46.0	42.0	44.8	2.7	62.7	61.0	61.4	70.2	65.1	67.7	4.0
4	34.1	34.7	42.0	42.1	42.3	2.3	64.0	62.9	63.5	70.3	68.2	69.4	3.0
0	33.4	34.0	47.0	46.6	47.2	5.0	57.5	55.1	56.6	65.3	62.6	64.0	8.0
0	38.2	38.9	48.2	45.4	47.6	4.7	57.1	55.0	56.2	64.8	63.5	64.1	6.0
0	38.0	38.7	49.5	48.2	48.7	4.3	-	-	-	-	-	-	-
0	29.7	30.9	47.5	46.0	47.0	4.0	62.5	58.7	60.0	72.3	68.7	70.2	8.0
3	34.5	36.4	47.5	47.2	47.3	4.0	59.6	59.1	59.4	69.7	68.7	69.2	5.3
5	34.6	35.1	43.0	42.0	42.5	4.0	44.5	43.5	44.0	58.0	56.0	56.8	5.3
1	35.9	36.0	40.8	40.7	40.7	4.3	43.6	43.3	43.5	57.7	56.4	57.1	6.0
5	31.4	31.9	38.8	38.1	38.4	4.0	50.4	50.2	50.3	66.9	58.3	59.3	4.3
0	30.6	33.2	41.6	37.0	39.0	3.7	52.3	51.6	51.9	61.0	60.4	60.8	5.0
5	35.1	35.4	40.8	40.4	40.4	3.3	-	-	-	-	-	-	-
5	36.9	38.5	47.5	43.2	44.7	5.0	-	-	-	-	-	-	-
5	34.4	35.1	46.6	46.0	46.5	6.0	44.4	43.5	44.3	59.0	56.0	58.3	5.3
5	36.2	36.7	48.8	47.2	48.1	5.7	44.8	44.2	44.6	59.0	55.2	56.6	8.0
4	34.6	35.1	45.6	44.5	45.0	6.7	-	-	-	-	-	-	-
5	36.4	36.6	47.4	46.0	46.8	6.0	-	-	-	-	-	-	-
5	33.5	34.2	44.0	43.0	43.7	6.0	43.3	43.0	43.2	57.8	55.7	56.9	8.0
5	35.6	36.0	46.0	44.7	45.6	5.7	44.0	43.0	43.6	57.8	56.6	57.3	8.0

in 1/2" samples. Q₁ = heat input in joules/in./in.
 from CO₂ = 157,500 joules per lb.)

comparable chilled and unchilled weld samples. $Q_2 = Q_1 \frac{V_2}{V_1} \sqrt{\frac{R_1}{R_2}}$
 ray Std = NAVORD OD7574.

Naturally Aged (30 days) After Welding						Porosity (avg.)(4)			
Yield (ksi)			Ultimate (ksi)			Elongation in 2" (%)	X-Ray Grade	% Frac.	Remarks
Max.	Min.	Avg.	Max.	Min.	Avg.				
33.1	32.9	33.0	49.9	49.6	49.7	3.5	0	0	Draw filed
35.8	35.0	35.5	46.6	44.0	45.5	4.0	0	0	" "
-	-	-	-	-	-	-	-	-	-
-	-	-	-	-	-	-	-	-	-
32.0	32.6	32.7	44.7	44.0	45.5	3.8	#1 SI	0	Draw filed
34.7	34.4	34.5	46.1	43.4	45.2	3.8	#1 SI	0	" "
38.3	29.9	33.5	40.6	39.6	40.2	4.0	-	-	-
36.9	31.4	36.6	41.3	39.5	40.4	4.0	-	-	-
29.5	27.1	28.8	47.7	47.6	47.4	6.3	#1 SI	0	Draw filed
33.1	31.4	32.1	48.2	47.5	48.3	6.0	#1 SI	0	" "
33.4	33.2	33.2	49.1	46.4	49.0	6.3	#1 SI	0	CO2 leaked
-	-	-	-	-	-	-	-	-	-
-	-	-	-	-	-	-	-	-	-
4.3	24.0	24.2	38.2	37.4	37.8	5.3	#3 LC	0	Draw filed
9.1	25.2	26.8	41.8	39.2	40.5	5.0	#1 LC	0	CO2 leaked
-	-	-	-	-	-	-	-	-	-
-	-	-	-	-	-	-	-	-	-
6.9	24.7	25.5	36.6	35.8	36.1	4.0	#3 LC	5	Wire brushed
5.8	25.6	25.7	38.1	36.5	37.3	4.3	#3 LC	2	" "
1.2	20.6	20.9	40.6	40.2	40.4	8.0	0	1	Wire Brushed
1.0	22.3	22.5	42.2	41.0	41.5	7.3	0	0	" "
.2	21.7	21.7	42.6	36.1	39.4	7.3	0	1	Draw filed
.8	21.2	21.6	40.9	40.6	40.8	8.3	#1 SI	1	CO2 leaked
.9	19.6	19.7	39.0	38.4	38.8	8.3	#1 SI	0	Draw filed
.5	19.3	20.2	40.8	39.9	40.2	7.8	0	0	" "

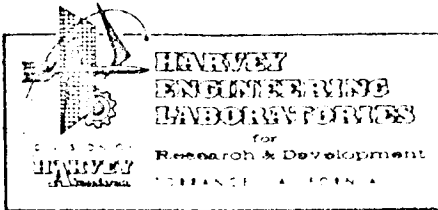


HA NO. 2283

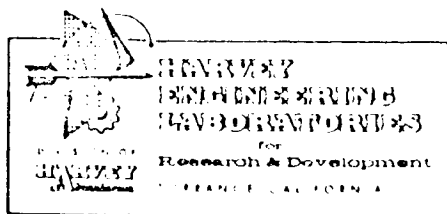
PAGE A.VII.

APPENDIX VII

TEMPERATURE MEASUREMENTS BY INFRARED RADIATION

TEMPERATURE MEASUREMENTS BY INFRARED RADIATION

Studies were made to determine the applicability of infrared radiometry to measurement of temperatures of the weldment during the welding process. A survey was made of various types of instruments available, and three were selected for experimental study. All contained a PbS detector with germanium lenses capable of small target size and focal length from 6 to 30 inches or more. Two were fixed spot and the third was a line scanner. Results of studies indicated that infrared radiometry could be adapted to this program by making provisions for the varying emittance of the work piece and interference from the welding arc. Fixed spot radiometers are more suitable for the work in this program, as monitoring of the temperature of one or more single points for weld parameter control will be the major purpose for radiometer use. Precise information on the temperature of a single point cannot readily be obtained from a line scanning radiometer, while fixed point radiometers are ideally suited for this application and are considerably less expensive. It is contemplated that future work would include the use of infrared radiometers in the instrumentation, with eventual application as a quality control device.



HEAT SOURCE: Weld seam

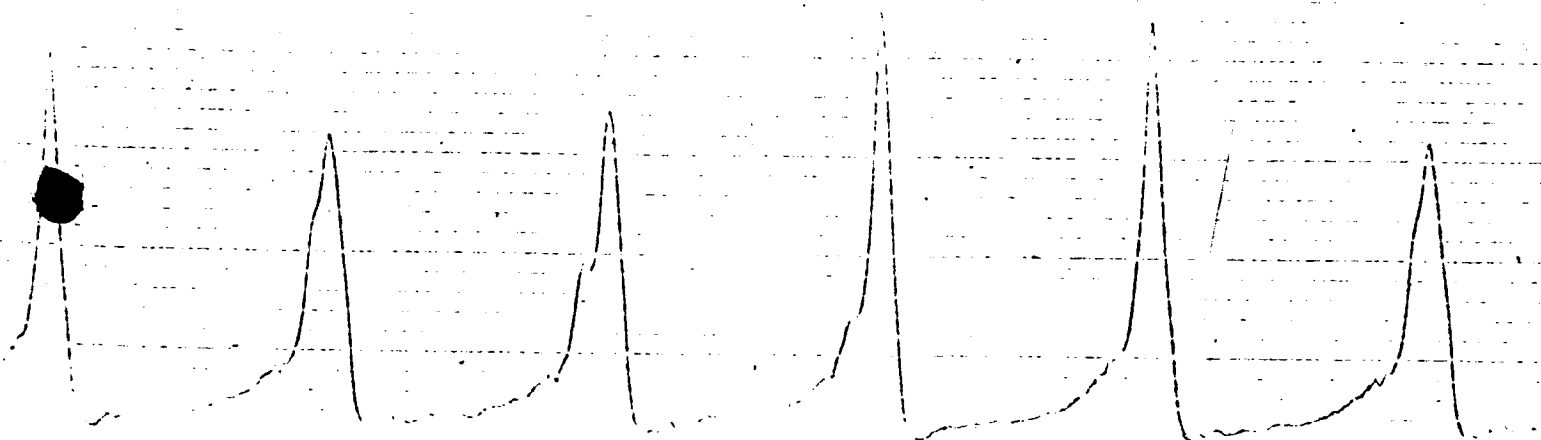
Location - Center of radiometer scan line

RADIOMETER: Germanium Lens, folding mirror, mask,
rotating reticle, PbS detector, amplifier, etc.

Scan speed = 50 in./sec.

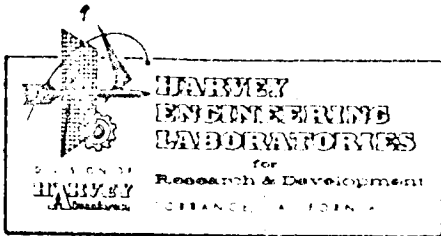
Scan line = 0.020" x 3" 1/2" ahead of electrode

RECORDER: Honeywell Visicorder, chart = 5 volts/in.



RADIOMETER GAIN = 1

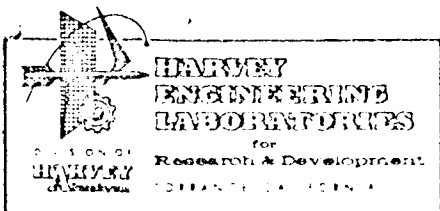
FIGURE 64 . TRACE OF BARNES SCANNING RADIOMETER DURING
WELDING, SHOWING SIX CONSECUTIVE SCANS



HA NO. 2283 PAGE A.VIII.

APPENDIX VIII

REFERENCES

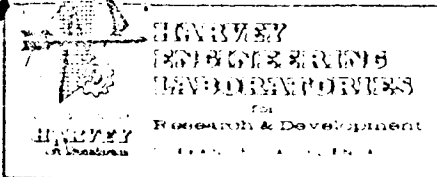


HA NO. 2283

PAGE A. VIII.01

REFERENCES

- (1) "Analysis of Time-Temperature Effects in 2219 Aluminum Welding," F. J. Jackson, Welding Journal, April, 1966, pages 1885-1923.
- (2) Welding Handbook, Fifth Edition, Section One, A.W.S., pages 5.19.
- (3) "Cooling Rates and Peak Temperatures in Welds," C. M. Adams, Jr., Welding Journal, May, 1958, pages 2105-2155.



HA NO. 2283

PAGE 1

DISTRIBUTION LISTAddresseeCopy No.

National Aeronautics and Space Administration
George C. Marshall Space Flight Center
Huntsville, Alabama 35812

Attn: Code PR-RC

Attn: Code MS-IL

Attn: Code MS-T

Attn: Code R-ME-MW

1

2 & 3

4

5 - 7, 9 - 13

Mr. John F. Rudy
Mail Stop G-0934
Martin Company
Denver, Colorado 80201

14

Robert E. Monroe
Battelle Memorial Institute
505 King Avenue
Columbus, Ohio 43201

15

R. H. Kilpatrick
Lockheed Georgia Co.
Marietta, Georgia 30061

16

Joseph Lempert
Westinghouse R&D Center
Pittsburgh, Pennsylvania 15235

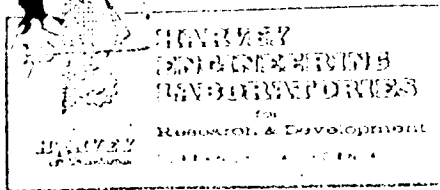
17

D. D. Pollock, A-263
Douglas Aircraft Company
3000 Ocean Park Avenue
Santa Monica, California 90405

18

Peter J. Tkac
Lear Siegler, Inc.
17600 Broadway Avenue
Cleveland, Ohio 44137

19



HA NO. 2283 PAGE 2

Addressee

Copy No.

F. D. Seaman
Westinghouse Electric Corporation
ASTRO Nuclear Division
Box 10864
Pittsburgh, Pennsylvania 15236

20

E. Strobel
Boeing Aircraft Company
P. O. Box 3707
Seattle 24, Washington

21

Mr. James R. Kennedy
(Plant #12, Dept. 234)
Grumman Aircraft Engineering Corporation
Bethpage, Long Island, New York 11714

22

Mr. Koichi Masabuchi
Battelle Memorial Institute
505 King Avenue
Columbus, Ohio 43201

23